JOURNAL OF CAVE AND KARST STUDIES

April 1998
Volume 60 Number 1
ISSN 1090-6924

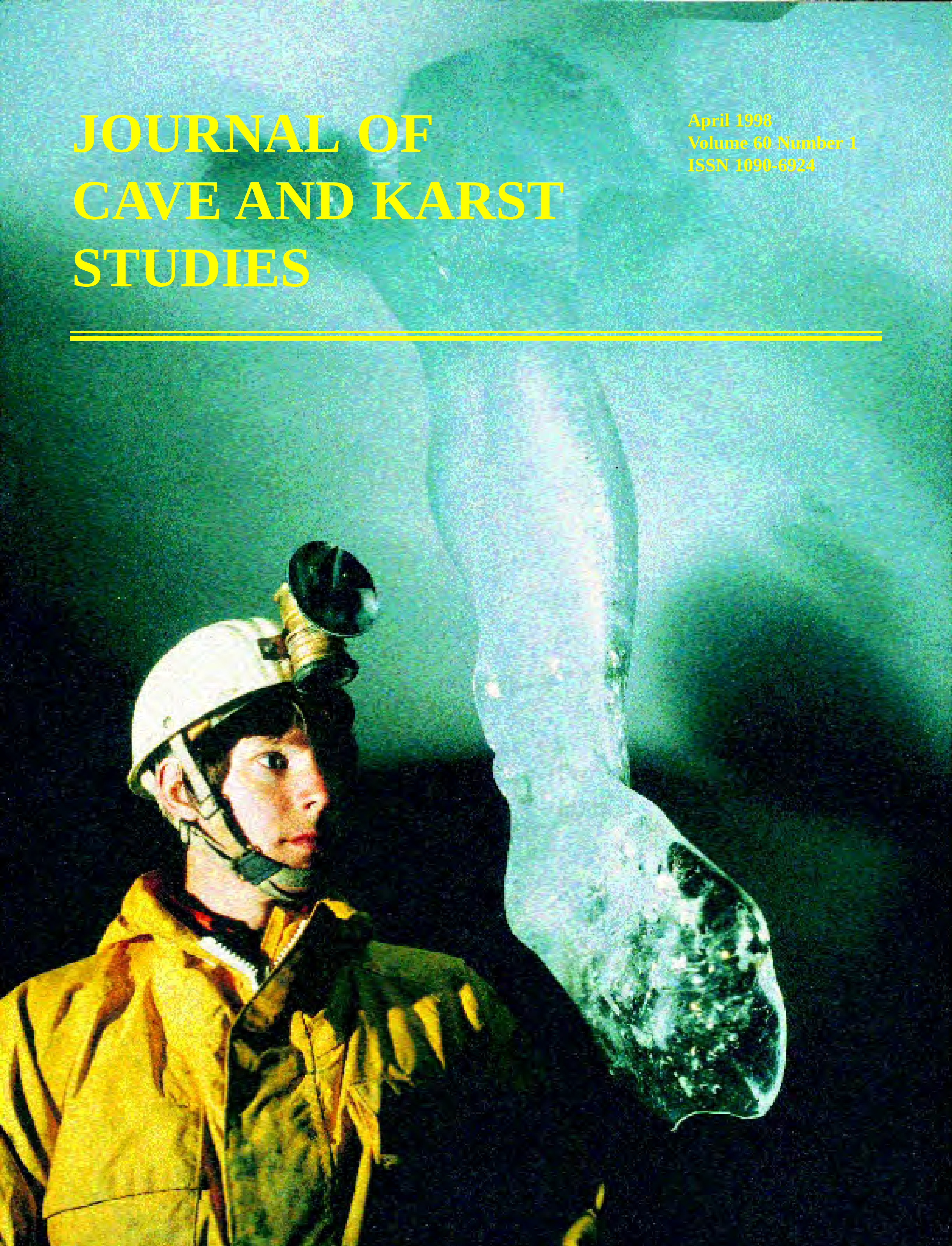

Journal of Cave and Karst Studies
Volume 60 Number 1 April 1998

CONTENTS

The *Journal of Cave and Karst Studies*, formerly *The NSS Bulletin*, (ISSN 1090-6924) is published three times a year by the National Speleological Society, 2813 Cave Avenue, Huntsville, Alabama 35810-4431; (256) 852-1300; FAX (256) 851-9241, e-mail: nss@caves.org; World Wide Web: http://www.caves.org/~nss/. The annual subscription fee, worldwide, by surface mail, is $18 US. Airmail delivery outside the United States of both the *NSS News* and the *Journal of Cave and Karst Studies* is available for an additional fee of $40 (total $55); The *Journal of Cave and Karst Studies* is not available alone by airmail. POSTMASTER: send address changes to the *Journal of Cave and Karst Studies*, 2813 Cave Avenue, Huntsville, Alabama 35810-4431.

Cover: Mark R. Vining in Paradise Ice Caves. See Anderson, Behrens, Floyd and Vining page 44.

THE PROBLEM OF CONDENSATION IN KARST STUDIES

VICTOR N. DUBLYANSKY
Simferopol University. 4, Yaltinskaya str., Simferopol, Crimea, 333036, UKRAINE

YURI V. DUBLYANSKY
Institute of Mineralogy & Petrography, Russian Academy of Sciences, Siberian Branch, 3 University Avenue, Novosibirsk, 630090, RUSSIA

Condensation in karst occurs over a wide range of natural settings, at latitudes from 25º to 70º and altitudes from sea level to 2600 m. In summer (April through September), condensation introduces a significant amount of water into the karst massifs (from 0.1% to as much as 20% of the total dry-season runoff). Contrary to common belief, in winter evaporation does not withdraw appreciable amounts of water from the massifs. Evaporating at depth, the water condenses near the surface within the epikarstic zone or on the snow cover and flows back. Condensation can sustain springs during prolonged dry periods (such as summer and winter) when there is no recharge by liquid precipitation.

Condensation can play a significant role in speleogenesis, and many forms of cave macro-, meso-, and micromorphologies are attributable to condensation corrosion. It can be particularly efficient in the latter stages of hydrothermal cave development (during partial dewatering) when the temperature and the humidity gradients are highest. Coupled with evaporation, air convection, and aerosol mass transfer, condensation can play a crucial role in the formation of a number of speleothems, as well as create peculiar patterns of cave microclimate.

Early statements advocating the condensation of moisture in caves can be found in texts of the ancient Greek philosophers Thales of Miletus, Empedocles, and Aristotle (VI-IV BC). Marcus Vitruvius Pollio (I AD) stated his belief that the moisture can condense from the vapors of hot waters rising from depth of the Earth (Fedoseev, 1975). During the following fifteen centuries, the natural phenomena were interpreted in accordance with theological dogmas. Only in XVI-XVIII AD, the European philosophers Georgius Agricola, Rene Descartes, and Athanasius Kircher brought back into scientific use the ideas of ancient natural philosophy. Eventually, O. Volger offered a more or less comprehensive hypothesis about formation of groundwater by condensation process (Volger, 1877). The hypothesis, however, came under severe criticism (Hann, 1880) and, after relatively short debate, was abandoned. It was A. Lebedev who revived the ideas of Volger in a series of publications of 1908-1926. The latter went largely unnoticed outside Russia due to the unfavorable historic background: World War I and Russian revolutions.

According to the concept of Lebedev (1936), the vapor moves from areas with elevated partial vapor pressure and air temperature to the areas with lower values of these parameters. For more than 70 years, the concept of Lebedev provided the basis for studies of natural condensation; only recently several papers suggesting re-consideration of the concept have been published (Tkachenko, 1978; Kuldzhaev, 1989). Applied to karst, the concept of Lebedev implies that condensation should occur in caves during warm seasons, and that evaporation must prevail there during cold seasons (Fig. 1).

Shestakov (1989) compiled a bibliography of more than 1,000 papers on condensation. About 10% of the researchers believe that only evaporation of soil- and ground water occurs and that condensation of atmospheric moisture underground is not possible; 40% think that the input of water due to summer

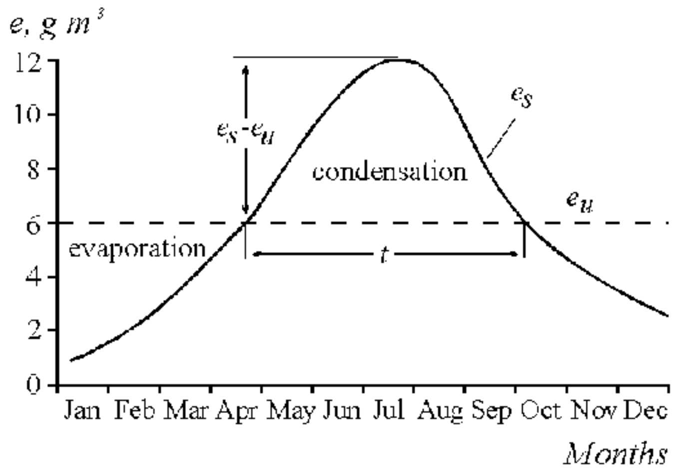

Figure 1. Potential of condensation and evaporation in the karst massifs of the Crimea Mountains (after Dublyankky & Lomaev, 1980; generalized). Many other karst massifs of the former Soviet Union exhibit similar patterns, though the concrete values of all parameters may vary. e_S is the absolute humidity on the surface; e_U is the absolute humidity underground; (e_S-e_U) - is the gradient of the absolute humidity of the air entering the cave; *t* - is the duration of condensation period. Condensation occurs when $e_s > e_u$.

condensation is balanced by water withdrawal due to winter evaporation; and ~50% consider the condensate an important component of the water balance, but abstain from numerical estimations.

Difficulties involved in quantifying the condensation are reflected in method and reference sources, which state that: "due to the fact that quantitative determination of condensation is difficult and time consuming, it is not expedient to take it into account in water balance studies" (Borevsky et al., 1976: 120); or: "due to practical difficulties in determining the condensation, the latter is conventionally lumped with the precipitation and the evaporation" (Pinneker, 1980: 89).

There is no agreement regarding the role of condensation among karst researchers, either. By way of example: Martel (1894) rejected the very possibility of it; Trombe (1952) and Gvozdetsky (1954) believed that it plays significant role in speleogenesis; and Gergedava (1970) assigned to condensation the leading role in speleogenesis.

By and large, the importance of condensation in karst and other hydrogeological processes seems to be underestimated. For instance, a fundamental review on karst geomorphology and hydrology by Ford and Williams (1989) only mentions seasonal condensation (p. 469) and condensation corrosion, mostly in hypogenic settings (p. 309). Meanwhile, the longstanding karst studies in the Crimea, Caucasus, and some other regions of the former Soviet Union reveal an important role of condensation in both formation of karst waters, and speleogenesis. Being published mostly in Russian, these data remain largely unavailable to the non-Russian researchers. This prompted us to prepare the present review.

Restricted volume of the paper does not allow us to present all pertinent references (many more references can be found in the bibliographic index by Shestakov, 1989), or to give detailed data on physical and geographical settings of studied objects (instead, we use statistical generalizations, such as the mean values and the coefficients of variation, C_v); as well as to provide all pertinent details about the methods used (in many instances we only outline their rationales). This should be viewed as an unavoidable shortcoming of a review paper.

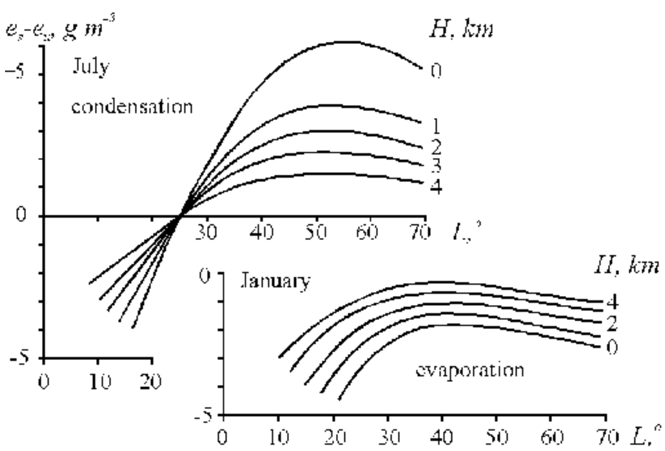

Fig. 2. Possibility of condensation in karst during warm (July) and cold (January) seasons at different latitudes L and altitudes above sea level H. Condensation occurs when $(e_s - e_u) > 0$ (after Dublyanskaya & Dublyansky, 1989).

DIFFERENT LEVELS OF CONDENSATION STUDIES

The discordant opinions about condensation, quite common in karst literature, often resulted from the difference in study methods and approaches. The latter strongly depend on the scale of studies. For the sake of simplicity, we will discuss separately four levels of condensation studies: global, regional, local, and object levels. It should be born in mind that the data and results obtained at one level cannot always be directly translated onto another level.

STUDY OF CONDENSATION ON THE GLOBAL LEVEL

The possibility of condensation can be assessed on the global scale in dependence on latitudes and altitudes. The attempt of such assessment was done by Dublyanskaya and Dublyansky (1989) (Fig. 2). They used data on latitudinal distribution of absolute humidity of the air (Khromov & Mamontova, 1963) along with the data on humidity in caves located at different latitudes and altitudes (by Moore and Sullivan (1978) with corrections by the data of other researchers). During the warm period (July) condensation can occur at latitudes from 25º to 70º; at lower latitudes evaporation prevails. During the cold period (January), evaporation prevails in caves at any latitude. The rates of condensation and evaporation change with altitude.

Naturally, Figure 2 is a broad generalization; it depicts only the possibility of condensation. Processes occurring in real caves depend on climatic zone in which the cave is located, position of the cave within karst massif, passage of frontal systems, and many other factors. Also, Figure 2 implies that the input of water from summer condensation is counterbalanced by its withdrawal during winter evaporation. However, the local-level studies of condensation suggest that this does not happen in natural settings (see section "Winter condensation" below).

STUDY OF CONDENSATION ON THE REGIONAL LEVEL

The regional-level studies deal with condensation within mountainous constructions (e.g., the Crimea) or individual karst massifs (e.g., Chatirdag massif, one of nine karst massifs of the Crimea). At this level, the following features are suggestive of condensation.

Low-discharge springs. Such springs exist within isolated karst-erosional or structure-denudational remnants which are located close to mountain summits, crests, and passes. In such settings, the recharge via infiltration is insignificant, which suggest condensation as the source of waters (Slavianov, 1955;

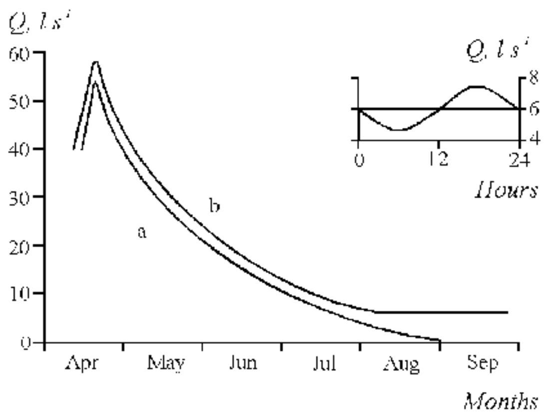

Figure 3. Discharge hydrographs (schematized). a - according to the model of the drainage of stored water; b - according to the condensation model. Inset shows the daily oscillations of the hydrograph during a period of condensation recharge (dry season; August-September on this graph). The values shown in the inset correspond to actual values measured for the Krasnopeshernaya River in the Crimea.

Protasov, 1959; Dublyansky, 1977; Dublyansky et al., 1985).

Constant summer discharges of karst springs. During summer dry season, karst springs display hydrographs which may be approximated by smooth recession curves. This type of hydrograph is normally interpreted by a model of drainage of karst in which water drains from storage in caves, fissures, and pores. A number of expressions approximate the observed recession curves; the one most frequently used is:

$$Q_t = Q_0 e^{-\alpha t} \quad (1)$$

where Q is the discharge [m^3 s^{-1}] at times t and 0, t is the time elapsed [days], and α is the recession coefficient [T^{-1}] (Ford & Williams, 1989; p. 196). Quite often, however, after reaching a certain minimum at $n \cdot 10^{-2}$-$n \cdot 10^{0}$ l s^{-1}, the falling hydrograph limb levels off and remains horizontal (Fig. 3) for a long period of time (1 to 4 months). This has been reported by Jenko (1959) as a "precise constancy of dry-season discharges" in karst springs of the Dinaric Karst (Yugoslavia). Similar patterns were found for karst springs in the Crimea, the Caucasus, and some other karst areas of the former Soviet Union (Dublyansky et al., 1984; 1985; 1989).

The analysis of daily hydrographs of the Krasnopeshchernaya River in the Crimea (fed by karst springs withdrawing water from the Dolgorukov karst massif, with its 13.7-km-long Krasnaya Cave) performed for the period from 1963 through 1988 revealed a fine structure of dry-season discharges. Having average daily value of 6 l s^{-1}, the discharge exhibits regular daily variations, increasing from 4 to 8 l s^{-1} and then lowering again (Fig. 3, inset). Thus, the drainage of stored water is overprinted by a certain dynamic process, which stabilizes the discharge of springs at some level (specific to each spring) and governs the systematic daily variations around this level. A similar pattern was observed in springs located at different altitudes. It does not depend on the presence and composition of vegetation, which could induce "evapotranspirational" cyclicity of discharge. Also, the relation between the discharge of springs and the variations of the gravitational field caused by the interaction of the Earth, the Moon, and the Sun, reported by Kinzikeev (1993), has not been confirmed in the Krasnaya Cave area. Thus, we believe that condensation provides the most appropriate explanation for the observed patterns of the dry-season discharges.

Meteorological data. The senior author, for a number of years, monitored the discharges of several springs which were suspected to be fed by condensation, along with meteorological parameters (Dublyansky, 1977). A strong correlation was found between dry-season discharge (nil precipitation during 1 to 4 months), and meteorological parameters for 15 springs in the Crimea and 6 springs in Western Caucasus located at altitudes from 30 to 1800 m and having discharge from 0.012 to 8.660 L s^{-1}. Systematic diurnal variations of discharge, Q, and water temperature, T_w, which were correlated with changes in dynamic parameters of the air, controlling condensation (that is, temperature of the air, T_A, and its absolute humidity, e_s) were observed during warm seasons (June-August) over a period from 1965 through 1994. These relations have statistically significant values of the coefficient of correlation (0.77-0.99 ± 0.05-0.21). The response of Q and T_w to the changes of T_A and e_s is normally delayed; hence, a travel-time correction (retardation Δt) must be applied. The latter ranges from 1 to 15 hours for different springs (Fig. 4 and Table 1). T_w changes during a day almost synchronously with Q and does not show appreciable correlation with T_A. One may assume that water controls

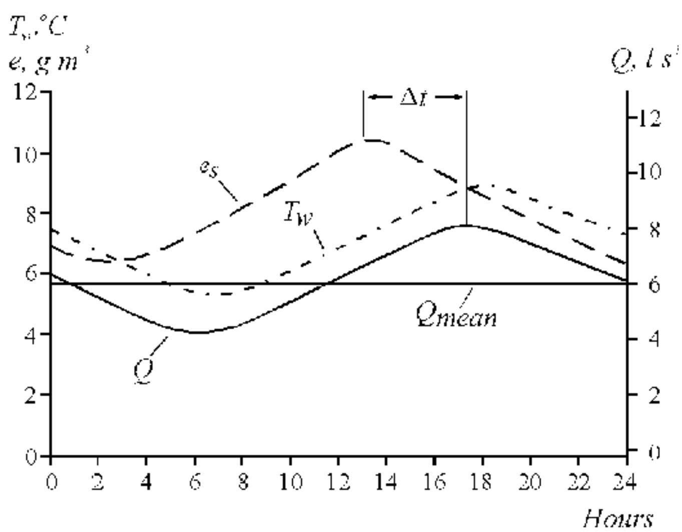

Figure 4. Daily variations of the discharge, *Q*, and the temperature, Tw, of a condensation-fed spring as compared with variation of absolute humidity of the atmospheric air, es. *t* - is the lag time (travel time).

Table 1
Discharge and water temperature in the condensation-fed springs in limestone massifs of the Crimea and Caucasus, and correlation between the discharge, Q, and absolute air humidity, e

Spring name	Altitude m	Period of observations	Mean discharge Q $l\ s^{-1}$	C_V	Mean T_W ºC	C_V	Lag time hours	Coefficient of correlation between Q and e
Crimea								
Ay-Petri	1100	July 1-2, 1959	0.012	0.03	7.2	0.04	2	0.95±0.09
Beshtekne	1000	June 26-27, 1989	6.100	0.07	6.5	0.01	3	0.78±0.17
Beshtekne	980	July 8-9, 1989	0.770	0.05	7.7	0.03	3	0.72±0.11
Pahkal-Kaya	960	June 27-28, 1994	0.014	0.07	10.1	0.04	6	0.80±0.12
Chatirdag	920	June 20-21, 1995	0.008	0.20	12.4	0.26	4	0.57±0.16
Alushta	920	July 20-21, 1991	0.054	0.04	6.5	0.03	3	0.86±0.09
Alushta	730	July 20-21, 1991	0.181	0.02	8.5	0.03	3	0.85±0.13
Mangup	575	July 25-26, 1971	0.370	0.06	10.6	0.03	4	0.92±0.12
Kizil-Koba	550	Aug 24-25, 1965	8.560	0.22	9.8	0.04	15	0.81±0.07
Aleshina Voda	550	Aug 25-26, 1965	2.350	0.17	9.6	0.03	6	0.85±0.14
Red Cave #33	510	June 26-27, 1984	1.460	0.02	9.6	0.02	8	0.81±0.16
Petrovski-1	420	June 18-19, 1986	0.110	0.05	10.9	0.04	2	0.74±0.16
Preduschelnoye	380	Aug 2-3, 1989	0.700	0.01	10.5	0.01	4	0.83±0.21
Petrovski-2	330	July 9-10, 1991	0.104	0.02	11.2	0.02	14	0.75±0.18
Yanishar	160	May 1-2, 1988	0.020	0.02	-	-	18	0.96±0.02
Opuka	30	July 2, 1991	0.105	0.04	13.3	0.02	10	0.73±0.18
Caucasus								
Bagia	1800	July 12-13, 1983	0.220	0.01	8.5	0.11	1	0.99±0.05
Gelgeluk	1780	July 19-20, 1984	1.400	0.03	4.1	0.02	5	0.92±0.09
Alek	960	Aug 5-6, 1971	0.220	0.03	9.2	0.06	5	0.88±0.07
Alek	920	Aug 6-7, 1971	0.170	0.04	9.6	0.05	5	0.92±0.09
Proval	600	Aug 21-22, 1975	0.830	0.04	30.0	0.03	16	0.72±0.19
Akhun	210	July 27-28, 1976	0.030	0.05	8.9	0.02	7	0.87±0.14
Mean	-	-	1.132	0.05	10.1	0.03	6	0.84±0.12

temperature during condensation, as the specific heat capacity of water (1 cal g^{-1} $degree^{-1}$) is 4 to 6 times as large as the specific heat capacity of karstifiable rocks (e.g., 0.16-0.24 cal g^{-1} $degree^{-1}$ for limestone and 0.20-0.25 cal g^{-1} $degree^{-1}$ for gypsum).

Geological engineering data. Much about condensation associated with construction works within karst terrains (residential and industrial buildings, asphalt and concrete covers, embankments, airdrome runways, etc.) has been published (Vedernikov & Larina, 1985). Condensation is viewed as a major factor in the rise of the groundwater (underflooding) within urbanized territories (Riazanova, 1987).

At the regional level, three groups of methods are used for quantitative determinations of condensation: (1) water balance studies; (2) calculation methods; and (3) microclimatic methods.

Water balance studies. A number of attempts have been undertaken for the Crimea Mountains to estimate condensation using water balance equation: [condensation = precipitation - (evapotranspiration+runoff)] (Golovkinsky, 1894; Vasilievski and Zheltov, 1932; Glukhov, 1963). The calculated values varied from 0.7 to 25.0% of the rainfall. This approach is inappropriate, as the calculated values are of the same magnitude as are estimated errors for other constituents of the water balance (15-20%).

Calculation methods. In 1938 through 1986 a number of researchers suggested methods for calculation of condensation within karst massifs. Most of those methods have important shortcomings: some of them contain terms which hardly can be determined; other are suitable for too general or, vice versa, too particular calculations. By way of illustration we present one of the suggested methods. Sitnikov (1986) studied the dynamics of moisture- and salt transfer in the aeration zone and suggested the following for estimation of condensation:

$$q(0,t) = -\frac{\beta\sigma(t)}{\gamma_L}\left\{P_W(0,t) - \left[P_L(0,t) - P_{AT}(0,t)\right]\right\}, \qquad (2)$$

where q is the condensation on or evaporation from a surface [m day^{-1}]; β is a coefficient accounting for the state of water on (from) the surface of which condensation (evaporation) occurs [m day^{-1}]; σ is a coefficient accounting for the effective surface of condensation (evaporation) [parts of unity]; γ_L is the density

Table 2. Condensation as related to recharge of some karst massifs of Ukraine, Russia, and Georgia (after Dublyansky, 1977; Dublyansky and Kiknadze, 1984; Dublyansky et al., 1985; and Vakhrushev, 1993). Calculations are by equation (3).

Karst massif	Surface area km²	The amount of condensed water mm	% of yearly total precipitation	Contribution to runoff l s^{-1} km^{-2} Annual	Per warm season
			Western Carpathians		
Ugolsk	12.0	1	0.1	0.02	0.11
			Crimea		
Aipetri	97.7	77	6.4	2.46	5.00
Dolgorukov	79.5	25	3.0	0.81	2.94
Karabi	217.4	27	3.2	0.86	3.09
Chatirdag	23.4	69	7.2	2.38	5.30
Inner Range	293.0	11	2.0	1.85	9.60
Opuka	2.7	36	9.1	1.15	1.70
			Western Caucasus		
Kavminvody	495.0	8	1.2	0.25	0.68
Alek-Akhtsu	28.8	82	3.4	2.60	6.12
Dzikhra-Vorontsov	38.0	41	1.9	1.85	4.20
Akhshtir-Akhun	19.0	22	1.1	0.69	1.40
Arabika	517.8	134	5.6	4.27	9.36
Bzib	297.8	121	4.8	3.85	8.40
Khipsa	186.8	149	5.8	4.72	10.13
Gumishkha	263.5	61	3.1	1.95	4.37
Duripsh	40.9	4	0.1	0.12	0.28
Mean		54	3.5	1.86	4.54
Cv		0.87	0.73	0.79	0.75

of water [kg m^{-3}]; P_L and P_w are the pressure of water [Pa]; and P_{AT} is the atmospheric pressure [Pa]. This equation can be used for covered karst, but is not applicable to the directly exposed karst or to individual caves.

Microclimatic method. It is based on the equation introduced by Obolensky (1944) and modified by Dublyansky (1969):

$$A = V \varepsilon (e_s - e_u)\, t\, J \qquad (3)$$

where A is the amount of condensate [g]; V is the volume of the active part of the karst massif [m^3] (estimated from topographic and geologic maps and considering the depth of caves); ε is the fissuration and karst porosity [parts of unity] (estimated by geological, geophysical, or hydrochemical methods by density of fissuration and the volume of caves); (e_s-e_u) is the difference of absolute humidities on the surface and underground [g m^{-3}] (determined by meteorological and climate data; see Fig. 1); t is the duration of condensation period [day] (see Fig. 1); J is the frequency of air exchange [day^{-1}] (estimated by air flow velocities measured in caves and scaled to the average fissure and/or cave dimensions; Dublyansky, 1969).

This method has several apparent shortcomings. For instance, it is difficult to determine ε and J accurately. Also, the diffusion of water vapor, which does not depend on air movement, is not considered. In actual practice, nevertheless, it gives satisfactory results. It has been calibrated on a monitored massif of the Krasnaya Cave (the Crimea) and gave fair agreement (±10%) with the values obtained by an independent method (measurement of the dry-season spring discharges).

The microclimatic method was used to determine the role of condensation in recharge of karst waters within 16 karst massifs of the former Soviet Union (Table 2). The data imply that condensation accounts for 0.1 to as much as 9.1% of the total annual precipitation (mean 3.5%, C_v = 0.73). The average yearly condensation runoff is 1.86 l s^{-1} km^{-2} (C_v = 0.79). Because condensation occurs only during the warm season, it is worthwhile to calculate seasonal (warm-season) runoff. Its mean value for the massifs studied is 4.54 l s^{-1} km^{-2}. Calculated values show good correlation with the dry-season discharges of springs located within the massifs (coefficient of correlation r = 0.7-0.8).

Microclimatic calculations reveal some interesting peculiarities of condensation in karst massifs located at different altitudes (Fig. 5). Equation (3) comprises both static (V, e) and dynamic (t, e_s, e_u, and, J) members. The values of the term (e_s-e_u) decrease with increasing altitude, whereas those of t increase. The coupled effect is the appearance of the conden-

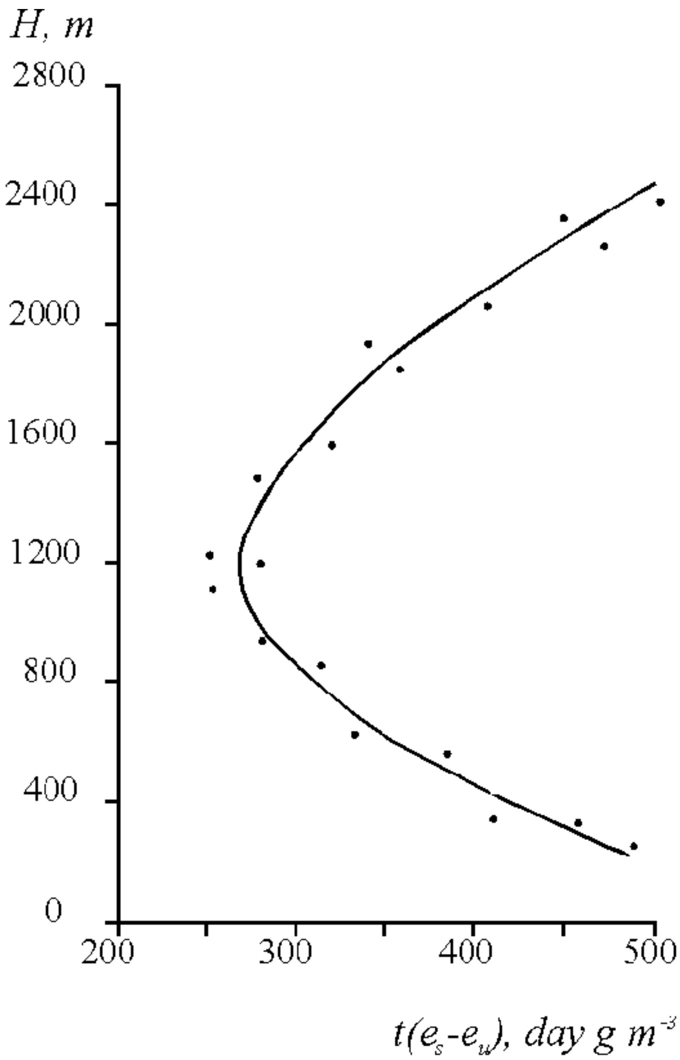

Figure 5. The dynamic parameter of condensation, t (e_s-e_U), as related to altitude above sea level, H. Data for the Bzib massif, Western Caucasus.

sation minimum at 800-1600 m and of two maximums below 800 and above 1600 m.

Naturally, the results presented in this section do not give an exhaustive account of all aspects of regional level condensation studies. For instance, of particular interest are the annual patterns of condensation in karst massifs located within different altitude zones having different vegetation cover; condensation in high altitude karst massifs; change of condensation pattern due to passage of frontal systems, etc. These problems are not yet explored adequately.

STUDY OF CONDENSATION ON THE LOCAL LEVEL

The local level deals with individual caves as well as with small karst remnants feeding karst springs.

Historical and archeological data. Water which condensed on naturally collapsed rock or within man-made piles of gravel was used for water supply in ancient and medieval settlements in Southern Europe and Central Asia (Zibold, 1904; Tugarinov, 1955; Klimochkin, 1973; Firsov, 1990; Vakhrushev, 1993). Destruction of such structures, as well as destruction of small isolated limestone remnants (e.g., their quarrying for gravel during road construction) led to decrease in discharge or even cessation of condensation-fed springs (e.g., Gaspra Isar and Morcheka springs in the Crimea).

Observations and microclimatic studies in caves. Studies through the past thirty years have revealed condensation in caves of varied location, morphology, and microclimate, as well as in underground mines (Ustinova, 1956; Protasov, 1959; Prokofiev, 1964; Lukin, 1969; Andrieux, 1970; Eremenko & Kolpashnikov, 1974; Dublyansky, 1977; Ginet, 1977; Racovitca & Viemann, 1984).

The possibility that there may be condensation occurring in a cave may be estimated by measuring the difference between absolute humidity on the surface and underground (e_s-e_u). Microclimatic observations from 290 caves of the Crimea and Western Caucasus (more than 10,000 measurements and 5,000 continuous daily records of air pressure, temperature, and humidity) demonstrated the existence of condensation and revealed its daily, weekly, and monthly variations (Dubljanski & Sockova, 1977; Tsikarishvili, 1981; Dublyansky et al., 1989). Condensation was observed in caves during the warm season (maximum in July and August). Evaporation prevails during the cold season, though in some particular settings condensation also can occur. The diurnal pattern of condensation is controlled by change of the temperature and humidity on the surface (maximum at 10 a.m. - 4 p.m. and minimum at 10 p.m. - 2 a.m.).

Condensation and chemosorption in caves and underground mines in hygroscopic rocks (massive halite and potash deposits) were reported by Maksimovich (1963), Eremenko and Kolpashnikov (1974), and Beltukov (1989). Korotkevich (1970) demonstrated that at relative humidity close to 100%, the rate of condensation there may be as high as 180-225 mm yr^{-1}.

Calculations of the amount of condensation in Kungur Ice Cave, Urals were performed by Lukin (1969). He calculated that some $2 \cdot 10^5$ m^3 of air passes through a cave per day. Each cubic meter of air leaves behind some 4.6 g of condensed water (which yields on a daily basis 920 kg). For five caves in the Crimea, Ustinova (1956) obtained somewhat lower values of 3 g m^{-3} at a rate of air exchange of $0.3 \cdot 10^5$ m^3 day^{-1}.

Detailed microclimatic studies carried out between 1960 and 1970 in 157 caves of the Crimea (Dublyansky et al., 1989) yielded an average value of condensation 19.9 g m^{-3} (C_v = 1.45). Condensation reaches a maximum of 75.8 g m^{-3} in July in vertical shafts; values of 0.7-4.0 g m^{-3} were measured in open caves located on the plateau, which agrees with earlier results by Ustinova (1956). Jameson and Calvin Alexander (1989) reported condensation rates of 30-90 g m^{-2} day^{-1} on vertical surfaces and 45-200 g m^{-2} day^{-1} on horizontal surfaces in Snedegar's Cave in West Virginia. Similar studies have been carried out in caves of Romania, France, and some other countries (Andrieux, 1970, Racovitca & Viemann, 1984).

Calculations of condensation. Several methods of condensation calculation in caves have been suggested; each method based on different theoretical premises. Mucke, Völker, and Wadewitz (1983) suggested an empirical equation for calculation of condensation:

$$m = (25 + 20W)(X_S - X_L), \qquad (4)$$

where m is the condensation rate [g m^{-2} $hour^{-1}$]; W is the velocity of the air motion [m s^{-1}]; X_s is the saturation humidity in the boundary layer between air and cave wall [g kg^{-1}]; and X_L is the humidity of the bulk of the air at the same temperature [g kg^{-1}].

Eraso (1969) pointed out that when warm air enters a cave, it cools down and a part of its moisture can condense. The decrease of the temperature is defined as:

$$\Delta T = (K - I)(1000 c_P \gamma)^{-1} \qquad (5)$$

where ΔT is the decrease of temperature [ºC]; K and I are the heat content of moist- and dry air masses [kcal m^{-3}]; C_P is the specific heat capacity of the air [cal g^{-1} $degree^{-1}$]; and γ is the air density [kg m^{-3}]. A similar approach was independently developed by Dublyansky and Iliukhin (1981).

Golod (1981) has developed a mathematical model of coupled aero-, thermo-, and hydrodynamic processes in caves. He assumed that condensation, being a low-intensity process, occurs at an equilibrium (along the curve of saturation). This allows calculation of condensation by:

$$P_H = P_0 \exp [\mu_n L_K/R] [(T_B - T_0)/(T_B T_0)] \qquad (6)$$

and

$$dQ_K = \rho_L L_K dV_K, \qquad (7)$$

where P_H is the pressure of saturated vapor; P_0 and T_0 are the pressure and the temperature at the triple point; μ_n is the molecular weight of the vapor; L_K is the specific heat of condensation; R is the universal gas constant; T_B is the absolute temperature; dQ_K is the heat released in process of condensation; dV_K is the amount of condensed water; and ρ_L is the density of the liquid phase.

Comprehensive thermodynamic calculations of condensation processes were performed by Bruent and Vidal (1981) in order to develop methods of protecting the Paleolithic paintings in the Lascaux Cave, France. The air conditioning system was constructed in the cave on the basis of these calculations.

Winter condensation. The local-level studies of condensation fostered some fundamentally new ideas about the formation of ground waters. The problem of special interest is the winter condensation (distillation). The warm-season condensation in caves is accompanied by an input of moisture from the outside atmosphere. The cold-season evaporation, however, does not remove all moisture from the rocks: the water evaporated deep within a karst massif condenses within the epikarstic zone or on the snow pack (Fig. 6). Thus, there occurs an "internal circulation of moisture", which does not increase the total amount of water stored in the massif, but significantly increases the residence time of water in the rock and thus enhances condensation-related karstification. Winter condensation sustains the runoff from high-mountain karst massifs during periods when they are devoid of recharge by liquid precipitation.

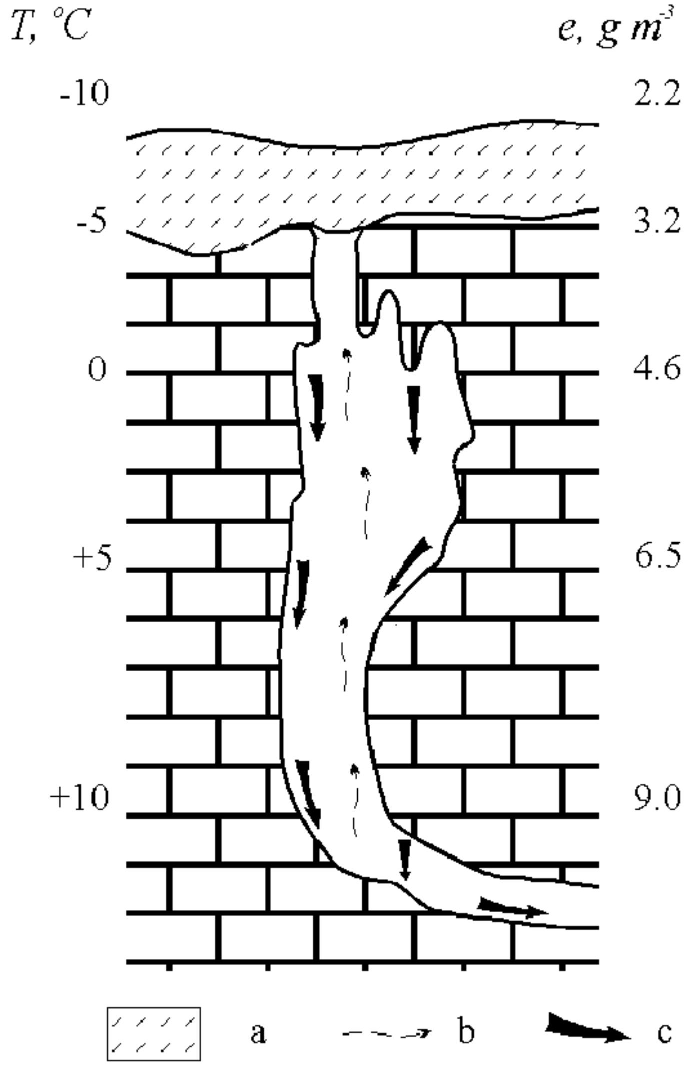

Figure 6. The pattern of air and moisture circulation characteristic of cold-season condensation setting. a - snow; b - movement of water in form of vapor; c - movement of water under the influence of gravity; T - the temperature of the cave air; e - absolute humidity.

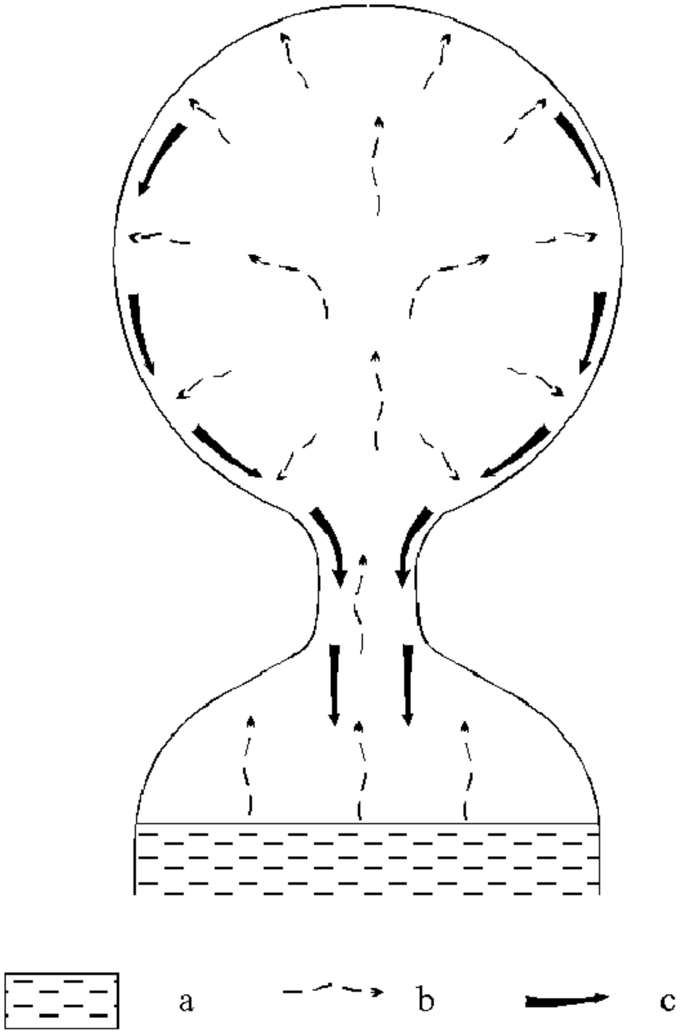

Figure 7. Condensation in a hydrothermal cave: a - thermal lake; b - movement of water vapor; c - movement of water as a liquid under the influence of gravity (after Szunyogh, 1982).

The winter condensation could be the mechanism, which prevents the large-scale removal of the moisture from karst massifs by evaporation during cold seasons. The surface area of open cave entrances through which such removal can take place is negligible relative to the total surface area of karst massifs.

Existence of winter condensation was confirmed by targeted observations in karst massifs of the Western Caucasus (Dublyansky et al., 1985). On some of them, the snow cover lies during 3-5 months and its thickness reaches 6-12 m (e.g., Bzib massif). There exists only insignificant runoff in caves; it is well correlated with the changes of negative air temperatures on the surface. Detailed microclimatic surveys have shown that this runoff cannot be accounted for by melting of snow at its base due to geothermal flux. The karst massifs are deeply cooled fragments of the Earth's crust, where the "normal" geothermal gradient begins to control the rock temperatures only at great depths.

Winter condensation was also determined in the Pinego-Kuloy karst region, Northern Russia, where Malkov and Frantz (1981) reported formation of condensate drops during 11 days, when outside air temperature varied from -7° to -42°C.

Hydrothermal condensation. A special case of condensation in caves is hydrothermal condensation occurring above the surface of underground thermal waters during the partial dewatering stage of hydrothermal caves (Fig. 7). Such a mechanism is believed to be responsible for the carving of peculiar spherical niches known in caves of Hungary (Müller, 1974), Italy (Cigna & Forti, 1986), and elsewhere. Theoretical consideration (Szunyogh, 1982; 1990, Dublyansky, 1987) as well as laboratory experimentations (Dreibrodt, 1994, pers. comm.) have shown that condensation in such a system is a naturally attenuating process: it slows down due to the low rate of heat transfer through the bedrock. In natural settings, however, hydrothermal condensation may become a powerful influence in karst formation if cooling of the bedrock occurs due to even minor ventilation. The latter is quite probable, as such caves develop not far from the topographic surface within the zone of aeration. A prominent example of such convection-condensation-corrosion is known in Grotta Giusti, Italy. The cave contains a lake of thermal water having a temperature of 32-34°C, while the temperature of the rock in the upper level of the cave is 20°C. The rate of condensation in this cave was estimated to be 8,640 l day^{-1}, and the estimated amount of bedrock $CaCO_3$ dissolved was 630 g day^{-1} (Cigna & Forti, 1986).

Study of condensation on the local level reveals many interesting problems, which require special detailed studies. Examples of such particular problems are: formation of condensation moisture in "mixing fogs", condensation in narrow passages due to increase of velocity of the air flow (accompanied by decrease of the pressure and temperature), influence of cave ice on condensation (sublimation), evaporation from the surface of inflowing water and further re-distribution of the moisture in the cave, and many others.

STUDY OF CONDENSATION ON THE OBJECT LEVEL

These studies deal with the separate parts of caves (e.g., isolated rooms, near-entrance zones, etc.), condensation devices of different design, as well as special tasks (e.g., studies of mineral formation, development of measures to preserve ancient graffiti and paintings, etc.).

Being studied at the object level, condensation appears to be quite a heterogenous process, and the pattern of condensation/evaporation within individual caves can be extremely complex. In some caves, the seasonal pattern of condensation and evaporation discussed above, can be interrupted by relatively short (from days to weeks) reversals (e.g., evaporation in summer due to passage of frontal systems and change of air circulation pattern).

Table 3
The output of different types of condensation setups constructed on the surface.

Author	Years	Location	Altitude m asl	Characteristics of the setup Volume m^3	Type of infilling	Yield l day-1 per each m^3 of infilling
Golovkinsky, N.A. and Peddakas, I.K	1864-1905	Crimea, Southern Coast	300	0.04-0.14	clay, sand	0.028
Zibold, F.I.	1912	Eastern Crimea	190	1117.0	pebble	0.320
Khudiaev I.E.	1931	Crimea, Southern Coast	480	0.03	gravel	0.980
Beliavsky, A.Y.	1940	Kiev	100	0.01	sand, loess	2.324
Tugarinov, V.V.	1951	Moscow area	280	300.0	gravel	0.620
Reiniuk, I.G.	1951-1965	Kolima Region	200	from 0.007	sand	0.022
				to 0.016	gravel	0.370
Protasov, V.A.	1955	Crimea, Southern Coast	400	0.25	gravel	0.018
Klimochkin, V.V.	1958-1970	Siberia and Kola Peninsula	?	0.01-0.05	sand	0.050
					pebble	0.060
					gravel	0.100
Dublyansky, V.N.	1960	Western Crimea	1100	900.0	gravel	0.016
Pribluda, V.D.	1963-1976	Western Crimea	900	22.0	gravel, cobbles	0.012
Mean						0.386
C_v						1.71

Condensation typically occurs on the surface of the cave bedrock, sediments (in the latter case it could be accompanied by different kinds of sorption), or water bodies. Besides, it can occur in the cave air itself, as warm, relatively moist surface air enters, cools and condensation fog eventually forms. This process can be classed as formation of aerosols (the fog particles must grow greater than ~5 µm in size to become visible). Though this process can occur through homogenous nucleation, more often it occurs heterogeneously (condensation of moisture on solid aerosol particles, which serve as condensation nuclei). If the water condensed on aerosol particles, its further migration inside cave will be governed by aerosol mechanics, rather than by gas dynamics.

Dripping and splashing water (from waterfalls, flowstone, etc.) can evaporate into cave air and be transported to other cave locations and condense. Splashing produces relatively large (~10 µm) hydroaerosol particles, which increases the specific surface of the liquid and fosters evaporation. Also, water for condensation/evaporation processes can be introduced as surface water flowing into a cave. The pattern of condensation/evaporation processes can be influenced by the airflow structure of the cave (see, e.g., data on the air flow directions inferred from the orientation of cave popcorn in Carlsbad Cavern; Queen, 1981).

Even though the data concerning condensation on the object level are abundant, these data are mostly descriptive, and studies presenting numeric estimations of condensation are quite scarce. Some examples are given below.

Studying archeology of the medieval cave towns in the Crimea, Firsov (1990) has noticed intensive condensation occurring in some crypts in summer. He estimated that a crypt carved in massive limestone and having the volume of 5.5 m^3 generates 0.25 l m^{-2} day^{-1} of condensate. Prokofiev (1964) was first to perform the direct measurements of the amount of condensate forming in different rooms of Vorontsovskaya Cave in the Western Caucasus. He used original traps for condensed (and partly infiltrated) water. The traps yielded up to 1300 g m^{-3} of water at an air exchange rate of $161.3 \cdot 10^6$ m^3 day^{-1}. Similar observations were carried out in a number of caves in Europe and Asia.

Condensation was also studied by means of lysimeters and condensers with differing designs (metallic cones, cylinders, boxes, casing tubes, polyethylene canisters, etc.), varying sizes (from 0.01 to 1120 m^3) and various types of filling material (sand, gravel, pebbles, limestone boulders). They were installed or constructed at altitudes ranging from 190 to 1100 m in the Crimea, Caucasus, Central Russia, Kola Peninsula, and Southern and Eastern Siberia. The yield of water in these experiments varied from 0.01 to 2.3 l day^{-1} from each cubic meter of the filling material (Table 3). Attempts to use these values directly to calculate condensation in adjacent karst massifs have failed (Glukhov, 1963; Klimochkin, 1973).

THE ROLE OF CONDENSATION IN KARST

There are several aspects of condensation in karst: (1) increase of the amount of water moving through the rock; (2) increase in the total volume of karst porosity; (3) formation and destruction of cave deposits; (4) alteration of cave microclimate. The data on these processes are scarce and often con-

Table 4
Chemistry of condensation waters.

Parameters	Moisture condensed on clean surface	Stationary drops on the ceiling	Trails and films on the walls	Source
Carbonate Karst				
Number of samples	7	55	66	DUBLYANSKY, 1977;
Mean TDS mg l-1	106	22.0	140.0	DUBLYANSKY et al., 1985;
Mean TDS CV	0.58	1.15	0.25	HOMZA, RAJMAN, & RODA, 1970
Hydrochemical type	HCO_3-Ca(Mg)	HCO_3-Ca	SO_4-HCO_3-Ca	KLIMOCHKIN, 1973;
Chemical denudation				NEMERIUK & PALTSEV, 1969;
µm×year-1				MAIS & PAVUZA, 1994;
calculated at 10ºC	-	-	2-19	MUCKE & VOLKER, 1978;
actual	-	-	0.5-4.0	PROKOFIEV, 1964
Carbonate Hydrothermal Karst				
Chemical denudation				SZUNYOGH, 1990
µm×year-1 (*)				
at 60ºC	-	-	200-50	
at 20ºC	-	-	30-4	
Sulfate Karst				
Number of samples	-	5	44	DUBLYANSKY et al., 1984;
Mean TDS mg l^{-1}	-	2000	2100	MALKOV & FRANTZ, 1981;
Mean TDS C_V	-	-	0.27	MUCKE & VOLKER, 1978
Hydrochemical type	-	SO_4-Ca	SO_4-Ca	
Chemical denudation				
µm×year-1				
calculated at 10ºC	-	-	92-730	
actual	-	-	90-121	
Rock Salt Karst				
Number of samples	-	-	17	BELTIUKOV, 1989;
Mean TDS mg l^{-1}	-	80000	322000	EREMENKO & KOLPASHNIKOV 1974
Mean TDS C_V	-	-	0.8	
Hydrochemical type	-	Cl-Na(K)	Cl-Na(K)	
Chemical denudation				
µm×year-1	-	-	21,000	

All samples are composite (many drops are mixed). They were typically collected at the end of a long period of nil precipitation or when the massif was covered by snow. (*) Growth of a spherical niche slows down with increase of its diameter; TDS - total dissolved solids

troversial.

INCREASE OF THE AMOUNT OF WATER AVAILABLE FOR SPELEOGENESIS

Our data suggest that the share of condensation in the water balance does not normally exceed 9% of the annual sum of precipitation (Table 2). However, condensation occurs during the warm season, when there is not much of precipitation. It plays, thus, an important role in the dry-season discharge of karst springs and rivers. Winter condensation does not increase the total amount of underground water, but prevents moisture from escaping the subsurface and creates specific local patterns of water circulation. These general conclusions need to be checked and numerically assessed by regional- and local-level studies.

DESTRUCTIVE PROCESSES

Many workers believe that condensed waters initially have exceptionally high aggressiveness with respect to bedrock limestone (Trombe, 1952; Gvozdetsky, 1954; Bernaskoni, 1966; Andrieux, 1970; Gergedava, 1970; Pasquini, 1973; Ginet, 1977; Mucke & Völker, 1978). The data on the composition of condensate from different karst massifs of Eurasia are compiled in Table 4.

Analyses were mostly performed on composite samples (up to 10,000 individual drops) collected from cave walls, which means these waters had the ability to dissolve the bedrock. Condensate has quite variable mineralizations (TDS; C_v up to 1.15), differing in karsts in different lithologies. Condensate water collected after a certain travel (30 to 100 m; flow as films and trails along walls) has higher mineralizations and lower coefficients of variation C_v (0.25 to 0.60). This suggests intensive corrosion of the bedrock.

The data on samples collected on a clean cool surface (ice-filled containers or refrigerators) are scarce. In some cases the measured TDS are low (e.g., 8.27-8.31 mg l^{-1} in Ochtinskaya Aragonite cave in Slovakia; Homza, Rajman, & Roda, 1970). In other cases, surprisingly high values of TDS were obtained (e.g., 130-170 mg l^{-1} in Hermanshöle in Lower Austria; Mais & Pavuza, 1994). Tarhule-Lips (pers. comm.) has found that the air moisture sampled in several caves of the Cayman Braker islands (Caribbean sea) can be slightly undersaturated to slightly supersaturated relative to bedrock limestone. This problem warrants further rigorous study.

Numeric estimation of the share of condensation in the water balance has been done only for one karst massif (Alek, Western Caucasus; Dublyansky et al., 1985). The total chemical runoff due to condensation in the warm period was calculated to be 41.2 tons (16.2 m^3) of limestone, which accounts for only 3.7% of the gross value of karst denudation. Condensation corrosion is most intensive in July (19%) and August (16%). At present, data are insufficient to estimate the speleogenetic role of winter condensation.

Many forms of cave macro-, meso-, and micromorphologies are attributable to condensation-corrosion. These are: spherical chambers 1 to 3 m in diameter in hydrothermal caves (Szunyogh, 1982; 1990); cupolas and ceiling bells (Andrieux, 1970; Mucke & Völker, 1978); solutionally widened fissures, niches, cells, vertical gutters, rills, edge patches, drop dents, indentations, etc. on cave walls (Bernaskoni, 1966; Eraso, 1969; Mais, 1973; Cigna & Forti, 1986; Davis & Mosch, 1988; Beltiukov, 1989; Jameson, 1989; 1995) (Fig. 8). Condensation corrosion often cuts through not only the bedrock, but also cave infilling (calcite, gypsum, salt, and ores) and speleothems (Hill & Forti, 1986).

Condensation may be particularly important in hydrothermal karst. During the stage of partial dewatering, when there is a free water surface in air-filled caves, thermal water may evaporate, move to the upper (cooler) parts of the cave due to convection, and condense on the cave walls (Fig. 7). The air

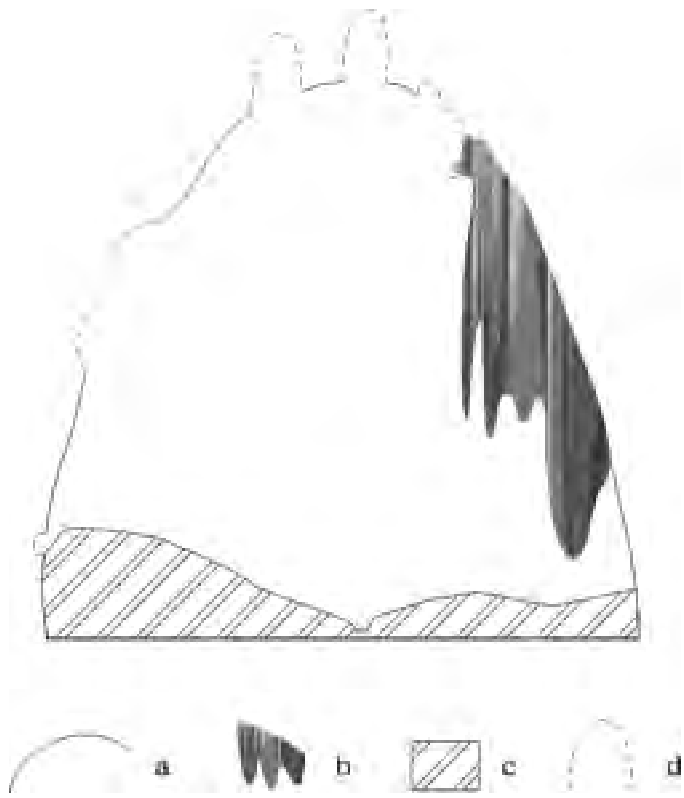

Figure 8. Destructive action of condensed waters. a - primary karst cavity; b - speleothems; c - cave sediments; d - morphologies caused by condensation corrosion (cupolas, niches, facets, grooves, pits, etc.).

mass above the surface of a thermal lake is thermodynamically unstable, because the warmer (less dense) air lies below the cooler (denser) air. Thus, air convection readily develops. Aggressiveness of the condensate is controlled by the content of CO_2 in the cave air and by the thickness and flow pattern of the films of condensate.

Another situation, particular to hydrothermal caves, is corrosion due to the presence of H_2S in the cave air. Worthington and Ford (1995) have shown that a high content of sulfate is characteristic of the thermal waters which contributes to dissolution of hypogene caves. During the stage of partial dewatering, the hydrogen sulfide in thermal waters escapes into the cave air. Some of it redissolves in films or droplets of condensate, where it is oxidized by dissolved oxygen. Produced sulfuric acid attacks limestone converting it to gypsum, forming fragile gypsum crust on the cave walls and ceiling. Such a mechanism, termed "replacement-solution", was suggested by Egemeier (1981). It is important to note that replacement-solution must be coupled with condensation (gypsum crust does not form on dry cave walls). Many caves of fossil hydrothermal karst exhibit morphological features which can best be explained by the discussed mechanism. Examples of such caves are known in Hungary (the Buda Hills), Kirghizstan (the Tyuya-Muyun), Algeria (the Bibans), and elsewhere. The process of replacement-solution is still active in caves of the Pryor mountains, Wyoming (Egemeier, 1981) and Grotta Grande del Vento, Italy (Cigna & Forti, 1986).

ACCUMULATIVE PROCESSES

Condensation coupled with evaporation and aerosol mass-transfer may play a significant role in the formation of a variety of speleothems. Hypotheses for a condensation origin of stalactites (though incorrect) were advanced by H. Jacob, E. de Clave, and J. Beumont in the seventeenth century (Shaw, 1992). Holland et al., (1964) included a group of condensation-related speleothems in their classification of cave formations. Cser and Mauha (1968) suggested an aerosol origin for one type of helictites and supported this hypothesis by means of an elegant experiment (fragments of calcite crystals were set in a plastic frame; 90 volts DC were applied to the base of the frame and the latter was exposed to the cave atmosphere; appreciable growth of crystals was observed after a several-month exposure). Many examples of speleothems supposedly related to condensation are given by Hill and Forti (1986). They suggest a condensation-related origin (along with other possible modes of formation) for a number of subaerial speleothems, such as: coatings and crusts (p. 29); coralloids (popcorn, coral, grape, or knobstone shapes; p. 33); rims (p. 54); ice frost crystals (p. 83); moonmilk (p. 116); as well as to clay vermiculations (p. 161). These speleothems are composed of calcite, gypsum, halite, carnallite, nitrates, and some other minerals. The list of specific formations of cave ice attributed to condensation is even larger (Mavliudov, 1989). More and more often, scientists resort to aerosol-condensation theory to explain the origin of some peculiar gypsum and carbonate speleothems (Calaforra & Forti, 1994; Turchinov, 1994; Klimchuk, Nasedkin, & Cunningham, 1995; Dublyansky & Pashenko, 1997).

CAVE MICROCLIMATE

The pattern of condensation in caves is controlled by cave microclimate. There exists, also, a feedback. Condensation of water is accompanied by significant yield of heat (585 kcal kg^{-1}). This affects cave microclimate; specifically it changes the fields of temperature and humidity (Andrieux, 1970; Molerio, 1981; Racovitca & Viemann, 1984). One of the prominent examples of such an impact is the short-periodic (seconds to tens of seconds) auto-oscillations of air movement, overprinting the more long-periodic “cave breathing” of barometric nature (Finnie & Curl, 1963; Dublyansky, 1977). Such auto-oscillations were reported from Krasnaya Cave in the Crimea (Dublyansky & Sotskova, 1989).

CONCLUSION

The problem of condensation in karst is a quite complex one. The data about condensation in the karstosphere are scattered in publications of karst researchers, physicists, chemists, meteorologists, hydrogeologists, mining geologists, soil scientists, geographers, glaciologists, biospeleologists, archeologists, construction engineers, etc. These specialists consider particular aspects of condensation and use research methods specific to their sciences. There is no consensus in the literature on the role of condensation in formation of karst waters, as well as on its role in formation of caves.

The problem of karst condensation can be studied with either a hydrogeologic or speleogenetic approach. Each line of approach is very different and the two approaches are seldom combined. The hydrogeological aspect of condensation deals with the role of condensation at the scale of a karst massif. Examples of typical problems are: (1) the share of condensation in water balance; (2) the role of condensation water in karst denudation; (3) the chemistry of condensed water; (4) patterns of moisture and condensate migration within karst massifs during different seasons; etc. Such a large-scale approach makes it necessary to generalize many characteristics, such as the fissuration of rock, or the coefficients of air-exchange at the scale of the karst massif, which necessarily decreases the preciseness of the results. In the framework of the hydrogeological approach, atmospheric moisture is considered to be a major source of water involved in condensation (and thus, karst) processes.

The speleogenetic approach deals with the role of condensation in the development of individual caves, the carving of smaller solutional forms, and the creation of speleothems. The smaller scale makes it necessary to perform more precise measurements of pertinent parameters (temperature of air and condensate; humidity, chemistry of condensate, etc.). These parameters can be used in laboratory- and theoretical modeling of cave-forming processes. The ultimate purpose of these studies is to explore the possible role of condensation in the creation of specific cave morphologies and speleothems, and to find the mechanism(s) involved in these processes.

When using the speleogenetic approach, one should consider more than just the moisture brought into the cave with the outside air. In caves containing water (lakes, streams, etc.), the water may evaporate from water surfaces, migrate, and then condense in different parts of the cave (Hill, 1987). Condensation of moisture from cave air and from evaporation of standing waters is also possible due to change of thermodynamic characteristics inside a cave (Dublyansky & Lomaev, 1980; Badino, 1995).

One important problem which has not been studied adequately yet is the relationship of condensation and cave aerosols. The moisture in the cave air may exist as more than just a form of vapor; it may also exist as all-water aerosol particles (hydroaerosols; Gádoros & Cser, 1986), as well as shells on solid aerosol particles (Pashenko et al., 1993; 1996). The laws of gas dynamics and aerosol mechanics are different, thus the migration of water in these two forms must have different patterns. Elevated contents of radon, typical of the cave air, foster the radiochemical reactions between hydroaerosol particles and gaseous components of the cave atmosphere. For instance, radiochemical processes may convert H_2S of the cave air (even in very small amounts) into H_2SO_4, which dissolves in water of hydroaerosols and drastically increases aggressiveness of the latter. It is becoming apparent that aerosols can play a significant role in mass transfer of moisture and speleothemic material inside caves, and can be particularly important in the formation of speleothems (Dublyansky & Pashenko, 1997).

Although awareness of the importance of these processes is growing, neither condensation nor cave aerosols have been adequately (quantitatively) studied to date. The future studies should develop a comprehensive theory of gas and aerosol mass transfer in caves, involving evaporation, convection, aerosol and gas mass transfer, and condensation. This problem is an interdisciplinary one; it warrants coupled efforts of hydrogeologists, meteorologists, physicists, and karst researchers.

ACKNOWLEDGMENTS

The paper has greatly benefited from thorough review and comments of R.A. Jameson and an anonymous reviewer of the *Journal of Cave and Karst Studies*.

REFERENCES

Andrieux, C. (1970). Evapo-condensation souterraine. *Ann. Spéléol*. 25(3): 531-559.

Badino, G. (1995). Fisica del clima sotterraneo. *Memoire dell'Istituto Italiano di Speleologia* 7, Serie 2, Bologna: 137 pp.

Beltiukov, G.V. (1989). On the formation of karst forms due to condensation. *Problemi Kompleksnogo Izuchenija Karsta Gornikh Stran*. Tbilisi-Tskhaltubo: 91-94. (In Russian)

Bernasconi, R. (1966). La condensation interne du karst profond. *Cavernes 10*(2): 41-46.

Borevskii, B.V., Khordikainen, M.A., & Yazvin, L.S. (1976). *Exploration and Assessment of Water Reserves in Fissure-Karst Reservoirs*. Moscow: Nedra: 246 pp. (In Russian)

Bruent, J. & Vidal, P. (1981). Etudes climatiques pour la conservation des Grott Ornees deux intervention. *Proceedings of the 8th International Congress of Speleology.* Bowling Green: 659-662.

Calaforra, J.M. & Forti, P. (1994). Two new types of gypsum speleothems from New Mexico: Gypsum trays and gypsum dust. *National Speleological Society Bulletin 56*: 32-37.

Cigna, A. & Forti, P. (1986). The speleogenetic role of air flow caused by convection. *International Journal of Speleology 15*: 41-52.

Cser, F. & Mauha, L. (1968). Contribution to the origin of "excentric" concretions. *Karszt és Barlangkutatás*, Budapest. *5*: 83-100.

Davis, D.G. & Mosch, C. (1988). Pebble indentations: a new speleogen from a Colorado cave. *National Speological Society Bulletin 50*(1): 17-20.

Dubljanski, V.N. & Sockova, L.M. (1977). Microclimate of karst cavities of the Mountain Crimea. *Proceedings of the 7th International Congress of Speleo*logy: 158-160.

Dublyanskaya, G.N. & Dublyansky, V.N. (1989). The role of condensation in the development of mountain karst. *Problemi Kompleksnogo Izuchenija Karsta Gornikh Stran*. Tbilisi-Tskhaltubo: 107-108. (In Russian)

Dublyansky, V.N. (1969). Methods of calculation of moisture condensation in fissure-karst reservoirs. *Bull. NTI, Series Hydrogeol. and Eng.-Geol*. n. 6, Moscow: ONTI VIEMS: 13-17. (In Russian)

Dublyansky, V.N. (1977). *Karst Caves and Shafts of the Crimea Mountains*. Leningrad: Nauka: 181 pp. (In Russian)

Dublyansky, V.N., Dorofeev, E.P., & Borodaeva, L.A. (1984). *Hydrochemistry of Kungur Ice Cave*. Simferopol. (Ukr. NIINTI, N603Uk 84): 37 pp. (In Russian)

Dublyansky, V.N. & Iliukhin, V.V. (1981). *Travels Underground*. Moscow. Physical Culture and Sport: 192 pp. (In Russian)

Dublyansky, V.N. & Kiknadze, T.Z. (1984). *Hydrogeology of Karst in Alpean Polded Zone of Southern USSR*. Moscow. Nauka: 125 pp. (In Russian)

Dublyansky, V.N., Klimenko, V.I., Vakhrushev, B.A., & Iliukhin, V.V. (1985). *Karst and Groundwaters of Mountain Massifs of the Western Caucasus*. Leningrad. Nauka: 150 pp. (In Russian)

Dublyansky, V.N. & Lomaev, A.A. (1980). *Karst Caves of the Ukraine*. Kiev. Naukova Dumka: 179 pp. (In Russian)

Dublyansky, V.N., Sotskova, L.M., & Ferbei, G.G. (1989). *Microclimate of Karst Caves in the Crimea Mountains*. Simferopol. (Ukr. NIINTI, N2495Uk 89): 132 pp. (In Russian)

Dublyansky Y.V. (1987). Theoretical modelling of the dynamics of formation of hydrothermal caves. *Metodi Izuchenija i Modelirovanija Geologicheskikh Yavlenij*. Novosibirsk: Inst. of Geology and Geophysics: 97-111. (In Russian)

Dublyansky Y.V. & Pashenko, A.E. (1997). Cave popcorn - an aerosol speleothem? *Proceedings of the 12th International Congr.ess of Speleology.* Chaux-des-Fonds. (In Press)

Egemeier, J.S. (1981). Cavern development by thermal waters. *National Speleological Society Bulletin 43*: 31-51.

Eraso, A. (1969). La corrosión climática en las cavernas. *Bol. geol. y Minero 80*(6): 564-581.

Eremenko, Y.P. & Kolpashnikov, G.A. (1974). On the methods of calculations of condensation runoff from spoils of potash mines. *Regim, Balans i Resoursi Podzemnikh Vod.* Minsk: 134-141. (In Russian)

Fedoseev, N.A. (1975). *The History of Study of the Major Problem of Hydrosphere*. Moscow. Nauka: 206 pp. (In Russian)

Finnie, J. & Curl, R. (1963). On the functioning of a familiar nonlinear thermodynamic oscillator. *Inernational. Symposium on Nonlinear Oscillation*. v. 3. Moscow: 121-123.

Firsov, L.V. (1990). Isars. *Novosibirsk*. Nauka: 470 pp. (In Russian)

Ford, D. & Williams, P. (1989). *Karst Geomorphology and Hydrology*. London. Unwin Hyman: 691 pp.

Gadoros, M. & Cser, F. (1986). Aerosols in caves - Theoretical consideration. *Proceedings of the 9th International Congress of Speleology*. Barcelona: 90-92.

Gergedava, B.A. (1970). The role of condensation and infiltration waters in cave origin. *Trudi. Vses. Geograficheskogo Obshchestva 102*(5): 196-198.

Ginet, R. (1977). Etude de la condensation atmospherique saisonneire dans la grotte de Hautcourt. *Pr. Acad. Sci.*, *18*: 1615-1618.

Glukhov, I.G. (1963). The role of condensation in water balance of mountains (on the example of the Crimea Mountains). *Izvestija VUZov*, geol. series, 3: 26-31. (In Russian)

Golod, V.M. (1981). Mathematical model of aerohydrodynamic processes in the aeration zone. *Akkumulatsija Zimnego Kholoda v Porodakh i Ego Ispolzovanije*. Perm: 6-8. (In Russian)

Golovkinskii, N.A. (1896). Observations on precipitation in soil. Attachment to the report of the hydrogeologist for 1896. Simferopol: 6 pp. (In Russian)

Gvozdetsky, N.A. (1954). *Karst*. Moscow. Geografgiz: 351 pp. (In Russian)

Gádoros, M. & Cser, F. (1986). Aerosols in caves - theoretical considerations. *Proceedings of the 9th International Congress of Speleol*ogy *2*., Barcelona: 90-92.

Hann, J. (1880). Uber eine neue Quellentheorie auf meteorologicher Basis. *Ztochr. Osterreichichen Gesellsch. fur Meteorol*. 15: 482-486.

Hill, C. (1987). Geology of Carlsbad Cavern and other caves in the Guadalupe Mountains, New Mexico and Texas. *New Mexico Bureau of Mines and Mineral Resources Bulletin 117*:151 pp.

Hill, C. & Forti, P. (1986**).** *Cave Minerals of the World*. Hunstville, Alabama: 238 pp.

Holland, H.D, Kirsipu, T.W., Huebner, I.I., & Oxburgh, U.M. (1964). On some aspects of the chemical evolution of cave waters. *Journal of Geol*ogy *72*: 36-67.

Homza, S., Rajman, L., & Roda, S. (1970). Vznik a vyvoj krasoveho fenomenu Ochtinskej aragonitovej jaskine. *Slovensky Kras. 8*: 21-68 (In Slovak)

Jameson, R.A. (1989). Features of condensation corrosion in caves of the Greenbrier karst, West Virginia. *Abstracts of the NSS Convention.*

Jameson, R.A. (1995). Condensation, condensation corrosion, and associated features in Snedegars and Greenville Saltpeter Caves: Underground the Appalachians. *A Guidebook for the 1995 Convention of the NSS*, Blacksburg, Virginia: 122-125.

Jameson, R.A. & Alexander, C.E. Jr. (1989). Hydrology and chemistry of condensation waters in Snedegar's and Greenville Saltpeter Caves, West Virginia. *Abstracts of the NSS Convention.*

Jenko, F. (1959). *Hidrogeologija i Vodno Gospodarstvo Krasa. Ljubljana*: 236 pp.

Khromov, S.P. & Mamontova, L.I. (1963). *Meteorological dictionary*. Leningra. Gidrometeoizdat: 250 pp. (In Russian)

Kinzikeev, A.R. (1993). Geodynamics and karst process. *Ingenernaja Geologija Karsta.* t. 2. Perm: 16-20. (In Russian)

Klimchouk, A., Nasedkin, V., & Cunningham, K. (1995). Speleothems of aerosol origin. *National Speleological Society Bulletin 57*: 31-42.

Klimochkin, V.V. (1973). The necessity of consideration of condensation processes when determining the balance of groundwaters. *Vlagooborot v Prirode i Ego Rol v Formirovanii Resursov Podzemnikh Vod*. Moscow. Stroiizdat: 288-290. (In Russian)

Korotkevich, G.V. (1970,). *Salt Karst*. Leningrad. Nedra: 256 pp. (In Russian)

Kuldzhaev, N.K. (1989). On the theory of a condensation origin for ground waters by A.F.Lebedev. *Izv. of Academy of Sci. of Tadzhik. SSR,* series Phys-Techn., Chem., and Geol. 1: 103-106. (In Russian)

Lebedev, A.F. (1936). *Soil and Groundwaters*. Moscow-Leningrad: 312 pp. (In Russian)

Lukin, V.S. (1969). Quantitative expression of evaporation and condensation of water in gypsum-anhydrite massifs of the Ufa plateau. *Zemlevedenije*, new series, *8*(48): 213-218. (In Russian)

Mais, K. (1973). Vorläufige Beobachtungen über Kondenswasserkorrosion in Schlenkendurhgangshöle. *Proceedings of the 6th International Congress of Speleology* 3. Praha: 203-207.

Mais, K. & Pavuza, R. (1994). Preliminary climatologic observations in Alpine caves of Austria. *Comptes Rendus du Colloque International de karstologie a Luxembourg*. Luxembourg, August 1992: 165-171.

Maksimovich, G.A. (1963). *Fundamentals of Karst Studies*. T. 1. Perm: Perm University: 444 pp. (In Russian)

Malkov, V.N. & Frantz, N.A. (1981). On winter condensation. *Akkumulatsija Zimnego Kholoda v Porodakh i Ego Ispolzovanije*. Perm: 97-99. (In Russian)

Martel, E.A. (1894). *Les Abimes*. Paris: 578 pp.

Mavliudov, B. (1989). Snow and ice formations in caves and their regime. *Proceedings of the 10th International Congress of Speleology 1*. Budapest: 295-297.

Molerio, L. (1981). Hidrogeologia y climatologia de la cueva La Mariana. *Volun. Hidraul*., 18, 57: 2-9.

Moore, G.W. & Sullivan, G.N. (1978). *Speleology*. Teaneck: Zephyrus Press: 150 pp.

Morozov, A.T. (1938). On the methods of study of moving vapor moisture in soil-ground. *Transactions of the Institute of Hydrology and Melioration,* t. *22*: 18-26. (In Russian)

Mucke, D. & Völker, R. (1978). Kondenswasserkorrosion. *Jahrb. des Höhlenforschers,* ss: 7-16.

Mucke, D., Völker, R., & Wadewitz, S. (1983). Cupola formation occasionally inundated cave roofs. *European. Conference on Speleology 2*. Sofia: 129-132.

Müller, P. (1974). A melegforrás-barlangok és gömbfülkék lebetheziséröl. *Karszt és Barlang*, *Budapest 1*: 7-11. (In Hungarian)

Nemeriuk, G.E. & Paltsev, V.P. (1969). On the methods of study of the ionic composition of vapor condensed from the air. *Proceedings of the 23th Hydrochem. Symposium.* Novocherkassk: 101-102. (In Russian)

Obolensky, V.N. (1944). *Course of meteorology*. Moscow-Sverdlovsk: 120 pp. (In Russian)

Pashchenko, S.E., Dublyansky, Y.V., & Andreichuk, V.N. (1993). Aerosol studies in Kungur Ice Cave. *Proceedings of the 11th International Congress of Speleology.* Beijing: 190-192.

Pashenko, S.E, Dublyansky, Y.V, Anderichuk, V.N., & Pashenko, E.F. (1996). Transformation of fractal atmospheric aerosol moving through natural cave. *J.Aerosol Sci.,* v. 27, Suppl. 1: S127-S128.

Pasquini, G. (1973). Aggressive condensation. *Proceedings of the 6th International Congress of Speleology 8*: 315-318.

Pinneker, E.V. (editor) (1980). Fundamentals of hydrogeology. *General hydrogeology*. Novosibirsk: Nauka: 230 pp. (In Russian)

Prokofiev, S.S. (1964). The role of condensation moisture in creation of karst caves. *Peshcheri,* Perm. *4*(5): 35-38. (In Russian)

Protasov, V.A. (1959). Condensation waters of Crimea Mountains and their role in underground runoff. *Proceedings of the 3rd Hydrol. Congress*, t. 9. Leningrad: 98-103. (In Russian).

Queen, J.M. (1981). *A Discussion and Field guide to the Geology of Carlsbad Caverns*. Unpublished report to Carlsbad Caverns National Park: 64 pp.

Racovitca, G. & Viemann, J. (1984). Sur le róle de la condensation souterraine dans la genèse des stalagmites de glace. *Trav. Inst. spéol. E.Racovitza 23*: 89-97.

Riazanova, E.A. (1987). Classification of factors and sources of groundwater level rise. *Voprosi Ingenerno-Geologicheskikh Issle Dovanii na Zastraivajemikh Territorijakh.* Moscow. Stroiizdat: 54-59. (In Russian)

Shaw, T.R. (1992). *History of Cave Science. The Exploration and Study of Limestone Caves to 1900*. Sydney: Sydney Speleological Society: 338 pp.

Shestakov, F.V. (1989). *Condensation of Water Vapor in Soil-Ground and in the Near-Surface Layer: Bibliography from 1877 till 1987*. Alma-Ata: Nauka: 77 pp. (In Russian)

Slavianov, V.N. (1955). About natural condensors of mountain slopes and about possibility of their usage for small-scale water supply. *Voprosi Izuchenija Podzemnikh Vod i Ingenerno-Geologicheskikh Processov*. Moscow: AN SSSR: 21-32. (In Russian)

Szunyogh, G. (1982). Theoretical problems of dissolution related to spherical niches formation. *Karszt és Barlang, Budapest, 2*: 83-88. (In Hungarian)

Szunyogh, G. (1990). Theoretical investigation of the development of spheroidal niches of thermal water origin - second approximation. *Proceedings of the 10th International Congress of Speleol*ogy. Budapest: 766-768.

Tkachenko, K.D. (1978). Importance of condensation moisture and dew in water balance of the aeration zone. *Geology Journal 38*(3): 27-34. (In Russian)

Trombe, F. (1952). *Traitè de Spéléologie*. Paris: 385 pp.

Tsikarishvili, K.D. (1981). Climatic particularities of karst caves in Georgia. *Proceedings of the European Conference on Speleology*. Sofia, t. 2: 386-390. (In Russian)

Tugarinov, V.V. (1955). Some results of study of water vapor condensation from the air. *Voprosi Izuchenija Podzemnikh Vod i Ingenerno-Geologicheskikh Processov*. Moscow: AN SSSR: 60-78. (In Russian)

Turchinov, I.I. (1994). Aerosol mineral formation in gypsum caves of Western Ukraine. *Voprosi Fizicheskoi Speleologii.* Moscow: MFTI: 51-63. (In Russian)

Ustinova, T.I. (1956). Conditions of condensation of atmospheric moisture in caves of western part of the Crimea Mountains. *Soveshchanije po Izucheniju Karsta*. v. 8. Moscow: 3-4. (In Russian)

Vakhrushev, B.A. (1993). Usage of condensation groundwater in Antique and Medieval times and in present time. *Dvizhenije v Noosphere: Theoreticheskie i Regionalnie Problemi*. Simferopol: 92-96. (In Russian)

Vasilievski, P.M. & Zheltov P.I. (1932). Hydrogeologic studies of the Chatirdag mountain in 1927. *Trudy Vserossiyskogo Geologo-razvedochnogo Ob'edinenija 142*: 1-99. (In Russian)

Vedernikov, V.V. & Larina, L.A. (1985). Calculation of water regime within constructional territories. *Raschet Vodnogo Rezhima Zastroennikh Territoriy*. Moscow: Stroiizdat: 52-56. (In Russian)

Volger, O. (1877). Uber eine neue Quellentheorie auf meteorologicher Basis. *Meteorol. Ztsechz.*

Worthington, S.R.H. & Ford, D.C. (1995). High sulfate concentrations in limestone springs: An important factor in conduit initiation? *Environmental Geology 25*(1): 9-15.

Zibold, F. (1904). The role of underground dew in water supply for Feodosia. *Pochvovedenije 4*: 21-29. (In Russian)

A SUMMARY OF DIVERSITY AND DISTRIBUTION OF THE OBLIGATE CAVE-INHABITING FAUNAS OF THE UNITED STATES AND CANADA

STEWART B. PECK
Department of Biology, Carleton University, Ottawa, Ontario, K1S 5B6, CANADA

A summary is given of families, genera, species numbers, and state distributions of the obligate subterranean (cave and groundwater) faunas of the contiguous United States and Canada. A total of 425 aquatic and 928 terrestrial species (1353 species in all) is now known. Total genus level diversity is greatest (in descending order) in the states of Texas, Alabama, Kentucky, Tennessee and Virginia. This genus and species richness is vulnerable to a variety of land use and pollution problems.

Nicholas (1960) provided the last complete list of the obligate subterranean fauna (troglobites and stygobites) of the United States. A total of 334 species and subspecies were then known. Since then, there has been much additional field work and taxonomic study on the U.S. cave fauna. Many taxonomic papers and state lists have been published, but they are too numerous to list here. No nationwide species-level list has been compiled since that of Nicholas. As a step towards this goal, I have compiled a summary list. This gives the taxonomic classification of obligate subterranean faunas to the genus level, and a numerical total of such species known in the genus, and the states or provinces in which they are known to occur. I believe this summary list to be a useful indicator of richness of subterranean faunas and their general areas of distribution. Reviews about the origin and ecology of this fauna are in Barr (1967, 1968), Barr, Culver and Kane (1995), Barr and Holsinger (1985), Culver (1982), Holsinger (1988) and Howarth (1983). In this paper I do not attempt to analyze the causes of the different state diversities.

METHODS

I started with the incomplete list in Barr et al. (1995) and worked to improve it. I then asked various taxonomic specialists to correct my preliminary summary lists. An attempt was made to exclude obvious troglophiles (species which may be known only from caves, but which show no morphological specializations for cave life). Troglobites (in terrestrial habitats) and stygobites (in aquatic habitats) are ecologically restricted to caves and subterranean groundwaters, and have usually had a long history of evolutionary specialization to these underground habitats. These animals usually have visibly distinctive cave-related body features (troglomorphies) and less evident physiological or behavioral specializations which restrict them to living only in pre-existing subterranean spaces and caves. These troglobites and stygobites are ecologically and evolutionarily the most interesting animals in caves and groundwaters. The faunas are here separated as terrestrial or aquatic in habitat because these two environments have entirely different faunas and environmental characteristics.

RESULTS

DIVERSITY

The list (Table 1) shows the genus and species level diversity and geographic occurrence by state and province of known troglobites and stygobites in the United States and Canada. This shows the extraordinary diversity of higher taxonomic categories, the species diversity, and geographic diversity of the USA cave fauna. Only one mite, one isopod, and two amphipods are cave-restricted in Canada. Note that the known total is now 425 aquatic species and 928 terrestrial species. Thus, at least 1353 animal species in the contiguous USA and Canada are restricted to cave and groundwater habitats, especially in the southeastern USA, Texas, and California.

DISTRIBUTION

In North America, cave-evolved species are mostly found to the south of the southern limits of the Pleistocene glacial ice sheet. But a few species were apparently able to survive subglacial conditions in the northern US and some parts of Canada. These are groundwater isopods and amphipods which now live in previously glaciated areas of New York, Vermont, Wisconsin, Alberta and British Columbia.

At the genus level, most USA cave fauna diversity occurs in the large limestone karst areas of Texas, the southeastern USA (Appalachian Mountains, Cumberland Plateau, Central Basin of Tennessee, the Bluegrass and Mammoth Cave regions of Kentucky), and the Sierra Nevada Mountain foothills of California. The states with the greatest total generic diversity are Texas, Alabama, Kentucky, Tennessee and Virginia (Fig. 1). The states with greatest troglobite (terrestrial) diversity are Alabama, Texas, Tennessee, Kentucky, California and Virginia (Fig. 2). The states with greatest stygobite (aquatic) diversity are Texas, Missouri, Kentucky, Virginia, Alabama, and West Virginia (Fig. 3). Northern and Central Florida, the Ozarks, southern Illinois, southern Indiana and other areas are secondary regions of medium level total diversity. Other smaller

Figures 1-3.

Frequency histograms by state of minimum number of genera with obligate subterranean species.

1. Combined (total) generic diversity by state.

2. Troglobite (terrestrial) generic diversity by state.

3. Stygobite (aquatic) generic diversity by state; the amphipod genus *Stygobromus* occurs in 36 states (not all shown here).

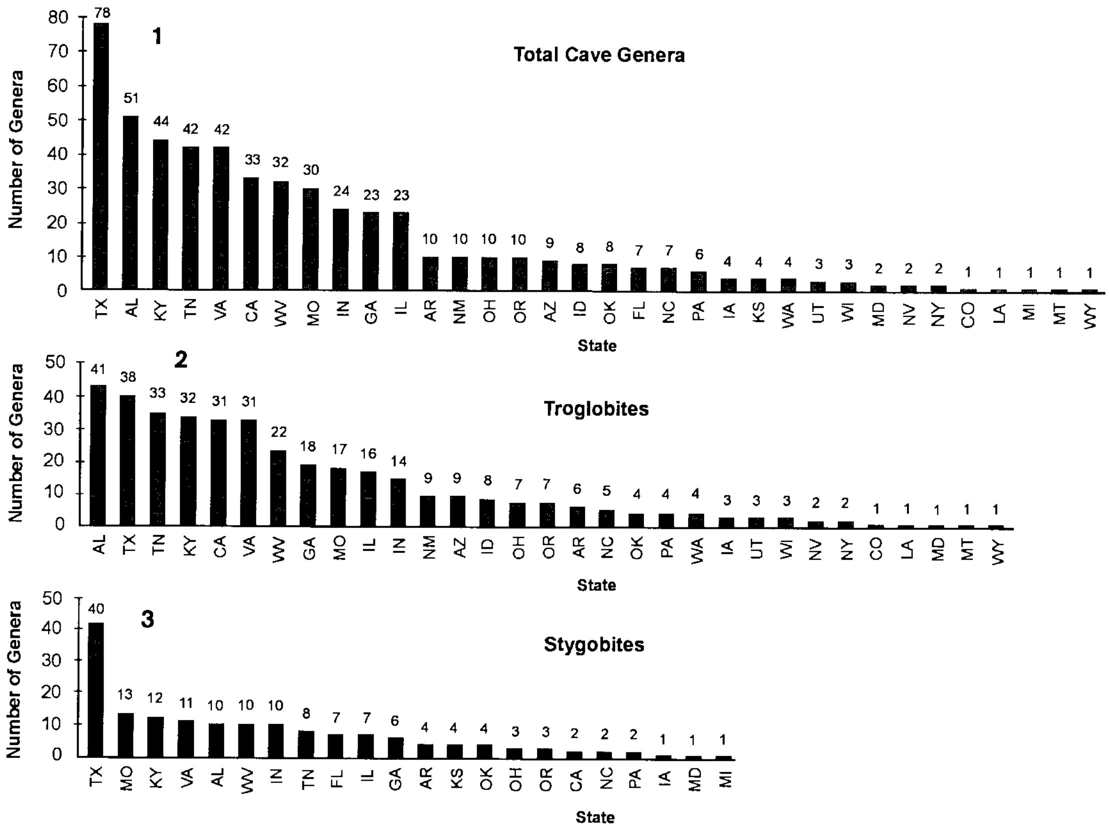

limestone regions in the east and west also have a cave fauna but it is more limited. Volcanic landscapes of the western US (and Hawaii - data not included here) have troglobites in lava tube caves and the extensive system of cracks and crevices which exist in volcanic basalt rocks.

PROSPECT

This summary list cannot yet be considered as complete. Although the faunal exploration of United States caves may now possibly be considered to be at a mature level, some new species will still be found. Some groups are known to have many still undescribed species, such as *Pseudanophthalmus* carabid beetles and *Pseudotremia* millipeds. And, compared to Europe, some subterranean habitats have been poorly sampled. The superficial subterranean environment ("MSS"), which has a rich fauna in Europe (Juberthie et al. 1980) has not been explored in North America. The hyporheic environment (groundwater beyond caves) is virtually unexplored in North America (Camacho 1992, Juberthie 1983). The list is also based on the traditional morphological definition of a species. There may be more "sibling-species" complexes that can be detected with modern molecular techniques (Laing et al. 1976).

Although there are certainly more species yet to be discovered, it seems unlikely to me that there are as many as the 6000 USA troglobite-stygobite species predicted by Culver and Holsinger (1992). Nevertheless, the presently known diversity of at least 1353 species shows the remarkable tendency for a great many groups of very different animals to move into all the many bio-spaces of groundwater and caves; habitats which seem so hostile to us. All of these species are vulnerable to many human land-use activities, and especially to karst groundwater pollution. There is certainly a need to work towards the protection and conservation of this special part of the world's biodiversity. I hope this list will help to alert officials to the richness of subterranean faunas in various states.

ACKNOWLEDGEMENTS

I thank the organizers of the Karst Waters Institute Conference on Conservation and Protection of the Biota of Karst (13-16 February 1997, Nashville, TN) for the invitation which led to the construction of this faunal summary. Field research has been supported in part by grants from the Natural Sciences and Engineering Research Council of Canada. Generous help with checking Table 1 and in providing additional data came from T.C. Barr, Jr. (carabid and pselaphid beetles), D. Chandler (pselaphid beetles), K. Christiansen (collembola), J. Cokendolpher (spiders and harvestmen), D. Culver (general groups), L. Ferguson (Diplura), J. Holsinger (amphipods and general faunas), J. Lewis (planaria and various aquatics), W.B. Muchmore (pseudoscorpions), W.A. Shear (millipeds), and J. Reddell (Texas faunas). I hope I have correctly summarised their information. Steve Goodacre, DeLancy Bishop, Jennifer Read, and Robert S. Anderson helped with data analysis and graphics.

Table 1. Summary of known (minimal) species diversity and state distributions of animals which are adapted for (and limited to) cavernous subterranean habitats in the contiguous United States and Canada. Both limestone karst and basaltic volcanic terrane faunas are combined here.

Higher Groups, families	Genera	Number of Species	States
I. AQUATIC HABITATS - Stygobionts			
PLATYHELMINTHES (flatworms)			
Lecithoepitheliata			
Prorhynchidae	*Geocentrophora cavernicola*	1	KY, VA
Tricladida			
Dendrocoelidae	*Dendrocoelopsis americana*	1	TX
Kenkiidae	*Kenkia* (= *Macrocotyla*)	4	MO, OR, WV
	Sphalloplana	14	AL, CA, GA, IN, KS, KY, MO, TN, TX, VA, WV
Planariidae	*Paraplanaria occulta*	1	VA
	Phagocata	6	IL, NC, PA, TN, WV
ANNELIDA			
Oligochaeta			
Haplotaxidae	*Haplotaxis brinkhursti*	1	WV
Lumbriculidae	*Spelaedrilus multiporus*	1	VA
	Stylodrilus beattiei	1	VA, WV
	Trichodrilus	2	TN, WV
MOLLUSCA			
Gastropoda			
Hydrobiidae (snails)			
Amnicolinae	*Amnicola*	4	AR, KY, MO
Emmericiinae	*Fontigens*	7	IL, MO, VA, WV
Lithoglypinae	*Balconorbis uvaldensis*	1	TX
	Holsingeria	2	VA
	Phreatoceras taylori	1	TX
	Phreatodrobia	9	TX
Littoridininae	*Antrobia culveri*	1	MO
	Antroselates spiralis	1	IN, KY
	Stygopyrus bartronensis	1	TX
Hirudinea			
Eropodbellidae	*Mooreobdella* n.sp.	1	TX
ARTHROPODA			
CRUSTACEA			
Eucopepoda			
Canthocamptidae	*Bryocamptus morrisoni*	1	IN, KY
Cyclopidae	*Cyclops* (?)	4	TX
	Diacyclops	2	IL, IN, TN
	Megacyclops	1	IN
Podocopa			
Entocytheridae	*Hobbsiella*	1	TX
	Sagittocythere	2	AL, IN, KY, TN
	Sphaeromicola moria	1	TX
	Uncinocythere	2	GA, MO

Candoniidae	*Candona* n.sp.	1	TX
	Prionocypris n.sp.	1	TX
Cyrididae	*Pseudocandona*	2	IN
Bathynellacea			
Parabathynellidae	*Iberobathynella bowmani*	1	TX
Thermosbaenacea			
Thermosbaenidae	*Monodella texana*	1	TX
Decapoda			
Astacidae (crayfish)	*Cambarus*	8	AL, AR, FL, GA, MO, OK, TN, WV
	Orconectes	4	AL, IN, KY, TN
	Procambarus	10	FL
	Troglocambarus maclanei	1	FL
Atyidae (shrimps)	*Palaemonias*	2	AL, KY
Palaemonidae (shrimps)	*Calathaemon holthuisi*	1	TX
	Palaeomonetes	2	FL, TX
Isopoda (isopods)			
Asellidae	*Caecidotea*	56+	AL, AR, FL, GA, IL, IN, KS, KY, MD, MO, OH, OK NC, PA, TN, VA, WV
	Calasellus	2	CA
	Lirceolus	5	TX
	Lirceus	2	VA
	Remasellus parvus	1	FL
	Salmasellus steganothrix	1	AB
Cirolanidae	*Antrolana lira*	1	VA
	Cirolanides texensis	1	TX
	Speocirolana hardeni	1	TX
Stenasellidae	*Mexistenasellus coahuila*	1	TX
Amphipoda (amphipods)			
Allocrangonyctidae	*Allocrangonyx*	2	MO, OK
Artesiidae	*Artesia*	2	TX
Bogidiellidae	*Parabogidiella*	2	TX
Crangonyctidae	*Bactrurus*	9	AL, AR, IA, IL, IN, KS, MI, MO, OH, OK, TN, VA
	Crangonyx	14	AL, FL, GA, IL, IN, KS, KY, MD, MO, OH, PA, TN, VA
	Stygobromus	180	in 36 states (not FL), AB, BC
	Stygonyx courtneyi	1	OR
Gammaridae	*Gammarus*	2	IL, VA, WV
Hadziidae	*Allotexiweckelia hirsuta*	1	TX
	Holsingerius	2	TX
	Mexiweckellia hardeni	1	TX
	Paramexiweckelia ruffoi	1	TX
	Texiweckelia texensis	1	TX
	Texiweckeliopsis insolita	1	TX
Sebidae	*Seborgia*	2	TX
INSECTA (insects)			
Coleoptera (beetles)			
Dytiscidae (water beetles)	*Haideporus texensis*	1	TX
	Stygoporus oregonensis	1	OR
Dryopidae (long-toed beetles)	*Stygoparnus comalensis*	1	TX
VERTEBRATA			
Pisces (fishes)			
Amblyopsidae	*Amblyopsis rosae*	1	MO

	Amblyopsis spelaea	1	KY
	Typhlichthys subterraneus	1	AL, KY, TN
	Speoplatyrhinus poulsoni	1	AL
Ictaluridae	*Satan eurystomus*	1	TX
	Trogloglanis pattersoni	1	TX
Amphibia (salamanders)			
Plethodontidae	*Eurycea latitans*	1	TX
	Eurycea neotenes	1	TX
	Eurycea tridentifera	1	TX
	Eurycea troglodyes	1	TX
	Eurycea n.sp.	2	TX
	Gyrinophilus subterraneus	1	WV
	Gyrinophilus palleucus	1	AL, TN
	Haideotriton wallacei	1	FL, GA
	Typhlomolge rathbuni	1	TX
	Typhlomolge robusta	1	TX
	Typhlotriton spelaeus	1	MO
	TOTAL AQUATIC SPECIES	**425**	

II. TERRESTRIAL HABITATS - Troglobites			
MOLLUSCA			
Gastropoda (land snails)			
Ellobiidae	*Carychium stygium*	1	KY, TN
Endodontidae	*Helicodiscus barri*	1	AL, GA, TN
Zonitidae	*Glyphyalina*	2	AL, KY, TN, WV
	Ogaridiscus	?	?
	Spelaeodiscoides spirellum	1	CA
CRUSTACEA			
Isopoda, Oniscoidea (terrestrial isopods)			
Trichoniscidae	*Amerigoniscus*	8	GA, OK, TN, TX, VA
	Brackenridgia	3	TX
	Miktoniscus	2	AL, KY, OH, VA
ARACHNIDA			
Schizomida			
Protoschizomidae	gen & sp	1	TX
Araneae (spiders)			
Cybaeidae	*Cybaeus* n.sp.	1	CA
	Cybaeozyga n.spp.	3	CA
Dictynidae	*Blabomma* n.sp.	6	CA
	Cicurina	58	AL, GA, TX
Leptonetidae	*Appaleptoneta*	5	AL, GA
	Callileptoneta n.sp.	1	CA
	Neoleptoneta	15	AL, TX
Linyphiidae	*Anthrobia monmouthia*	1	KY, TN, VA, WV
	Bathyphantes weyeri	1	VA
	Erigone sp.	1	TX
	Islandiana	3	KY, VA, TX, WV
	Oreonetides n.sp	1	VA
	Phanetta subterranea	1	AL, KY, TN, VA, WV, etc.
	Porhomma cavernicolum	1	AL, AR, KY ,IL, TN, VA, WV, etc.
	Smilax n.sp	1	IA, WI
Nesticidae	*Eidmannella*	6	TX
	Nesticus	9	AL, CA, GA, NC, TN, VA
Telemidae	*Usofila* n.spp.	6	CA

Tetragnathidae	*Meta dolloffi*	1	CA
Theridiidae	*Thymoites*	3	AZ, NM
Pseudoscorpiones (pseudoscorpions)			
Superfamily Chthonioidea			
Chthoniidae	*Aphrastochthonius*	7	AL, CA, NM, TX
	Apochthonius	24	AL, AR, CA, GA, IL, IN, MO, NM, OH, OR, VA, WV
	Chthonius	2	AL, IL, IN, KY ,OH, TN, VA
	Kleptochthonius	40	AL, IN, KY, TN, VA, WV
	Mexichthonius n.sp.	1	TX
	Mundochthonius	2	IL, MO, VA
	Neochthonius	2	CA
	Tyrannochthonius	35	AL, KY, TN, TX
Superfamily Feaelloidea			
Pseudogarypidae	*Pseudogarypus*	3	AZ, CA
Superfamily Garypoidea			
Garypidae	*Archeolarca*	4	AZ, CA, TX
	Larca laceyi	1	CA
Superfamily Neobisioidea			
Bochicidae	*Leucohya texana*	1	TX
Ideoroncidae	*Albiorix* n.sp.	1	AZ
Neobisiidae	*Alabamacreagris*	2	AL
	Americocreagris colombiana	1	OR
	Australinocreagris grahami	1	CA
	Fissilicreagris imperialis	1	CA
	Lissocreagris	4	AL, GA, VA
	Minicreagris pumila	1	AL, GA, TN
	Parobisium charlottea	1	OR
	Setigerocreagris phyllisae	1	CA
	Tatarocreagris	10	TX
Syarinidae	*Chitrella*	7	TN, TX, VA, WV
	Chitrellina n.sp.	1	AZ
Superfamily Cheiridioidea			
Cheiridiidae	*Cheiridium* reyesi	1	TX
Superfamily Cheliferoidea			
Chernetidae	*Dinocheirus cavicolus*	1	TX
	Hesperochernes	3	AL, AR, GA, IN, KY, MO, OH, OK, TN, VA
	Neoallochernes stercoreus	1	TX
	Tuberochernes	2	CA, AZ
Acari (mites)			
Rhagidiidae	*Elliotta howarthi*	1	ID, WA
	Robustocheles occulata	1	AB, IA, WA
	Flabellorhagidia pecki	1	ID
	Foveacheles	2	CA
	Rhagidia varia	1	VA
Opiliones (harvestmen)			
Ceratolasmatidae	*Hesperonemastoma*	3	AL, ID, KY, UT
Cladonychiidae	*Speleomaster*	2	ID
Phalangodidae	*Banksula*	10	CA
	Bishopella jonesi	1	AL
	Calicinia cloughensis	1	CA
	Crosbyella	2	AR
	Hoplobunus	2	TX
	Phalangodes	2	AL, KY, TN

	Phalangomma virginicum	1	VA
	Texella	14	CA, NM, TX
Travuniidae	*Speleonychia sengeri*	1	WA
	Erebomaster flavescens	1	IN
Triaenonychidae	*Cryptobunus*	2	MT, NV, UT
ATELOCERATA (= "TRACHEATA")			
DIPLOPODA (millipeds)			
Callipodida			
Abacionidae	*Tetracion*	2	AL, TN
Dorypetalidae	*Colactis*	1	CA
Spirostreptida			
Cambalidae	*Cambala*	3	AL, FL, GA, KY, TN, TX, VA,WV
Chordeumatida			
Caseyidae	*Speoseya grahami*	1	CA
	Opiona siliquae	1	CA
Cleidogonidae	*Pseudotremia*	30	AL, GA, IN, KY, TN, VA, WV
Conotylidae	*Achimenides pectinata*	1	IL, WI
	Austrotyla specus	1	MO
	Conotyla	2	IN, MD, NY, PA
	Idagona westcotti	1	ID
	Lophomus	2	WA
	Macromastus	2	ID, OR
	Plumatyla humerosa	1	CA, OR
Striariidae	*Striaria*	2	CA, VA
	Speostriaria shastae	1	CA
Tingupidae	*Tingupa pallida*	1	IL, MO
Trichopetalidae	*Scoterpes*	30	AL, GA, IL, KY, MO, TN
	Trichopetalum	4	?KY, VA, WV
Polydesmida			
Fuhrmannodesmidae	*Speodesmus*	10	CO, NM, TX
	Tidesmus hubbsi	1	NV
Macrosternodesmidae	*Chaetaspis*	3	KY, TN
Nearctodesmidae	*Ergodesmus remingtoni*	1	IL
Polydesmidae	*Brachydesmus pallidus*	1	VA, WV
Xystodesmidae	gen.sp.	1	TX
Julida			
Zosteractinidae	*Ameractis*	2	AL, NC, TN
	Zosteractis interminata	1	IL, MO, NC?
CHILOPODA			
Scolopendromorpha			
Cryptopidae	*Theatops*	3+	TX
Geophilomorpha			
Himantariidae?	gen.sp.	3	TX
Lithobiomorpha			
Lithobiidae	gen. sp.	2	TX
HEXAPODA; PARAINSECTA			
Collembola (springtails)			
Sminthuridae	*Arrhopalites*	14	AR, KY, IL, IN, MO, OK, TX, VA, WI
Entomobryidae	*Entomobrya*	12	
	Pseudosinella	22	AL, GA, IN, KY, MO, NC, NM, OH, OK, TN, TX, VA, WV

	Sinella	8	CA, IN, KY, MO, OH, TN, VA, WV
Hypogastruridae	*Schaefferia*	5	AL, TX, VA
Oncopoduridae	*Oncopodura*	3	CA, MT, NM, OR, TX, VA, WY
Onychiuridae	*Onychiurus*	3	AL, IA, IL, IN, KY ,MD, MO, NC, OH, OR, PA, TX, VA, WA, WI, WV
Tomoceridae	*Tomocerus*	4	AL, CA, IL, KY, LA, MD, MO, NM, TN, VA, WV
INSECTA			
Diplura (bristletails)			
Campodeidae	*Allocampa*? n.sp.	1	TX
	Eumesocampa	2	IL, MO, WV
	Haplocampa	11	AZ, CA, ID, IL, MO, OR, UT, WA
	Litocampa	23	AL, AR, GA, IN, KY, MO, NC, NM, TN, VA, WV
	Genus A	1	NM, TX
	Genus B	1	TN
	Genus C	1	NV
Japygidae	*Mixojapyx reddelli*	1	TX
Thysanura (silverfish)			
Nicoletiidae	*Texoredellia texensis*	1	TX
Coleoptera (beetles)			
Carabidae	*Ameroduvalius*	5	KY
(ground beetles)	*Darlingtonea kentuckensis*	1	KY, TN
	Horologion speokoites	1	WV
	Neaphaenops	4	KY
	Nelsonites	5	KY, TN
	Pseudanophthalmus	250+	AL, GA, IL, IN, KY, MD, OH, PA, TN, VA, WV
	Rhadine	11	TX
	Xenotrechus	2	MO
Leiodidae	*Ptomaphagus*	19	AL, AZ, GA, KY, TN
(scavenger beetles)	*Glacicavicola bathyscioides*	1	ID, WY
Pselaphidae	*Arianops*	6	AL, TN, VA
(pselaphid beetles)	*Batriasymmodes*	4	AL, KY, TN, WV
	Batrisodes	19	AL, IN, KY, OH, TN, TX
	Tychobythinus (=*Bythinopsis)*	3	AL, KY, TN
	Speleochus (=Macherites)	12	AL, TN, GA
	Spelobama vana	1	AL
	Subterrochus	3	AL
	Texamaurops reddelli	1	TX
Diptera (flies)			
Sphaeroceridae (small dung flies)	*Spelobia tenebrarum*	1	AL, AR, GA, IL, IN, KY MO, NY, PA, TN, VA, WV

REFERENCES

Barr, T.C. (1967). Observations on the ecology of caves. *American Naturalist 101*: 475-492.

Barr, T.C. (1968). Cave ecology and the evolution of troglobites. *Evolutionary Biology 2*: 35-102.

Barr, T.C., Culver, D., & Kane. T. (1995). Biospeleology in the United States. In: Encyclopedia Biospeologica, C. Juberthie & V. Decu (eds.), *Société de Biospéologie, Moulis, France I*: 403-416.

Barr, T.C. & Holsinger, J.R. (1985). Speciation in cave faunas. *Annual Review of Ecology and Systematics 16*: 313-337.

Camacho, A.I. (1992). A classification of the aquatic and terrestrial subterranean environments and their associated fauna. In A.I. Camacho (ed.), *The Natural History of Biospeleology*. Museo Nacional de Ciencias Naturales, Madrid, Spain: 57-103.

Culver, D.C. (1982). *Cave life: Evolution and Ecology*. Harvard University Press, Cambridge, MA, USA.

Culver, D.C. & Holsinger, J.R. (1992). How many species of troglobites are there? *National Speleological Society Bulletin 54*: 79-86.

Holsinger, J.R. (1988). Troglobites: the evolution of cave-dwelling organisms. *American Scientist 76*: 146-153.

Howarth, F.G. (1983). Ecology of cave arthropods. *Annual Review of Entomology 28*: 365-389.

Juberthie, C. (1993). Le milieu souterrain: étendu et compositon. *Mémoires de Biospéologie 10*: 17-65.

Juberthie, C., Delay, B., & Bouillon, M. (1980). Extension du milieu souterrain en zone non-volcanic: description d'un nouveau milieu et son pueplement par les Coléoptères troglobies. *Mémoires de Biospeologie 7*: 19-52.

Laing, C.D., Carmody, G.R., & Peck, S.B. (1976). How common are sibling species in cave-inhabiting invertebrates? *American Naturalist 110*: 184-189.

Sullivan, G.N. (1960). Checklist of macroscopic troglobitic organisms of the United States. *American Midland Naturalist 64*: 123-160.

AIR TEMPERATURE AND RELATIVE HUMIDITY STUDY: TORGAC CAVE, NEW MEXICO

JEFFREY FORBES
Daniel B. Stephens & Associates, 6020 Academy NE, Albuquerque, NM 87109 USA

Torgac Cave, located in south-central New Mexico is remarkable for at least three reasons: its extraordinary gypsum speleothems, its large bat population, and the unusually cold temperatures within the cave. It has been proposed that the presence of the bats and the speleothems may be related to the anomalous temperatures observed in the cave. This paper reports the results of a five week study of cave air temperature and relative humidity conducted during January-February 1995.

Several different techniques were employed to measure the temperature and relative humidity (RH) of the cave atmosphere. A sling psychrometer was used to make spot measurements of temperature and RH at 11 locations throughout the cave on two successive dates. In addition, hourly measurements of air temperature and RH at a single location were recorded over a five week period using a capacitance probe and data logger.

A novel technique for inferring RH was also attempted in which kaolinite clay samples were placed at different locations throughout the cave, and at different elevations above the cave floor at a single location, and allowed to equilibrate with the cave air. Subsequent laboratory analysis of the water activity and gravimetric water content of the clay samples following equilibration allowed the time-averaged RH to be inferred, and these data were used to reconstruct the vertical RH profile of the cave atmosphere.

Cave air temperatures measured with the sling psychrometer ranged from 5.4 to 11.1ºC, while RH values ranged between 47% and 89%. The driest conditions were encountered close to the entrance, where cold, dense winter air sinks into the main entrance, drying the cave passages below as it warms. The data logger and capacitance probe recorded subtle, but distinct diurnal temperature and RH fluctuations in the Tray Room located some 75 m from the nearest entrance. These measurements suggest that the cave generally becomes progressively drier throughout the winter months, then again becomes wetter during the summer, both in response to inflow of surface water from summer thunderstorms, and stable thermal stratification of the cave atmosphere during the warmer months, which prevents the density-driven influx of outside air.

Values of RH inferred from laboratory analysis of clay samples placed in the cave correlated well with those measured directly using the sling psychrometer or capacitance probe. Analysis of the clay samples indicated the existence of large vertical variations in time-averaged RH from floor to ceiling of the cave passage. Based on these preliminary results, the clay equilibration method could prove useful in other studies of humidity stratification of cave air.

Torgac Cave is remarkable for its gypsum speleothems. These include claw-shaped gypsum stalactites, knobby gypsum stalagmites, and unusual gypsum trays (Doran & Hill, 1998). The cave is located in gentle, semi-arid, sparsely vegetated karst terrain in southern New Mexico at an altitude of about 1550 m (5075 ft) above sea level. The cave is located within the West Pecos Slope physiographic province of Kelley (1971).

Torgac Cave is a solution cave developed in Permian rocks of the Fourmile Draw Member (uppermost member) of the San Andres Formation, (Kelley, 1971). The Fourmile Draw consists of a nearly flat-lying alternating sequence of carbonate and evaporite sedimentary rocks, primarily dolostone and gypsum. While frequently described as a "gypsum cave," examination of the rocks exposed in the cave walls shows that the majority of passages are developed in thick dolostone units, and most of the gypsum visible in the cave actually consists of secondary gypsum dripstone deposits. The only significant gypsum beds observed in or near the cave are those exposed at the surface in the two entrance sinkholes. This uppermost gypsum unit overlies most of the cave passages, and the spectacular gypsum speleothems within the cave are derived from the dissolution and subsequent reprecipitation of this gypsum.

Torgac Cave has two known entrances (Fig. 1), including a large Main (west) Entrance and a smaller East Entrance. Because the large sinkhole surrounding the Main Entrance acts as a cold trap for outside winter air, the air temperature in the cave is noticeably colder than other caves in the vicinity. It had also been noted by cavers that some areas of the cave were much colder than others. This in turn raised the question of

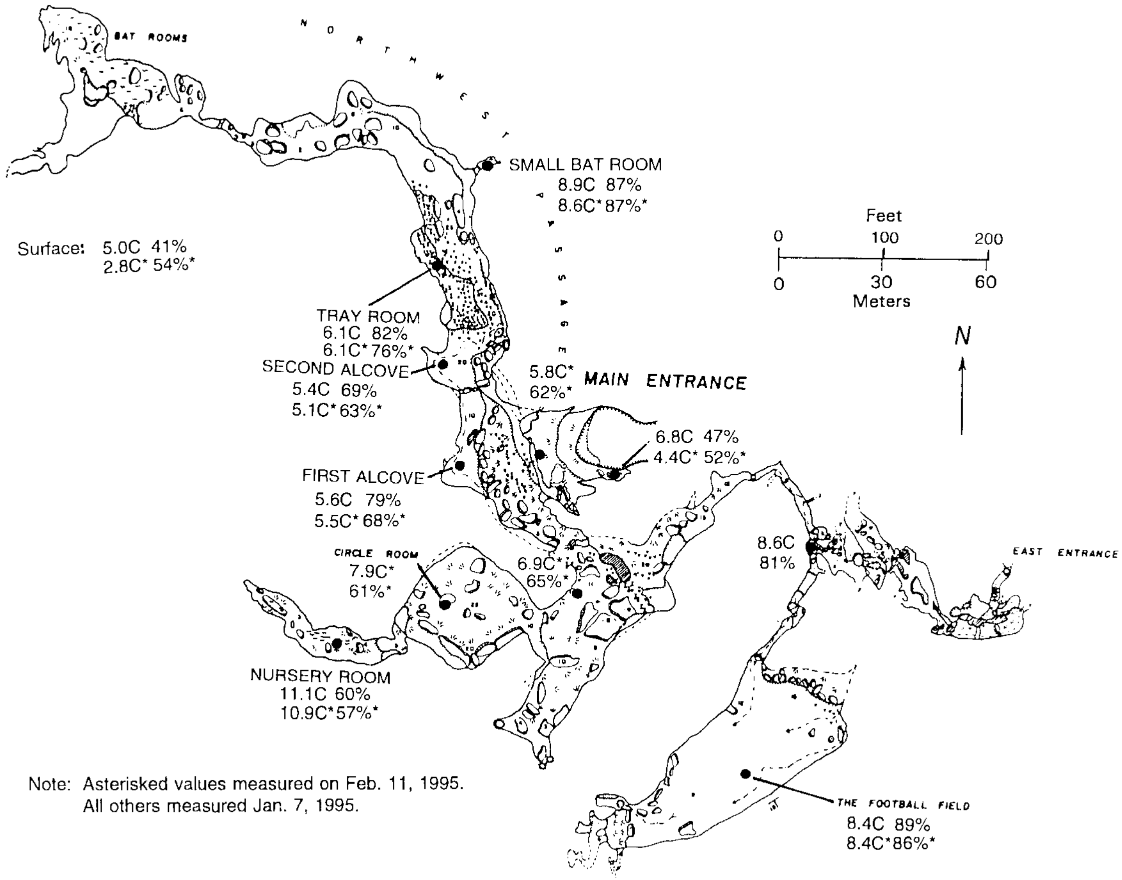

Figure 1.

Air Temperature and Relative Humidity in Torgac Cave.

whether spatial variations in cave microclimate could in some way account for the unusual speleothem development, particularly the gypsum trays (Doran & Hill, 1998).

In order to address this question, we conducted a study during January and February 1995 to measure air temperature and relative humidity (RH) in several areas of Torgac Cave. The impetus for the cave meteorology study was, in part, to ascertain whether vertical air temperature and/or humidity stratification could account for the growth of the gypsum trays in some areas of the cave. Specifically, it had been hypothesized that perhaps gypsum trays "refuse" to grow downward because the air below the level of the tray is drier than that above. The cave meteorology study was intended to test this hypothesis. Torgac Cave also serves as a winter hibernaculum for approximately 1000 bats (Jagnow, 1998), and the microclimate information was considered important with respect to the roost requirements of these bats.

MATERIALS AND METHODS

Air temperature and relative humidity were measured on January 7, 1995 and again on February 11, 1995 at the surface and at 11 locations throughout the cave (Fig. 1) using a research-grade sling psychrometer. The dry bulb and wet bulb temperatures were recorded to the nearest 0.1ºC using the psychrometer, and the barometric pressure (mbar) was determined to the nearest 5 mbar at each location using a Casio watch barometer. These data were subsequently used to calculate RH using the computer program HumiCalc™. At these temperatures and pressures, a change in temperature of 0.1ºC results in a change in RH of about 1%, which is taken to be representative of the magnitude of RH errors in our measurements.

In addition to the two psychrometer surveys, a portable data logger equipped with a temperature/RH sensor was used to continuously monitor air temperature and RH during the period between January 7, 1995 and February 11, 1995 at a single location in the Tray Room (Fig. 1) where gypsum trays are particularly well-developed. A Campbell CR-10 data logger was used for this purpose, along with a Vaisala capacitance-type temperature/humidity probe. The data logger was programmed to query the Vaisala sensor once every hour, and the sensor was placed about 0.3 meter (1 foot) above the floor of the Tray Room. The data logger collected data for 34 days in this mode.

A novel method for assessing vertical variations in RH in the Tray Room was also attempted. On the first day that the data logger began acquiring hourly temperature and humidity measurements, 11 small plastic cups containing 2 to 3 gm of dry, powdered kaolinite clay were suspended at different elevations above the floor of the cave, using a vertical piece of steel conduit pipe with clothes pins attached (Photo 1). The clay samples were spaced at 0.3-m (1-foot) intervals above the floor, and were allowed to equilibrate with the cave atmosphere for the five-week period of the study. The initially dry clay imbibes water from the cave air until at equilibrium the water activity (a_w) of the clay is equal to that of the surrounding atmosphere. This is the RH analogy of the temperature profile work reported by Benedict (1974).

In addition to the 11 kaolinite clay samples suspended vertically in the Tray Room, four identical clay samples were placed throughout the cave at some of the same locations where spot measurements of air temperature and RH were made with the sling psychrometer. These four samples were intended to check whether or not the clay equilibration method indicated similar time-averaged RH values to those measured during the two temperature surveys.

Following the five-week equilibration period in the cave, the cups containing the clay samples were capped and sealed with electrical tape, and returned to the laboratory, where a_w was measured using a Decagon Aqualab CX-2 water activity meter. The CX-2 water activity meter is a chilled-mirror psychrometer device, in which the clay sample is placed in a sealed chamber with a polished metal mirror that is alternately warmed and chilled. As the chamber is warmed, water in the clay sample evaporates into the air above it. When the mirror is chilled, condensation occurs and fog forms on the mirror, thereby altering its optical properties. The circuitry of the instrument allows precise determination of the temperature at which condensation first occurs (dew point), which in turn is related to the water activity of the sample. The instrument provides a direct readout of a_w, which is equivalent to the fractional relative humidity (a_w = %RH/100), with an estimated precision of ±0.5% RH. The water activity of the equilibrated clay samples should thus provide a measure of the time-averaged RH at the specific locations in the cave where the samples were placed.

Following the water activity measurements, the gravimetric water content of each clay sample was determined by weighing the sample, then reweighing it following drying overnight at 105ºC in a lab oven. The weight of the water lost during drying divided by the weight of the dried clay represents the gravimetric water content, expressed in grams water per gram of clay. The precision of the gravimetric water content is approximately ±0.005 g/g.

RESULTS AND CONCLUSIONS

Measured wet bulb and dry bulb temperatures and calculated RH values for the January and February monitoring events are shown in Table 1. Figure 1 shows the measured air temperatures and RH values at each monitoring location. The dry bulb temperature represents the temperature of the cave air. During January, cave air temperatures ranged from 5.4ºC to 11.1ºC, with the coldest temperatures being measured in the lowest part of the streamway passage directly inside the Main Entrance (First and Second Alcoves). The warmest temperature on that date was in the Nursery Room, a small area somewhat isolated from the rest of the cave by a constricted climb down that connects the Nursery Room with the Circle Room. The floor of the Nursery Room is covered with a blanket of dry bat guano approximately one meter thick; however, only a few bats were observed hibernating in the room during the period of this study.

Photo 1. "Tray Room" in Torgac Cave showing kaolinite clay samples suspended at 0.3 m intervals along steel pipe (left) to monitor vertical variations in relative humidity. Data logger in sealed bucket in foreground makes hourly measurements of air temperature and relative humidity.

Cave air temperatures measured during February were generally slightly colder than during January, although temperatures remained unchanged at two of the locations. All of the temperature values are significantly colder than the estimated mean annual temperature for this location of approximately 14.4ºC (Gabin & Lesperance, 1977). Cave temperatures depressed below the mean annual temperature are characteristic of "cold trap" type caves, including many ice caves (Halliday, 1954). In these instances, the cave entrance and pas-

Table 1. Temperature and Relative Humidity Measurements in Torgac Cave.

Location	Date	Time	Dry Bulb Temp[1] (C)	Wet Bulb Temp[1] (C)	Barometric Pressure[2] (mbar)	RH[3](%)
Surface (parking lot)	1/7/95	1905	5.0	0.3	846	41%
	2/11/95	1100	2.8	-0.6	844	54%
Main (west) Gate	1/7/95	1845	6.8	2.2	850	47%
	2/11/95	1125	4.4	0.7	846	52%
First Alcove	1/7/95	1425	5.6	3.9	852	79%
	2/11/95	1205	5.5	3.0	849	68%
Second Alcove	1/7/95	1500	5.4	3.0	852	69%
	2/11/95	1220	5.1	2.2	849	63%
Tray Room	1/7/95	1520	6.1	4.7	851	82%
	2/11/95	1310	6.1	4.2	846	76%
Small Bat Room	1/7/95	1620	8.9	7.8	850	87%
	2/11/95	1400	8.6	7.5	845	87%
Nursery Room	1/7/95	1400	11.1	7.2	852	60%
	2/11/95	1540	10.9	6.7	847	57%
Football Field	1/7/95	1800	8.4	7.5	853	89%
	2/11/95	1610	8.4	7.2	847	86%
Circle Room Ent.	2/11/95	1510	6.9	4.0	846	65%
Circle Room	2/11/95	1530	7.9	4.6	846	61%
Main Ent. Climbdown	2/11/95	1140	5.8	2.8	846	62%
East Ent. Climbdown	1/7/95	1825	8.6	6.9	852	81%

[1] Dry and wet bulb temperatures measured using sling psychrometer

[2] Barometric pressure measured using barometer function on Casio Alti-Depth wristwatch.

[3] Relative humidity calculated from dry & wet bulb temperatures and barometric pressure using HumiCalc™ software, available from Thunder Scientific (tel. 505-265-8701).

sage geometry permits cold dense air to sink into the cave during winter, where it pools in a low portion of the cave (Smithson, 1993).

During a previous study of bat roosting requirements conducted in Torgac Cave during the winter of 1966-67, Howell (1967) noted that between December and late April "temperatures remained low and constant with a 6.5ºC average in most rooms." This observation is consistent with the measurements shown in Table 1, except that the Small Bat Room was significantly warmer during this study (8.9ºC) than during the 1966-67 investigation, where temperatures of between 1.7ºC and 4.4ºC were noted in the "Velifer Room" (aka Small Bat Room). The reason for the difference is not known, but apparently cannot be ascribed to variations in the hibernating bat population in this room. During the 1966-67 study, approximately 560 *Myotis velifer* (Cave Bat) were counted in the room, whereas during bat counts at the start and end of the present study, about 270 of these bats were present (Jagnow, 1998). Thus, the higher temperatures reported here are not attributable to extra heat generated by greater numbers of bats.

Relative humidity values measured at waist-height (about 1 m above floor) during this study ranged from 47% to 89%, with the driest air found closest to the Main Entrance, as expected. There, cold, dry outside air sinks into the cave, warming slightly as it enters, lowering the RH even further as a result of the temperature dependence of this parameter. The highest RH values were observed in the Small Bat Room (87%) and the Football Field (86%-89%), both located in "dead end" areas with relatively poor air circulation from the entrances. At most locations, the RH values for February are several percent lower than those measured during January, which probably reflects the progressive drying of the cave throughout the course of the winter via entry of cold, dry outside air. Howell (1967) also observed that the Small Bat Room (aka Velifer Room) was among the most humid areas of the cave during the winter months.

Figure 2 shows variations in air temperature and RH recorded by the data logger in the Tray Room over the month-long monitoring period. Temperatures at this location ranged between 4.4ºC and 5.1ºC, while RH varied between 86% and 96%. Several trends are evident in the data. First, there is a small, but unmistakable diurnal fluctuation in both temperature and RH. The amplitude of the temperature oscillation is about 0.1ºC, while that of RH is 2% to 4%. Daily minimum temperatures occur at about 8:00 AM, and maxima at about 2:00 PM. The cave air temperature fluctuations appear to correlate with

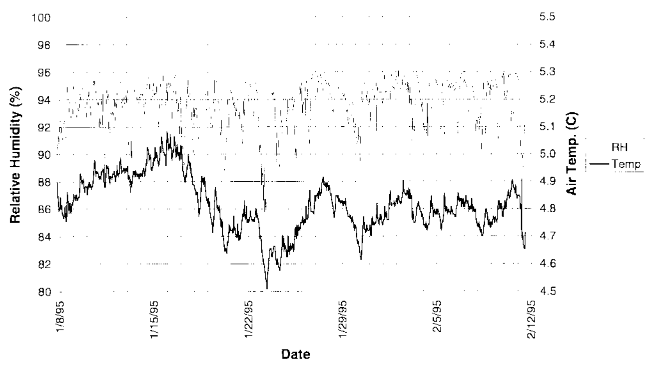

Figure 2. Temperature and RH recorded with data logger in Torgac Cave Tray Room.

external temperature cycles, with the coldest cave temperatures occurring near dawn following the end of a cold night. The Tray Room is located approximately 75 meters from the Main Entrance. Apparently, pulses of outside air are able to penetrate to this distance.

In general, the temperature and RH curves track each other, indicating that as temperatures fall, so too does RH. At first this appears counterintuitive, because cooling of an air mass should cause a rise in RH, not a decline. The explanation for this is probably simply that outside air is both colder and drier than "cave air." Pulses of outside air entering the cave cause both the cooling and the drying of the cave. Influx of outside air is facilitated when the temperature gradient between inside and outside is greatest, which occurs at the coldest time of day, generally in the early morning. This suggests that the RH in Torgac Cave should be lowest towards the end of particularly cold winters, and should reach a maximum in late summer or early autumn.

Upon close examination, exceptions to the positive correlation between temperature and RH sometimes occurred during the warmest part of the day. On these days, when temperature peaked in the Tray Room shortly after noon, a sharp downward spike in RH occurred at nearly the same time. The explanation for this phenomenon is unknown, but it is possible that strong outside winds that typically occur during the warmest part of the day caused short-duration pulses of dry outside air to move into the cave on those days.

As described above, small powdered clay samples were placed in the cave and left to equilibrate with the cave air. The clay samples were intended to serve as proxy recorders of the time-averaged RH at the location where they were left. To my knowledge, this technique has not been tried in previous studies, in caves or elsewhere.

Figure 3 shows the correlation between relative humidity measured with the sling psychrometer and that inferred from the equilibrated clay samples left in the cave. The two psychrometer values are the different readings obtained on the two days. This plot shows reasonably good agreement between the two methods, especially considering that the psychrometer values represent the RH at the moment of the measurement, whereas the values inferred from the clay samples are integrated over the clay equilibration time constant. This time constant is unknown, but is probably on the order of a week or two, based on experiments conducted in the laboratory with saturated salt solutions of known RH. Thus the clay equilibration technique appears to provide at least a qualitative indication of the average RH.

Figure 4 shows the RH inferred from clay samples suspended at different heights above the floor in the Tray Room. A large variation in RH is apparent over the vertical interval monitored. The highest RH is observed 0.3 m above the floor (92.4%), which correlates well with the average of the RH values recorded using the Vaisala sensor (Fig. 2), also located about 0.3 meter above the floor and approximately one meter away horizontally. Decreasing RH values were observed up to a height of 1.2 m where an RH minimum occurred at 83.4% (Fig. 4). This height generally corresponds with the point furthest from any cave wall, floor, or ceiling. Although air velocity measurements were not made, the low RH observed at the 1.2 m level also probably corresponds to the zone of maximum airflow, given that locations closer to the floor and walls are subject to the drag effects imposed by these surfaces.

Because the walls in the Tray Room are uniformly wet, it is reasonable to expect that the RH approaches 100% in the thin stagnant boundary layer immediately adjacent to the cave surfaces. Although the water films in Torgac Cave are saturated with gypsum, the effect of such calcium and sulfate concentrations on the vapor pressure of water in the solution is negligible, and equilibrium RH that would exist very close to such a wetted surface would be well over 99% RH.

RH increases gradually above the 1.2 m level to approximately 90% at a height of 3.3-3.5 m). These two samples were located within about one meter of the cave wall, and thus are probably also influenced by evaporation of water films from the wet surface.

As a check on the RH values measured using the water activity meter, the gravimetric water content of the clay sam-

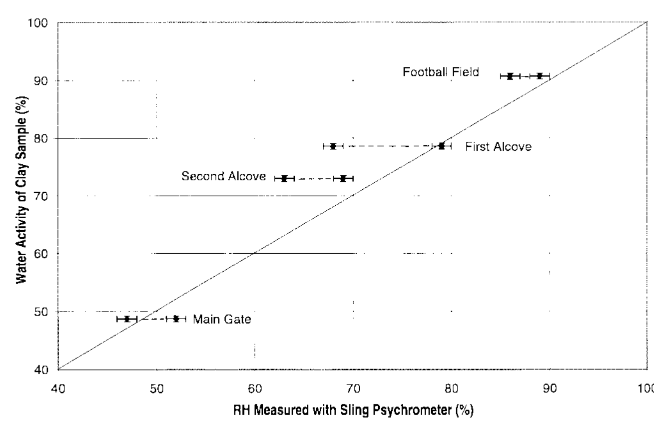

Figure 3. Measured RH vs. RH inferred from Equilibrated Clay Samples.

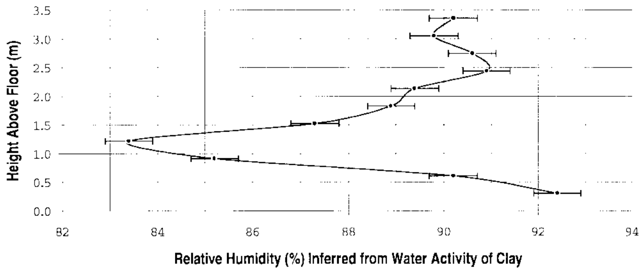

Figure 4. Water activity of clay samples suspended at different heights in Torgac Cave Tray Room.

ples was also determined. This provides an independent check on the water activity data. Figure 5 shows the gravimetric water content of the different clay samples versus height above the floor. The shape of the curve is qualitatively similar to that in the previous figure, indicating that the RH variations observed are real and significant.

Figures 4 and 5 demonstrate that the cave atmosphere within the Tray Room is vertically stratified with respect to RH, and can vary substantially over short vertical distances in a cave passage. The humidity profile (Fig. 4) suggests that maximum evaporation in the Tray Room should occur furthest from the ceiling, walls, and floor. This generally corresponds with the location of maximum gypsum tray development (Doran & Hill, 1998), although more measurements will be needed to verify this preliminary hypothesis.

Figure 4 raises the question of what is being measured when we determine "the RH" using a sling psychrometer or other device that stirs the air throughout a considerable volume. This study indicates that considerable "fine scale" variation in RH may exist, depending upon the measurement height and distance to the nearest wet cave surface. The role of such RH variations in speleogenesis or speleothem deposition is unknown, but recent studies of the condensation corrosion and evaporation deposition in caves of the Guadalupe Mountains of New Mexico indicate that this phenomenon could be important.

ACKNOWLEDGMENTS

The author would like to acknowledge the Bureau of Land Management for access to the cave, and cavers Deb Harrison, Dave Jagnow, John Lyles, Lois Bergthold, Linda Doran, Lynne Lazelle, and Leslie O'Toole who helped install and remove instruments from the cave. Thanks are also due to Daniel B. Stephens & Associates, Inc. for the use of the water activity meter, and anonymous reviewer for the careful review of this paper.

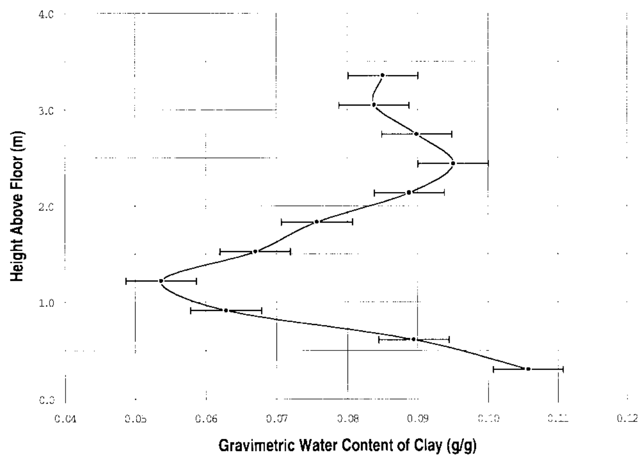

Figure 5. Gravimetric water content of clay samples suspended at different heights in Torgac Cave Tray Room.

REFERENCES

Benedict, E.M. (1974). Hot Air Rises. *Speleo Digest 1974*: 215-216.
Doran, L.M. & Hill, C.A. (1998). Gypsum trays in Torgac Cave, New Mexico. *Journal of Cave and Karst Studies 60*(1): 39-43.
Gabin, V.L. & Lesperance, L.E. (1977). *New Mexico Climatological Data: Precipitation, Temperature, Evaporation, and Wind Monthly and Annual Means, 1950-1975*. W.K. Summers & Associates.
Halliday, W.R. (1954). Ice caves of the United States. *National Speleological Society Bulletin 16*: 3-28.
Howell, D.J. (1967). *Bats of Fort Stanton Cave and Torgoc's Cave*. Unpublished report from Bureau of Land Management files.
Jagnow, D.H. (1998). Bat usage and cave management of Torgac Cave, New Mexico. *Journal of Cave and Karst Studies 60*(1): 33-38.
Kelley, V.C. (1971). Geology of the Pecos Country, southeastern New Mexico. *New Mexico Bureau of Mines and Mineral Resources Memoir 24*: 75 p.
Smithson, P.A. (1993). Vertical temperature structure in a cave environment. *Geoarchaeology 8*(3): 229-240.

BAT USAGE AND CAVE MANAGEMENT OF TORGAC CAVE, NEW MEXICO

DAVID H. JAGNOW
1300 Iris St. #103, Los Alamos, NM 87544 USA

Torgac Cave, New Mexico, is a dolomite and gypsum cave that provides a stable winter hibernaculum for several species of bats, primarily Myotis velifer*, the cave myotis;* Corynorhinus *(formerly* Plecotus) townsendii*, Townsend's big-eared bat; and* Myotis ciliolabrum*, the western small-footed myotis. Occasional bat count studies between 1966 and 1996 indicate a total hibernating population ranging from 649 to 3951 individuals. Temperature and relative humidity studies have established the preferred habitat of each species. Through wise management by the Bureau of Land Management (BLM) and volunteers of the Southwestern Region, NSS, the population has remained stable over the past 30 years, even though the cave has been gated and off-season visitation has increased substantially. The construction of bat-friendly gates and the seasonal closure of Torgac Cave from November 1 to April 15 have helped maintain a stable bat population. It is recommended that the BLM continue the winter bat counts on an annual basis, and that studies be initiated of the summer bat flights.*

Torgac Cave (aka: Torgoc Cave, Torgoc's Cave) is located in central New Mexico, about 100 km northeast of the town of Capitan. The cave is located on public land administered by the Bureau of Land Management (BLM). It is gated, and access is controlled by the BLM. The purpose of this review is to determine the size, variety, stability and trends of the winter bat population using Torgac Cave as a hibernaculum. This information will be used by the BLM to better manage the cave and bat population.

According to tradition, Torgac Cave was discovered and named after a hunter who found it in the 1950s. Reports of bats using Torgac Cave date back to about 1965 when cavers began to visit this gypsum-dolomite cave. Large, knee-deep piles of dried bat guano in the Bat Rooms, in the northwest end of the cave (Fig. 1), attest to the fact that bats have used that portion of the cave much more extensively in the past than at present. The Bat Rooms are presently accessed by tight crawls through a large breakdown collapse area. It appears that the extensive dried deposits of bat guano predate the breakdown collapse. Within recent years, only a few individual bats have been observed in that portion of the cave, and only very minor amounts of fresh guano are found there.

There were also large mounds of bat guano present in the Bat Nursery Room, the western extension off the Circle Room. This room remains easily accessible to the main cave, and was reportedly occupied by small maternity colonies, perhaps 300-400 individuals, during the summer months in the late 1960s. However, within recent years, only a handful of bats have occupied this once-popular roost (Corcoran III, personal communications, 1996).

The earliest study of the bats in Torgac Cave was done by D. J. Howell from September, 1966 to April, 1967, as an unpublished report to the BLM. Approximately every two weeks, Howell measured the fluctuations in temperature, humidity, and ammonia concentrations, and tracked bat movements as a result of changing microclimates. This baseline study indicated about 560 cave myotis and about 100 Townsend's big-eared bats at the peak of the winter hibernation.

The author attended the Southwestern Regional held at Torgac Cave the weekend of October 26, 1968. The approximately 40 cavers were shocked by recent vandalism to the unique gypsum speleothems. Members of the Sandia Grotto, NSS, met on October 29, 1968, to discuss how to protect the cave. Even at that time, one of the main concerns was the protection of the bats. "Gating the cave was another suggestion; however, a sufficient opening will have to be created in order for the bats to enter and leave the cave freely. Horizontal bars across the main entrance will fulfill this purpose." (Rohwer, 1968: 3)

The following weekend, members of the Sandia Grotto again visited Torgac Cave. Jim Hardy, John Corcoran, Jennifer and Robbie Babb showed the vandalism to BLM Cave Specialist Don Sawyer, and they made plans to gate the entrance. "Sunday we did a little more caving; then the main entrances were sealed off, officially, as well as practically, ending the trip." (Mauser, 1968: 2) At this time, the bats were forced to use many small openings around the perimeter of the large entrance sink. I'm sure this move did not help the bat population, but it did serve to protect the beautiful gypsum speleothems.

Torgac Cave was subsequently gated at two entrances in late 1970. Both gates were designed to be bat-friendly, and were later rebuilt. In 1992, Jim Cox rebuilt the main gate to be even more vandal-resistant and more bat-friendly. Now the bats not only exit through both gates during the summer months, but also through small openings too tight for human entrance.

There is no record of any bat counts between 1967 and 1987. The hibernating bat colony study at Torgac Cave was

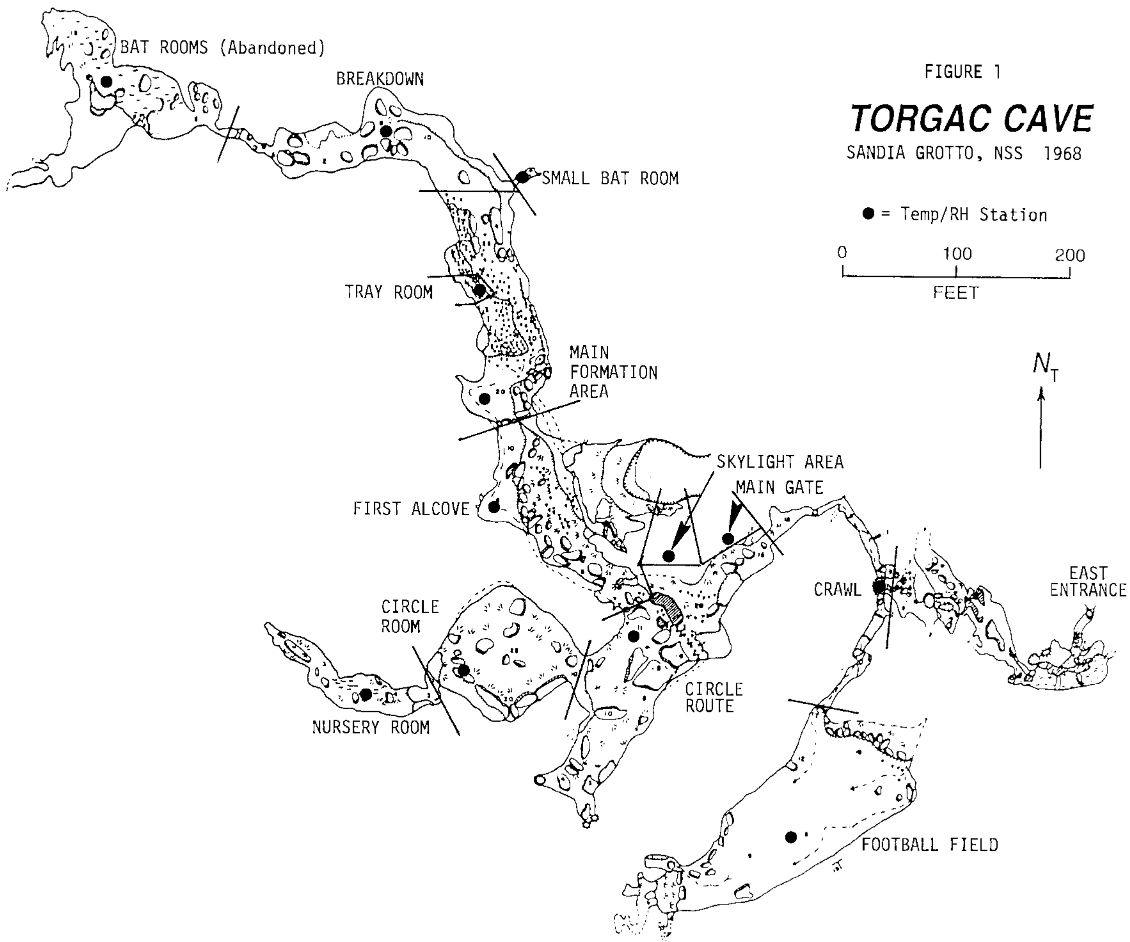

Figure 1. Map of Torgac Cave showing temperature and relative humidity collecting stations.

initiated by BLM cave specialist Matt Safford in the winter of 1987/88, and two counts were made (Safford, 1988). Safford continued these studies annually until January 6, 1990, at which time he was transferred to a different district. Since then, the bat counts have been conducted by volunteers. Rebecca Jagnow led a bat count on February 2, 1991. David Jagnow led the most recent bat counts from January 7, 1995 to February 11, 1996 (Table 1). Plans are to continue an annual census by members of the Pajarito Grotto, NSS. The results of these bat surveys are summarized in Table 2 and Figure 2.

Because Torgac Cave is recognized as a bat hibernaculum, the BLM decided in 1993 to seasonally close the cave from November 1 to April 15 to protect hibernating bat populations and to maintain the natural microclimate (Bilbo, 1993). Within the Roswell Resource Area, the BLM has enforced the seasonal closure of Torgac and nine other caves to protect these critical bat hibernacula (BLM, 1993).

DESCRIPTION OF ENVIRONMENT

GEOLOGY

Torgac Cave is located in eastern Lincoln County, New Mexico, at an elevation of 1550 m (5075 ft). The large sinkhole entrance is located in the extensive gypsum karst area created by the Fourmile Draw Member of the San Andres Formation of Permian age. The interbedded gypsum and dolomite dip approximately 10m/km (50ft/mile) to the east. Bedding is disturbed locally by numerous subsurface collapses caused by karst drainage to the Pecos River in the east. The surface topography consists of sparsely vegetated rolling gypsum hills with about 20 m of local relief. Within Torgac Cave, the roughly-weathered dolomite beds provide a good purchase

Figure 2. Torgac Cave bat census.

Table 1.
Torgac Cave Bat Count Statistics, February 11, 1996.

Area	Temp	RH	MV	CT	MC	PH
Bat Rooms	9.8	54%	-	3	-	-
Breakdown	(no readings)		-	-	-	-
Small Bat Room	C 9.5 F 7.6	73% 59%	658	-	2	-
Tray Room	C 5.7 F 9.9	62% 52%	-	-	51	-
Main Formation Area	C 5.7 F 3.8	62% 46%	6	70	51	-
First Alcove	F 3.9	46%	6	67	1	-
Skylight Area	6.1	32%	1	2	-	-
Main Gate	7.4	26%	-	-	-	1
Circle Route	5.1	37%	-	3	1	-
Circle Room	7.7	38%	-	2	-	-
Nursery Room	9.4	42%	-	1	-	-
Crawl	7.2	54%	39	-	-	-
Football Field	7.7	61%	1	-	2	-
Total			711	148	108	1

MV = *Myotis velifer* (cave myotis)
CT = *Corynorhinus townsendii* (Townsend's big-beared)
MC = *Myotis ciliolabrum* (western small-footed myotis)
PH = *Pipistrellus hesperus* (western pipistrelle)
C = Ceiling Temperature (°C)/Relative Humidity
F = Floor Temperature (°C)/Relative Humidity

for the bat clusters. Mineralogy of Torgac Cave is discussed in Doran and Hill (1998).

SPELEOGENESIS

Torgac Cave is an inactive vadose cave with the main passage located about 30 m below the surface. From the main entrance, the dry vadose passage extends approximately 300 m to the northwest, through the Northwest Passage, to some abandoned Bat Rooms where the passage is terminated by collapse. Also from the main entrance, the vadose passage extends approximately 300 m to the south through two main branches, the Circle Room, and the Football Field, both of which are also terminated by collapses. The current water table is well below the main vadose level of Torgac Cave, and the flat dirt floors of the main passage are now only occasionally flooded by water entering from the main entrance sink.

TEMPERATURE

The entrance sink is approximately 25 m in diameter and lies on the side of a much larger surface depression that opens to the southwest. This topography forms a cold-air trap that funnels cold air into the center of Torgac Cave. This forms a stable bat hibernaculum during the winter months, with temperatures ranging from a low of 4°C near the main entrance sink, and warming to about 10°C near the extremities of the cave. The annual temperature high for Torgac Cave is 14°C, recorded in August (Rolfe, 1967). Average summer temperature is about 11°C. Most of the passages are 15-18 m in width, with a ceiling height of two to six meters. The bats typically cling to resistant dolomite beds or gypsum-encrusted dolomite beds that form the ceilings of these passages.

BATS OF TORGAC CAVE

CAVE MYOTIS

By far the most populous bat in the study is *Myotis velifer*, the cave myotis. These bats vary in color from dark gray to a light buff with a dark gray face and short gray ears. They typically form large clusters during hibernation. In Torgac Cave the typical cluster size is from 25 to 40 individuals. They tend to hibernate in relatively warm, high humidity areas of the cave and often appear quite alert when encountered.

TOWNSEND'S BIG-EARED BAT

The second most common bat in Torgac Cave is *Corynorhinus townsendii*, the Townsend's big-eared bat. Until recently, this bat species was identified as *Plecotus townsendii*. Townsend's big-eared bats vary in color from dark to light gray to dingy yellow, but are most readily identified by their large ears, approximately three centimeters in length. However, the ears may be folded back against the body and largely covered by their wings, with only the tragus visible. If their ears are folded back, they can sometimes be distinguished from the cave myotis by their slightly larger size. These big-eared bats typically hibernate in small clusters or singly. They are usually found hibernating in the coldest areas of the cave and at lower relative humidities than the cave myotis prefer.

WESTERN SMALL-FOOTED MYOTIS

Torgac Cave also hosts a small population of *Myotis ciliolabrum*, the western small-footed myotis. These bats can be identified by their dark gold (brassy) fur in striking contrast to their dark short ears and dark mask around their eyes. Small-footed myotis tend to hibernate individually or in small clusters up to 25 individuals on open, moist ceilings. They also love to cram themselves into moist ceiling cracks. They prefer cold to moderate temperatures, and congregate in areas of high humidity.

OTHERS

Other bats occasionally found in Torgac Cave include the big brown bat (*Eptesicus fuscus*), which can be identified by its large size (almost twice as large as the other species); its small, dark ears with a large, rounded tragus; and its beautiful brown fur. The western pipistrelle (*Pipistrellus hesperus*) is occasionally found hibernating as individuals. They can be identi-

Table 2. Annual Bat Cenus: Torgac Cave.

Bats	66/67	87/88	88/89	89/90	90/91	94/95	95/96
Cave myotis	560	2821	655	2039	3778	450	711
Townsend's big-eared	100	141	46	68	147	87	148
Western small-footed myotis	10	30	7	0	26	111	108
Big Brown	-	1	-	-	-	-	-
Pallid	-	-	-	-	-	?(8)	-
Western Pipistrelle	-	-	-	-	-	1	1
Total	670	2993	708	2107	3951	649	968

fied by their very small size, light gray to yellowish fur and their black leathery mask. There have also been possible sightings of pallid bats (*Antrozous pallidus*). They can be identified by their pale-colored fur, light yellow above and cream to white below, and their long naked ears and pale pink face. These bats were recorded only occasionally as solitary individuals and, thus, are probably transient inhabitants.

CENSUS METHODS

Population numbers were obtained by direct count of the bats during hibernation. Care was taken not to create undue disturbance and the animals were not handled, except by Howell (1967). Torgac Cave was divided into sections to facilitate counting and to determine if the bats were changing locations during the winter months. Temperature and relative humidity readings were taken either by sling psychrometer or by electronic instruments at established data stations. When possible, floor and ceiling readings are taken.

During the bat counts, the volunteer cavers followed the bat survey guidelines developed by Mike Ballistreri (1995), bat biologist at the University of New Mexico. We avoided nylon clothing or coveralls that would make noise while walking. We used electric lights, and covered the lenses with red automotive tail-light repair tape in those areas where bats were present. Unnecessary packs and clothing were left outside the cave, and all dangling metal objects such as zipper pulls or metal shoulder-strap connectors were silenced by taping over with duct tape. Talking was held to a minimum and at a low volume, and the volunteers moved as smoothly and quietly through the cave as possible.

RESULTS

NUMBER OF BATS

The annual bat census data for Torgac Cave are summarized in Table 2 and Figure 2. Note that there are gaps in the collected data between 1967 and 1987, and again between 1991 and 1994. The total number of bats varied from a high in the winter of 1990/91 of 3951 to a low of 649 in the winter of 1994/95. The data can be divided into three high-count years (87/88, 89/90, & 90/91) and four baseline years (66/67, 88/89, 94/95, & 95/96).

The cave myotis have consistently accounted for the highest percentage of the total population. The greatest variation from year to year is in the number of cave myotis, from a low of 450 in 94/95, to a high of 3778 in 90/91. The high cave myotis count the winter of 1990-91 may be questionable. During that count, the Small Bat Room (Velifer Room) was so loaded with bats that they estimated the size of each cluster and totaled the number of square feet of bats. At that time, the BLM used the packing ratio of 166 velifer/square foot to determine the number of bats. There is some error associated with this calculation, as the packing ratios probably vary with temperature and relative humidity during the hibernation period. Over the years, the cave myotis population has averaged 1573 during the peak of hibernation.

The Townsend's big-eared bat population has remained very stable over the past 30 years. The low count was 46 individuals in 88/89, with the highest count of148 individuals in 95/96. These counts of the Townsend's big-eared bats are probably accurate, because they tend to hibernate in pairs or small clusters that are well-exposed and easy to count. The big-eared count has averaged 105 over the seven years of data.

The western small-footed bat population has always remained relatively small, varying from 0 in 89/90 to 111 in 94/95. The count has averaged 42 over the seven years of data. These counts are probably the least accurate because the western small-footed bats tend to hibernate out of sight, in small cracks and pockets.

Other bats include one big brown bat, counted by Matt Safford on January 16, 1988. The big browns are rare in Torgac Cave, but are commonly found in small numbers in other caves in the Roswell Resource Area.

The author found eight possible pallid bats on January 7, 1995. One, just beyond the Main Gate, was a positive identification. The other small cluster of seven possible pallids was located in the First Alcove/Breakdown area. Their fur was extremely light colored, but their faces were light gray and ears were shorter than the other pallid. Bill Ellis also spotted a possible pallid bat on November 12, 1995. This large, very pale bat with large ears was sighted at the very end of the Nursery Room, but flew before it could be examined closely.

One western pipistrelle has consistently visited Torgac Cave from 94/95 to 95/96. He moves about the cave during hibernation, from about 30 m past the Small Bat Room, to just outside the entrance to the Small Bat Room, and most recently was located on a breakdown block about six meters above the Main Gate.

TEMPERATURE AND RELATIVE HUMIDITY

Torgac Cave provides an ideal bat hibernaculum because of the very stable cave environment and wide variety of temperatures. Detailed temperature and relative humidity studies are discussed by Forbes (1998). Torgac Cave does not have multiple entrances, other than around the perimeter of the main collapse, so there is very little air movement through the cave other than atmospheric pumping. Even though surface winds average 17 kph out of the south during the winter months (Howell, 1967), Torgac Cave is colder and more independent of the external environment than other caves in the vicinity.

The Main Entrance sink provides a cold air trap, with the coldest temperatures measured at the base of the breakdown collapse pile. The First Alcove and Main Formation Area have reached a low temperature of 4°C (95/96), and over the years have averaged 4.9°C during the bat counts. The Townsend's big-eared bats prefer roosting on the dry dolomite ceilings of these coldest portions of the cave. The relative humidity (RH) of these portions varied from 46% (95/96) to 79% (66/67 & 94/95), averaging 62% over the years that data is available. Within these areas, the cold dry air is at floor level, with warmer humid air along the ceiling, as is typical of many portions of Torgac Cave. The most recent measurements in the Main Formation Area revealed 3.8°C and 46% RH near the floor, and 5.7°C and 62% RH near the ceiling where the bats roost.

The western small-footed bats prefer slightly warmer and more humid conditions. They pack into a five-centimeter-wide dripping crack in the ceiling of the Main Formation Area, and also like to cluster on the dripping ceiling of the Tray Room—an isolated portion of the Main Formation Area. The relative humidity of the Tray Room has varied from 52% near the floor to 96% near the ceiling (Forbes, 1998).

The cave myotis obviously prefer the warmer and more humid conditions of the Small Bat Room (Velifer Room) off the east side of the Northwest Passage. This small room, approximately one to two meters in height and about 10 m in diameter, contains an average of 1375 cave myotis. Temperature and relative humidity have varied from 2°C and 99% RH (Howell, 1967) to 13.5°C (11/30/88 & 1/6/90) and 73% RH (2/11/96). Some years, the ceiling in this room is dripping, and many of the velifer are soaking wet. On average, this room measures 8.5°C and probably over 86% RH.

The second-largest concentration of cave myotis occurs where the East Entrance passage joins with the Crawlway between the Main Entrance and the Football Field. In this area, approximately 40-100 cave myotis can be found in small clusters up a steeply-dipping gypsum-encrusted wall for about 30 m. Temperature and relative humidity probably vary greatly over the expanse of this wall, well out of reach of our instruments.

The warmest areas of Torgac Cave are also the most isolated from the central collapse cone. The (abandoned) Bat Room, at the northwest end of the Northwest Passage, is typically 10°C and 55% RH during the winter months. Although it contains knee-deep piles of dried guano, the room has only been occupied by a small number of bats in recent years. The Nursery Room, off the west end of the Circle Room, averages 11°C and 50% RH during the winter months. This room may contain one or two active bats during the winter months, and occasionally contains small clusters of cave myotis during the summer months. A very large mound of guano indicates this room was probably a favored summer roost prior to the cave's discovery by cavers in the mid-1960s. The Nursery Room is flagged as "off limits" due to the strong smell and dusty conditions of the bat guano.

Temperatures throughout the cave are relatively stable from year to year. However, relative humidity varies widely, depending on recent rains. In 94/95 the cave was about 20% more humid on average than the corresponding areas in 95/96. The streambed had recently flooded in 1994, and the ceiling of the Velifer Room and other areas were very actively dripping. However, 1995 was a dry year, the stream bed sediments were dry, and areas like the Velifer Room were not dripping as much. The humidity within the cave is probably highly dependent on the local path of the late summer thunderstorms, which can dump tremendous amounts of water within a very narrow storm track.

DISCUSSION

The author has no good explanation for why the cave myotis are so numerous in certain years. The population variation does not appear to track well with climatic conditions. Safford (1989) had enough data from nearby Fort Stanton Cave to see a five year cycle of highs and lows in population numbers. The data for Torgac Cave is too sparse and contains too many gaps to do a similar comparison.

Relatively low-count baseline years are essentially identical to the earliest studies done by Howell (1967). Howell's studies were comprehensive and were performed before Torgac Cave experienced much visitation, prior to closing many small entrances and installing the two gates. It appears that the subsequent installation of the gates has protected the unique gypsum speleothems of Torgac Cave, while not noticeably impacting the hibernating bat populations. It is possible that the caver traffic and/or gates have affected the summer nursery usage.

RECOMMENDATIONS

It is recommended that the BLM continue to close Torgac Cave to visitation from November 1 to April 15. The current policy of limiting visitation to one trip (six person maximum) per month during the summer months is also recommended.

It is further recommended that members of the Pajarito Grotto on an annual basis continue the winter bat count program. Howell recorded an unusual year in 1966 when Torgac

Cave reached its coldest temperature immediately following a cold snap in November. During most years, however, the greatest number of bats and the deepest state of hibernation occurs early in February. This is approximately midway through the hibernation cycle, and it is recommended that bat counts be performed at this time each year. To minimize disturbance, it is further recommended that only one bat count be performed each year.

At present, the United States Fish and Wildlife Service lists the three main species of bats found in Torgac Cave as C2: "Species of special concern. Listing as endangered or threatened may be appropriate, but conclusive data are not currently available." For each of these species, human disturbance of the maternity and/or hibernating roosts was cited as the primary cause of decline. It is well known that the Townsend's big-eared bat is highly susceptible to disturbance (Barbour & Davies, 1969; Mohr, 1972). It is therefore extremely important that both summer and winter roosting sites be protected through thoughtful management if this species is to survive. The author is especially appreciative that the BLM Roswell Resource Area has recognized this concern, and has enforced seasonal closure of their bat caves. It is hoped that other federal and state agencies across the United States will take similar actions to protect sensitive bat habitats.

Much more research could be conducted on the bats of Torgac Cave. Summer studies of the bats have not been done. It would be good to have each group of summer visitors report the location and numbers of bats observed, and be aware of their presence so as to cause minimal disturbance. Evening bat counts of exiting bats could be performed at both gates and other various small exits. On May 6, 1994, Bill Ellis and Paul Reynolds (Ellis, 1994) counted 64 bats exiting Torgac Cave through a small hole about 12m east of the Main Gate between 8:30 and 9:30pm. Similar data would help expand our knowledge of the bats year round.

It would be interesting to core an undisturbed portion of the bat guano piles in the Bat Room and in the Nursery Room for radiocarbon dating and species identification. It is believed that bat skulls present in the cores could provide species identification.

ACKNOWLEDGMENTS

Special thanks for all the caver volunteers who have assisted with the bat counts over the years. The Bureau of Land Management, Roswell District, New Mexico, provided research permits and allowed access to Torgac Cave. Mike Bilbo, cave specialist for the Roswell District, provided access to the BLM data as well as professional and personal support for this project. Dr. Mike Balistreri, University of New Mexico, trained many of the volunteers in bat identification, and provided very useful guidelines for performing the bat counts with minimal disturbance.

REFERENCES

Balistreri, M. (1995). *Bat Survey Guidelines (Crystal, Torgac, Crockett's Caves), & Bat Species of New Mexico*. unpublished report: 4p.

Barbour, R.W. & Davis, W.H. (1969). *Bats of America*. The University Press of Kentucky: 286 pp.

Bilbo, M. J., et. al. (1993). *Seasonal Closure of Bat Hibernaculum Caves: BLM (Roswell) Amendment to Ft. Stanton Cave, Torgac's Cave, Crockett's Cave, Cave Management Plans and Interim Cave Visitation Policy*: 6p.

Bureau of Land Management. (1993). Closure and restriction order: Roswell resource area bat hibernaculum. *Federal Register*, 9/17/93, *58*(179): 48668-48669.

Doran, L.M. & Hill, C.A. (1998). Gypsum trays in Torgac Cave, New Mexico. *Journal of Cave and Karst Studies 60*(1): 39-43.

Ellis, B. (1994). *Torgac's Cave Trip Synopsis*. unpublished report in BLM Roswell Resource Area files: 3 p.

Forbes, J. (1998). Air temperature and relative humidity study: Torgac Cave, New Mexico. *Journal of Cave and Karst Studies 60*(1): 27-32.

Howell, D.J. (1967). *Bats of Fort Stanton Cave and Torgoc's Cave*. unpublished report, BLM Roswell Resource Area: 57 pp.

Mauser, M. (1968). Trip report, Torgac's. *Underground Experience: Sandia Grotto Newsletter 1*(3) (November 6): 2.

Mohr, C. (1972). The status of threatened species of cave-dwelling bats. *National Speleological Society Bulletin 34*: 33-47.

Rohwer, R. (1968). Vandalism of Torgac's. *Underground Experience: Sandia Grotto Newsletter 1*(2) (October 30): 3.

Rolfe, E. (1967). Personal communication to D.J. Howell.

Safford, M. (1988). Hibernating bat population studies. *Southwestern Cavers* (Nov-Dec): 65-67.

Safford, M. (1989). Bat population study Fort Stanton Cave. *National Speleological Society Bulletin 51*: 42-46.

GYPSUM TRAYS IN TORGAC CAVE, NEW MEXICO

LINDA M. DORAN
700 Adams SE, Albuquerque, NM 87108 USA

CAROL A. HILL
17 El Arco Drive, Albuquerque, NM 87123 USA

The gypsum trays in Torgac Cave, New Mexico are only the second reported occurrence of this speleothem type in the world. They differ from most other (carbonate or gypsum) trays in that they often have stalactites growing on their flat undersides (thereby forming "claw" shapes), and in that they can exhibit multiple tray growth in the vertical direction on a single stalactite. This deviation from "normal" tray development indicates that for gypsum trays to form, equilibrium must be reached between infiltration and evaporation of water. If infiltration exceeds evaporation, then gypsum stalactites ("claws") will form; if evaporation exceeds infiltration, then trays (with flat-bottomed surfaces) will form. Drier climatic conditions during the Holocene (last 10,000 years) may have influenced the growth of gypsum trays in Torgac Cave.

Torgac Cave is located in central New Mexico, ~100 km northeast of the town of Capitan, on Bureau of Land Management property. The cave is developed in the Permian Fourmile Draw member of the San Andres Formation, a silty-limy dolomitic unit containing gypsum interbeds. Short-grass prairie vegetation and a semiarid climate exist in the vicinity of the cave. The entrance area is a collapse sinkhole approximately 100 m in diameter and 30 m deep (Fig. 1). The entrance sink funnels cold, dry air down into the cave, especially in the winter. The temperature and humidity of Torgac Cave were monitored by Forbes (1998) in January and February of 1995. Temperatures at that time ranged from 5.5° to 10.9°C. Relative humidity ranged from 56% to 96% in different parts of the cave. The cave serves as a hibernaculum for several species of bats (Jagnow, 1998).

Hill (1982) was the first to discuss the mineralogy of the cave, reporting gypsum stalactites ("claw" and anemolite), stalagmites, popcorn and crust, and epsomite flowers, cotton and crust. This report expands on Hill's earlier description; in particular it discusses the gypsum trays in the cave, a type of speleothem not previously recognized there. Other speleothems/minerals in the cave not previously reported are gypsum rims ("eggshell" variety; Fig. 2), gypsum flowers, gypsum blisters, gypsum flowstone, and epsomite stalactites (growing on the tips of gypsum stalactites). The gypsum dripstone and flowstone has a macrocrystalline texture, with individual gypsum crystals up to 3 cm in diameter. This texture gives these speleothems a "bumpy" appearance. Gypsum spar crystals, up to 10 cm long and dating from an earlier phreatic episode (Fig. 3), are found within bedrock cavities (vugs) in the Football Room (Fig. 1).

DESCRIPTION OF TRAYS

Trays are a speleothem type composed of sprays or clusters of popcorn or grape coralloids and frostwork, the composite mass of which ends in a flat, horizontal, traylike surface (Hill & Forti, 1986). Often these flat-bottomed masses occur in tiers or ledges, that is, separated from one another at different levels along a cave wall, in a stairstep-like manner. Maximum development of trays is along their flat, bottom surfaces (trays seemingly "refuse" to grow farther down). The elevation of the flat surface coincides with wall irregularities, the tips of bedrock pendants, or the tips of stalactites.

Both carbonate (calcite-aragonite) and gypsum trays have been reported in the literature. Martini (1986) was the first to formally name and describe this speleothem type from carbonate occurrences in South African caves. These speleothems had been called "flat-bottomed popcorn" by cavers in the Guadalupe Mountains, New Mexico, for many years (Hill, 1986; 1987). Gypsum trays were first documented by Calaforra and Forti (1994) in Rocking Chair Cave, near Carlsbad, New Mexico. Torgac Cave has the second reported occurrence of gypsum trays anywhere in the world.

Gypsum trays can be found at several locations in Torgac, including the Main Formation Area, a smaller room called the Tray Room just off the Main Formation Area, the main north-south passage halfway between the Main Formation Area and the Circle Room, and the Football Room (Fig. 1). In the Main Formation Area, several dozen trays are suspended from the lower ends of gypsum stalactites at a height of about 4 m above the floor. The stalactites, which are ~1.2 to 1.5 m long, widen at their tips to form small trays 0.3 to 0.5 m wide. Often the flat lower surfaces of these trays are not completely horizontal but may be inclined at up to about 10° from the horizontal. Some of the trays in this area are actively dripping, with tiny gypsum stalactites forming on the bottom of the trays, thus giving the composite mass a "clawlike" appearance. Other of the trays are flat and dry, with no stalactitic growth beneath them. Trays in the southwest half of the room appear to have developed as multiple tiers from which small gypsum stalactites have grown, connecting the tiers to one another (Fig. 4).

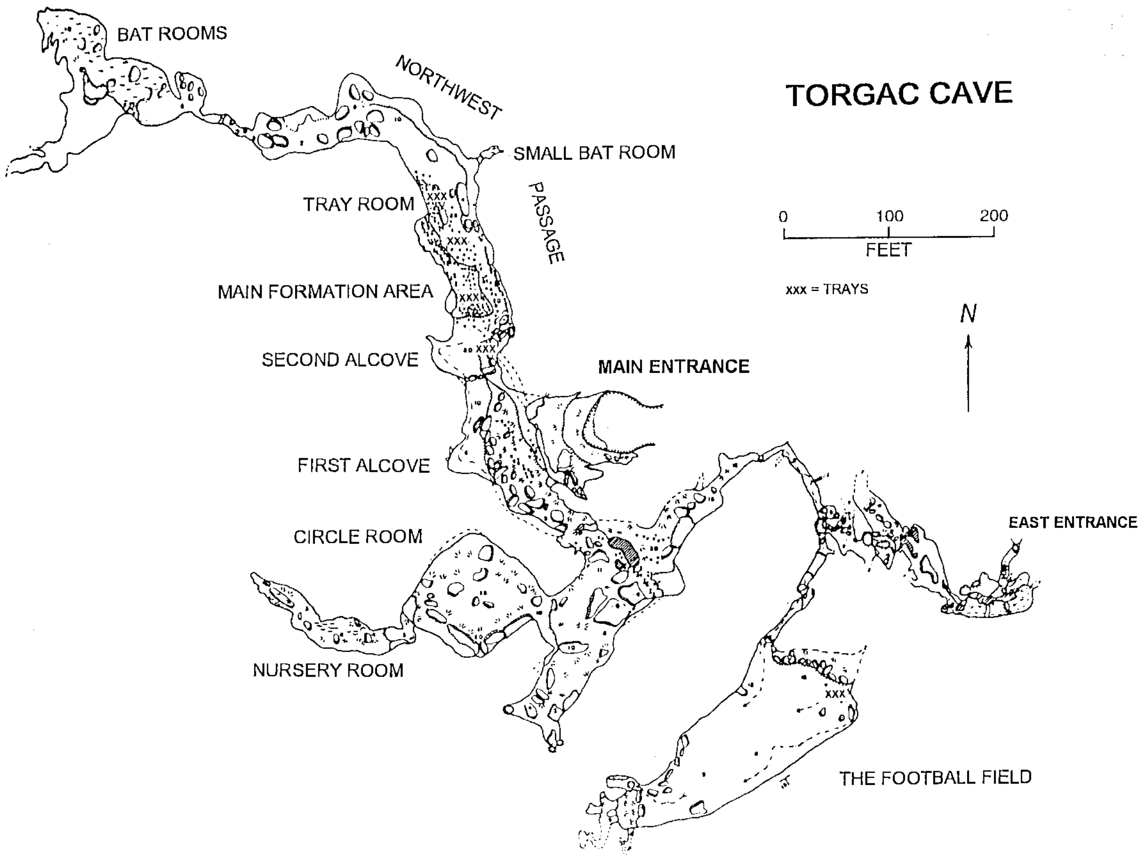

Figure 1. Map of Torgac Cave showing location of trays ("xxx" denotes trays).

On the northeast side of the room the trays are about the same size but are more uniformly flat and have no stalactites extending downward from their bottom surfaces. The flat-bottomed surfaces of the trays are characterized by macrocrystalline gypsum popcorn rosettes in their centers surrounded by gypsum frostwork around their edges. Along the east side of this portion of the cave, the passage slopes sharply upward toward the eastern entrance, a configuration that may result in higher evaporation rates as cold, dry air sinks into the passage from the entrance.

In the Tray Room, at the back of the Main Formation Area, tray tiers extend outward from the walls in the upper half of the gallery. These tiers begin at about 1 m above the floor and can be found at several levels up to about 4 m. These trays are elongated in a north-south direction and measure up to 25 cm in diameter. Many have tiny, actively growing gypsum stalactites extending downward from their flat lower surfaces, and also gypsum stalagmites on the floor beneath these drip points. The highest tray in this room is attached to and nearly flush with the ceiling.

Trays can also be found at the tips of stalactites above the slope on the east side of the passage between the Main Entrance and the Main Formation Area. These trays are suspended from the ceiling between 1.3 m and 2.1 m above the floor. The lower set of trays appears to have developed successive stages of tray growth like some of the trays in the Main Formation Area. The upper trays are much drier and flatter. Like those in the Main Formation Area, these are composed of gypsum rosettes surrounded by gypsum frostwork (Fig. 5). The enlarged mass of the trays is ~0.3 m to 0.5 m in diameter and ~0.3 m long. Several other incipient trays can be seen on the wall behind and around the higher trays.

Well-formed gypsum trays occur in the Football Room near the south end of the cave. One tray (the one closest to the south wall) is suspended from a ~0.8 m-long stalactite and has a stalagmite and a series of drip holes in the sediment floor beneath it. This tray is 1.9 m above the stalagmite and 2.4 m above the floor. It thus appears that some of the dripping water is oversaturated with respect to dissolved calcium sulfate and precipitates gypsum when it reaches the floor; other dripping water is undersaturated and creates drill holes instead. Nearby, a separate cluster of five gypsum trays is suspended 3.4 m above the floor. These trays are 7 to 15 cm in diameter and are attached to three branching stalactites, each about 0.6 m long. Some 25 drill holes occur in the mud floor beneath these wet and dripping trays; however, no incipient stalactites or "claws" extend downward from the bottoms of this cluster of trays.

ORIGIN OF TRAYS

The origin of trays is not well understood and it is hoped that the description of gypsum trays in Torgac Cave will con-

Figure 2. "Eggshell" gypsum rims, in passage leading into the Football Field Room. Photo courtesy of D. Jagnow.

Figure 3. Phreatic tabular gypsum crystals in a bedrock cavity, Football Field Room. Photo courtesy of D. Jagnow.

tribute to the model of origin for this speleothem type. Martini (1986) was the first to speculate on the origin of carbonate (calcite-aragonite) trays, saying that these are subaerial, rather

Figure 4. Tiers of gypsum trays connected by stalactites, Main Formation Room. The tiers may represent alternating wet (stalactites) and dry (trays) climatic episodes. Photo courtesy of D. Jagnow.

than subaqueous, speleothems. According to Martini's model, slightly undersaturated (with respect to calcite and aragonite), thin-film solutions flow down a rock pendant (or stalactite) and reach saturation by evaporation. Where evaporation of these thin films of water occurs, aragonite frostwork is precipitated. Subsequent thin-film solutions rise in this frostwork by capillarity, so that later frostwork growth is upward or lateral, away from the pendant tip (or stalactite), causing a flat-bottomed surface to form. And, since different rock pendants (or stalactites) differ in elevation, trays can form as multiple flat-bottomed tiers or ledges. Aragonite frostwork continues to grow along the edges of a carbonate tray where evaporation is at a maximum, but frostwork in the interior of the tray is gradually replaced by calcite popcorn because these interior solutions (where evaporation is relatively less) are undersaturated with respect to aragonite but oversaturated with respect to calcite. Martini's (1986) model was for carbonate trays, but Calaforra and Forti (1994) proposed essentially the same genetic mech-

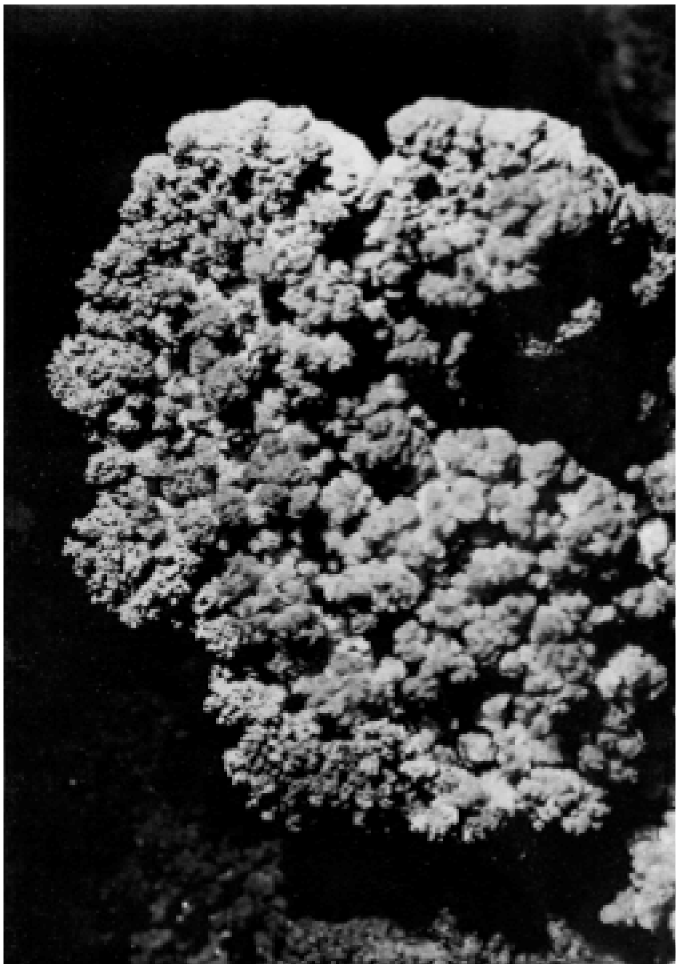

Figure 5. Looking straight up at the flat bottom of a gypsum tray, between Main Entrance and Main Entrance Area. Popcorn rosettes of gypsum make up the center of the tray and gypsum frostwook forms along the edges of the tray. Photo courtesy of D. Jagnow.

anism for the growth of gypsum trays. However, in the case of gypsum trays there is no replacement of one mineral by another (i.e., aragonite by calcite), but a recrystallization of gypsum (from frostwork to popcorn) takes place in the interiors of trays.

DISCUSSION

The gypsum trays in Torgac Cave show that the mechanism for tray growth as described by Martini (1986) is incomplete. Gypsum trays develop frostwork exteriors, popcorn interiors, and flat-bottomed surfaces, even though they are not formed by the replacement of one mineral by another. Instead, tray morphology may be a function of growth from thin films due to microclimate variations. Thin films in a more highly evaporative environment (i.e., the outer surfaces of trays directly subjected to air flow) may promote a dendritic, frostwork morphology, whereas in the center of trays, a less evaporative (less air flow) environment promotes the rounded, botryoidal form of popcorn—either calcite popcorn (replacing aragonite frostwork) or gypsum popcorn (recrystallizing from gypsum frostwork).

In Torgac, gypsum trays commonly form both on wall pendants and stalactites, but some stalactitic trays are different from those in other caves in that they are multiply stacked, with separate tiers of trays forming as part of the same stalactite (Fig. 4). This seems to show that the evolution of these trays is dependent on equilibrium conditions established between the amount of infiltrating water and evaporation. If there is an insurge of water (as during a wetter climatic interval), then dripping water may form stalactites ("claws") on the bottom of trays (the trays are the "hands" from which the stalactite "claws" hang). But if the infiltration of water slows down or stops (as during a drier climatic interval), a new tray tier may grow at the bottom of these stalactites. The fact that the gypsum trays in Torgac Cave only occur at or near the ends of large (3 to 4 m long) gypsum stalactites (Fig. 4) may reflect drier climatic conditions during the Holocene in the central New Mexico area (Harris, 1985). During wetter periods in the Pleistocene (e.g., the Wisconsin glacial), the large gypsum stalactites may have formed. Then, during the much drier Holocene, the trays could have formed, with small oscillations in climate during this time causing the multiple tray tiers. The fact that some of the trays appear to be "dead" while others are "active" (with water dripping off them) may be the result of seepage patterns, or it may indicate different evaporative conditions within different parts of the cave due to air flow patterns. Where dry desert air descends into the cave along entrance breakdown, evaporation may cause certain trays to be inactive, whereas in more humid passages, the trays may still be growing.

In Torgac, the trays are present in the middle to upper (above ~2m) portions of the passages, but documented trays (both carbonate and gypsum) in other caves are located closer to the floor. This aberrant distribution may reflect microclimate variations in Torgac brought about by its multiple collapse entrance. In a large cave system like Carlsbad Cavern, cold, dry air flows into the cave along the floor, and it is always here, near the floor, that "popcorn lines" and associated trays form (Hill, 1987). But in Torgac, air flow is down many entrance holes, causing local evaporation gradients where trays are not necessarily located near the floor. This distribution also correlates with the findings of Forbes (this issue) where the highest microclimate relative humidities in Torgac were measured within 0.3 m of the floor (92%) and ceiling (90%), and with a relative humidity minimum (83%) at 1.2 m. This height may correspond to the zone of maximum air flow and region of preferred growth for gypsum trays in Torgac.

CONCLUSION

Trays are a speleothem type whose origin and mechanism of formation is still not well understood. Further work needs to be done on the critical microclimate conditions needed for gypsum (and carbonate) tray development.

ACKNOWLEDGEMENTS

Support for this paper was provided by Dave Jagnow, who helped with observations, took photographs, and led trips into Torgac Cave; Jeffrey Forbes, who conducted meteorologic measurements in the cave; and Cyndi Mosch, who provided insight into climatic processes and mineralogy. The Bureau of Land Management, Roswell District, provided research permits and allowed access to the cave; Mike Bilbo, cave specialist for the Roswell District, provided professional and personal support for this project.

REFERENCES

Calaforra, J.M. & Forti, P. (1994). Two new types of gypsum speleothems from New Mexico: gypsum trays and gypsum dust. *National Speleological Society Bulletin 56*(1): 32-37.

Forbes, J. (1998). Air temperature and relative humidity study: Torgac Cave, New Mexico. *Journal of Cave and Karst Studies 60*(1): 27-32.

Harris, A.H. (1985). *Late Pleistocene Vertebrate Paleoecology of the West*. University of Texas Press, Austin: 293 pp.

Hill, C.A. (1982). Mineralogy of Torgac Cave. *Cave Research Foundation Annual Report*: 17-18.

Hill, C.A. (1986). The origin of "trays" (Flat-bottomed popcorn) in Carlsbad Cavern. *Cave Research Foundation Annual Report*: 14-16.

Hill, C.A. (1987). Geology of Carlsbad Cavern and other caves in the Guadalupe Mountains, New Mexico and Texas. *New Mexico Bureau of Mines and Mineral Resources Bulletin 117*: 150 pp.

Hill, C.A. & Forti, P. (1986). *Cave Minerals of the World*. National Speleological Society. Huntsville, Alabama: 286 pp.

Jagnow, D. (1998). Bat usage and cave management of Torgac Cave, New Mexico. *Journal of Cave and Karst Studies 60*(1): 33-38.

Martini, J. (1986). The trays: an example of evaporation-controlled speleothems. *Bulletin of the South African Speleological Association 27*(1): 46-51.

Charles H. Anderson, Jr., Christopher J. Behrens, Gary A. Floyd and Mark R. Vining-Crater Firn Caves of Mount St. Helens, Washington. *Journal of Cave and Karst Studies 60*(1): 44-50.

CRATER FIRN CAVES OF MOUNT ST. HELENS, WASHINGTON

CHARLES H. ANDERSON, JR., CHRISTOPHER J. BEHRENS, GARY A. FLOYD AND MARK R. VINING
International Glaciospeleological Survey
547 SW 304 St., Federal Way, WA 98023 USA

Systematic observation, photo-reconnaissance, mapping, and sampling were performed in the crater firn caves of Mount St. Helens, Washington, from 1981 through 1996 by members of the International Glaciospeleological Survey in cooperation with the United States Forest Service and Mount St. Helens National Monument.

Mount St. Helens is an active dacitic volcano, which is currently in a semi-dormant state after a catastrophic explosive eruption in May 1980. A dacite dome occupies the crater and plugs the volcanic vent. The crater area has been progressively covered by a layer of snow, firn, and glacier ice since as early as 1986. Heat, steam, and volcanic gases from the crater fumaroles melted over 2415 meters of cave passage in the crater ice mass. The caves are in approximate balance with the present geothermal heat release. Future changes in the thermal activity will influence the dimensions, location, ceiling, wall, and wall ablation features of these caves. Cave passages are located above fumaroles and fractures in and adjacent to the crater lava dome. Cave passages gradually enlarge by ablation, caused by outside air circulation and by geothermal sources beneath the ice. The passages form a circumferential pattern around the dome, with entrance passages on the dome flanks. Passages grow laterally and vertically toward the surface, spawning ceiling collapse.

The crater ice body has been expanding since 1986 and its mean density increases each year. It possesses at least two active crevasses. Trends and changes in geothermal activity in the crater of Mount St. Helens have been noticeable through cave passage observation and re-mapping.

This paper describes the crater firn caves of Mount St. Helens, Washington, a system of melt passages in firn ice in the crater of an active Pacific Rim volcano. Observations described were conducted from 1981 through 1996. Glaciologists have made mention of firn, crater, steam, and geothermal caves (Kiver & Mumma, 1975; Kiver & Steel, 1975), and sometimes have dealt with their origin to a limited degree. No one has provided timely observation of the evolution of geothermal ice cave systems in detail. International Glaciospeleological Survey (IGS) members are currently conducting these studies in the crater firn caves of Mount St. Helens, and have done so in an ongoing fashion throughout the development of the crater snowpack. This study documents an unique opportunity to capture data on the interaction of geothermal energy and alpine snowpack accumulation from its inception after the eruption of the volcano in 1980.

Crater reconnaissance in 1981 preceded annual surveys that began in 1982 with mapping, documention, and photography of cave passages, snow, firn, and glacier ice (Fig. 1). Several years of observations and data have been collected, but they have not been systematically interpreted at this point. We have examined temporal relationships of the behavior of the system in terms of cause and effect. Our conclusions are based on preliminary results and qualitative interpretation. We intend to offer what explanation we can for the trend of development observed in crater firn caves at Mount St. Helens.

Figure 1. One of the crater firn caves of Mt. St. Helens. Photo courtesy of Rob Huff.

GEOLOGIC SETTING

LAVA DOME AND CRATER

Pringle (1993) summarized the geology of Mount St. Helens. The Lava Dome consists of dacite. The west crater wall exposes a good cross-section of the volcano before the 1980 eruption. The lower section of the crater wall consists of a dacite dome of Pine Creek age (~3000-2500 yrs B.P.). This dacite dome is cut by dikes of the Castle Creek age

Figure 2. Photo showing a cross section of the volcano before the 1980 eruption and the 330 m high lava dome in the crater of Mt. St. Helens. Photo by Charles H. Anderson, Jr.

(~2500-1500 yrs B.P.), some of the feeder dikes for the Cave Basalt Eruption that formed Ape Cave. Above the Cave Basalt is the dacite summit dome of Kalama Age (~500-200 yrs B.P.), the pre-1980 summit dome of Mount St. Helens (Fig. 2).

ERUPTION HISTORY

Mount St. Helens is located in the southwest Cascade Mountains of Washington State, U.S.A. Mount St. Helens has been called the most violent, active volcano in the United States. It erupted at 8:32 a.m. on May 18, 1980, sending billowing columns of ash high into the atmosphere (Tilling et al., 1990). The eruption was preceded seconds earlier by a magnitude 5.1 earthquake, which caused a large portion of the north flank of the mountain to slide. Immediately afterward, an explosive lateral blast was directed northward through the still-moving slide block, closely followed by a summit eruption of ash and steam.

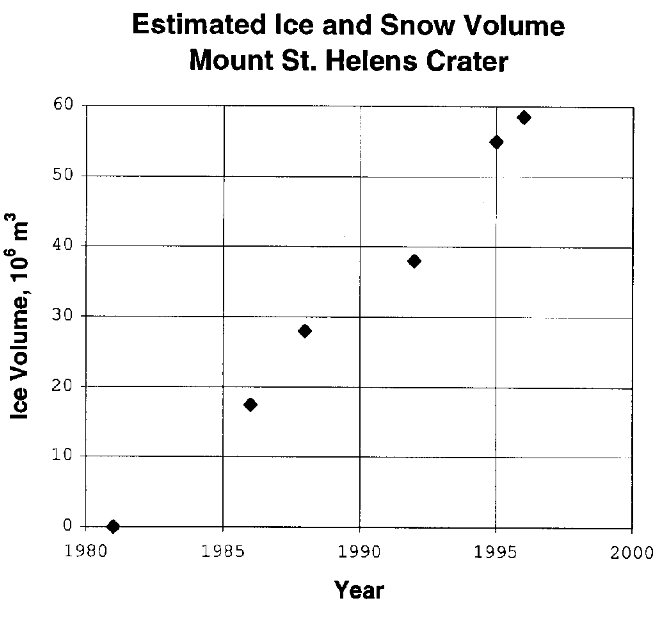

Figure 3. Ice and snow volume in the crater of Mt. St. Helens.

On May 19, 1980, when the extent of damage to the volcano was revealed, the entire north flank was gone. The greatly enlarged and deepened crater was horseshoe-shaped, open to the north with the south of the mountain then the highest part of the volcano at ~2502 m msl. The lip of the open crater on the north was estimated to be about 1890 m msl. Mount St. Helens remains a potentally active and dangerous volcano, though it now (1997) appears quiescent. In the last 515 years, it produced four major explosive eruptions and dozens of lesser eruptions.

On June 15, 1980, the formation of a small lava dome on the floor of the crater was evident. The ~185 m in diameter dome was less than 37 m high. By June 23, 1980, it had grown to be 200 m long and 60 m high. From May 1980 to October 1986, there have been a series of 16 dome-building eruptions, constructing the new 305 m (1,000 feet) high and 915 m wide lava dome in the crater formed by the May 18, 1980, eruption (Swanson & Holcomb, 1989). The nearly 1.6 km wide, 3.2 km long, 610 m deep crater is so large it makes the lava dome seem small (Fig. 2). The Washington Monument placed in the crater would only be half as high as the lava dome.

EFFECTS ON PRE-EXISTING GLACIERS OF MOUNT ST. HELENS

From analysis of USGS topographic maps, the May 1980 eruption removed all of the Loowit and Leschi Glaciers and parts of the Ape, Forsyth, Nelson, Toutle, Shoestring, Smith and Wishbone Glaciers, more than 70% of the pre-eruption ice volume. Only two unnamed glaciers on the south side suffered no net volume loss of ice during the eruption. The eruption removed Forsyth and the Shoestring Glaciers zones of snow accumulation and ~75% of their volumes of glacier ice. As a result, the Shoestring Glacier has suffered significant ablation.

In 1981, following the great eruption, a surge occurred in Shoestring Glacier. Apparently, the weight of volcanic debris, added to a fairly heavy snow load in the winter of 1980-81, produced a sudden budget overbalance in spite of removal of a substantial portion of the original ice volume. The surge behavior was not repeated the following year.

SNOW, FIRN, AND ICE IN MOUNT ST. HELENS CRATER

The shade from the high, steep crater walls to the south and west protects a large volume of the snow and ice that is presently accumulating in Mount St. Helens Crater. Crater ice volume increased from ~2.8 x 10^7 m^3 of uncompacted snow and firn in 1988 to over 5.5 x 10^7 m^3 in 1995. These figures are derived from published USGS figures modified by consideration of thickness data collected from direct cave observation. As of late 1996, the crater was estimated to have 5.85 x 10^7 m^3 of ice, firn, and snow (Fig. 3).

During the winters since 1982, snow and ice avalanches from the crater walls contributed to the formation of a snow and ice field on the south (interior) side of the lava dome. The accumulation of avalanche material from the crater walls

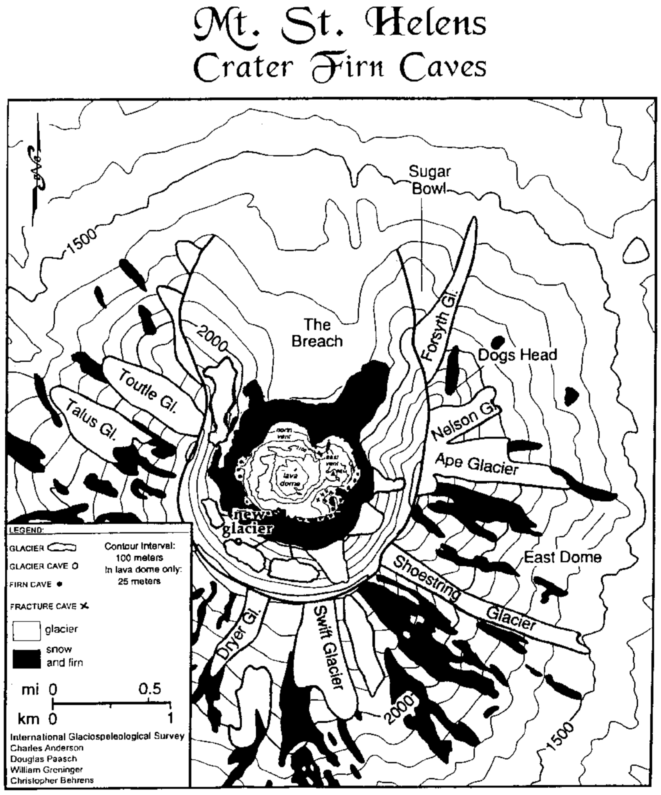

Figure 4 (above) and Figure 5 (below).

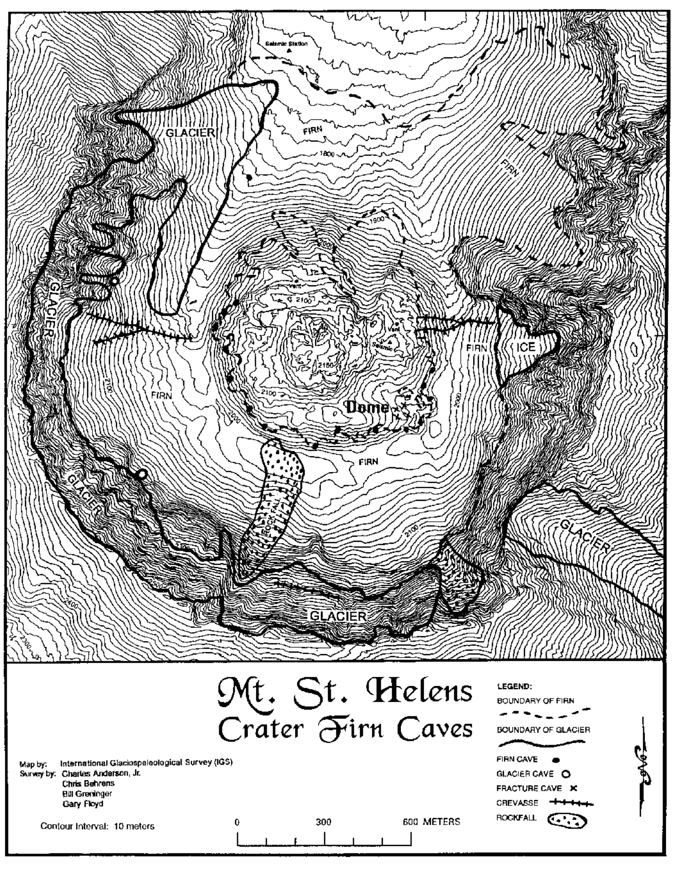

helped form an ice field ~60 m thick, based on crater firn cave surveys. The crater icefield is an incipient glacier that continues to grow.

The snow and ice on the south crater wall behind the lava dome have crevasses and flow features that show that a new glacier is forming (Fig. 4). The ice mass shows signs of ice flow around both sides of the lava dome and flowing out to the front of the dome. The rate of advance may be greater than any other glacier in the contiguous U.S. in recent centuries. The new glacier is forming between the south crater wall and the lava dome (Fig. 5). Snow stacking higher each year locally compresses the lower layers into glacial ice. There are at least two radial crevasses in the permanent ice field. One crevasse is located on the northwest side and another is on the northeast side of the crater, near the lava dome. Both crevasses penetrate through the lowermost layers of the permanent ice field. The crevasse on the northwest side was revealed when the roof of an ice cave collapsed, due possibly to thrust fault activity in the crater floor around September 1994. The ice density in

Figure 6. The firn section of the ice mass in the crater of Mt. St. Helens showing a large crevasse. Crevasses are located at the northwest and northeast sides of the crater near the lava dome. Photo by Charles H. Anderson, Jr.

September 1994 at the base of this crevasse was 0.85 g/cm^3. The ice density in the lowest cave passage was 0.86 g/cm^3 (September 1996; see Fig. 6). Density measurements were performed using a cylindrical saw, and by weighing and measuring the cut samples in the field.

PROGRESSIVE RECRYSTALLIZATION

When winter's snowpack survives the summer and is buried by the following winter pack, the buried snow layer compacts and recrystallizes. New-fallen snow has a density of 0.06 to 0.08 g/cm^3. As water percolates through the snowpack and daily temperatures fluctuate, individual snowflakes metamorphose first to subspherical porous grains and later to granules of solid ice (corn snow). Density of the snowpack rises from ~0.1 to ~0.3 g/cm^3. When snow recrystallizes so that its density reaches an arbitrary value of 0.55, it becomes firn. As long as the firn has air pockets, the recrystallization process can increase its density. After 25 to 150 seasons, the density in a glacier reaches 0.88 g/cm^3 or more. Density of solid ice is ~0.92 g/cm^3. The process only continues if the confining pressure increases (Sharp, 1960).

Generally in the ice caves, firn is distinguished from recrystallized recent snow (corn snow) by stratigraphic relationships. Glacial ice forms from firn at a density of 0.82 g/cm^3, at which point the individual crystals become firmly interlocked with one another and the material possesses an inherent hardness (Sharp, 1960).

Multiple years of winter snowpacks were preserved between 1986 through 1997 and provided the pressure necessary to convert crater snowfall into a permanent firn field. As recrystallization continued in the deepest layers, the glacial ice formed a rigid fabric with limited permeability. From 1986 to 1996, gradual increases in basal ice densities were subjectively observed (though not measured) in cave passages, including the transition from snow to firn to ice. An apparently abrupt decrease in percolating water was noted in the final stage of this transition. We interpret this condition to result from bulk freezing in intergranular pores. Clearly, after a series of heavy winters and/or mild summers, there can be such a sequence of yearly net accumulations that it would take many years to degrade the body enough to remove them. In this way a "permanent" glacial core developed and is perpetuated in the Mount St. Helens crater.

GEOTHERMAL ACTIVITY IN THE CRATER

The Mount St. Helens lava dome is the locus of the active volcanic vent. It, therefore, is a source of volcanic gas emissions. The caves are a primary result of the concentration of heat in an ice-and-snow covered terrain. They are localized at active fumaroles and form as conduits of escape for the heated gases. They are further modified by the drainage of heated surface water from the dome directly into the ice body.

Periodic observations and resurveys of cave passages, noting changes in passage dimensions and location, enabled the detection of heat-flow changes and of locations of volcanic emanations. Sulfurous fumes locally occur in the caves. Hundreds of small fumaroles emit considerable quantities of steam that frequently impair visibility in the firn caves and make mapping, photography, and other observations difficult. Some of these fumaroles make audible hissing and gurgling noises. Although the rising heat and steam cause the ice walls and ceilings to drip constantly, no appreciable quantities of standing or flowing water have been observed in the caves.

Gases from the numerous fumaroles and slowly circulating surface air mix throughout the cave passages. The degree of such mixing is most obviously recognized by the presence of breathable air throughout the known cave system. We have not observed stagnant or poisonous air compositions. Routine safety practice include carrying portable hydrogen sulfide and carbon monoxide detectors during new passage exploration. Many of the larger cave rooms provide a protected environment for monitoring volcanic gas composition. These rooms are ideal sites for prolonged monitoring of changes in volcanic emanations because they are relatively easy to find and their narrow connections with the upslope cave passages prevent rapid mixing with outside air.

If Mount St. Helens were to begin another eruptive phase, the first indications may be changes in the firn cave morphology (triggered by increased heat flow), together with increases in volcanic gas concentrations and microseismic activity. Passages may enlarge due to increases in the volume and temperature of steam and gas emissions from the fumaroles. Such observations might signal danger.

CRATER FIRN CAVES OF MOUNT ST. HELENS

The crater firn caves are located in firn ice behind the lava dome of Mount St. Helens. The firn ice field is elongated east-to-west with a steep crater headwall rising up to 2550 m (8365 ft) on the south margin (Fig. 5). The firn ice field proper is

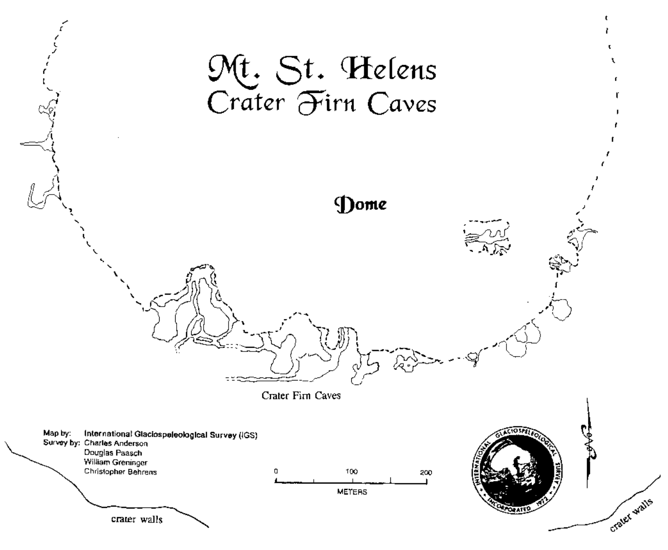

Figure 7. The Mt. St. Helens Crater Firn Caves System as mapped in 1996.

Figure 8. One of the crater firn caves, looking up at scallops on the cave walls. Photo by Charles H. Anderson, Jr.

Figure 9. Ice stalagmite in the crater firn caves near the lowest passage. Photo by Charles H. Anderson, Jr.

below the headwall on the southeast wall of the crater, rising to a maximum elevation of 1990 m (6520 ft) on the south side of the lava dome, and sloping downward to the northeast. Further to the northeast, the firn ice field rises gently to a saddle (1890 m or 6200 ft msl) adjacent to the crater wall.

The caves are called firn caves because ice density ranges from 0.55 to 0.82 g/cm^3. Sub-ice fumaroles and warm air currents form and maintain the cave passage beneath the ice field behind the lava dome. Heat and steam from the crater fumaroles melted over 2,415 m of cave passage in the crater ice mass (Fig. 7). The caves are interpreted to be approximately in balance with the present geothermal heat release because they have reached an apparently stable morphology. Future changes in the thermal activity will influence the dimensions, location, ceiling, wall, and wall ablation features of these caves. Rapid enlargement forms "steam cups" (Kiver & Steel, 1975). Air circulation converts these to the typical scalloped ceiling and wall form ubiquitous in ice caves (Anderson et al., 1994).

Entrances to 15 firn caves have been identified around the perimeter of the lava dome. These caves were mapped in 1996 (Fig. 7). Some have spectacular large rooms. Most have small rooms and crawlways. Cave features include scalloped surfaces of ceilings and walls, moulins in the ceiling, multiple domes connected by crawlways, skylights, and, in winter, helictites, stalactites, and stalagmites of ice (Figs. 8 & 9). Room sizes in 1996 varied from 12 m x 24 m x 6 m high to 4.6 m x 4.6 m x 2.4 m high. The caves are generally associated with fumaroles. Other caves form on the crater and dome walls where melt water undermines the firn and glacial ice.

Six main entrances and numerous smaller ones behind the lava dome lead down the 40º sloping crater floor immediately adjacent to the dome (Fig. 10). The perimeter passage is surprisingly horizontal. The horizontality may be controlled by localized thermal activity along an arcuate fault or fracture zone within the lava dome. An arcuate distribution of thermal anomalies suggests that volcanic emanations are escaping around a plug-like lava body (the dome itself) in the vent and also suggests a circumferential trend. Descending passages have vertical sides and ceilings that are convex upward. Passages paralleling the slope contours are commonly shaped like right triangles with the 90º angle located at the junction of the downslope ice wall and the ice ceiling. The floor slopes are about 30º where mud to boulder-size volcanic rubble occur and occasionally over 40º where bedrock is

Figure 10. Team members climbing down the lava dome to the entrance of the lowest passage which is parallel to the lava dome. Photo by Charles H. Anderson, Jr.

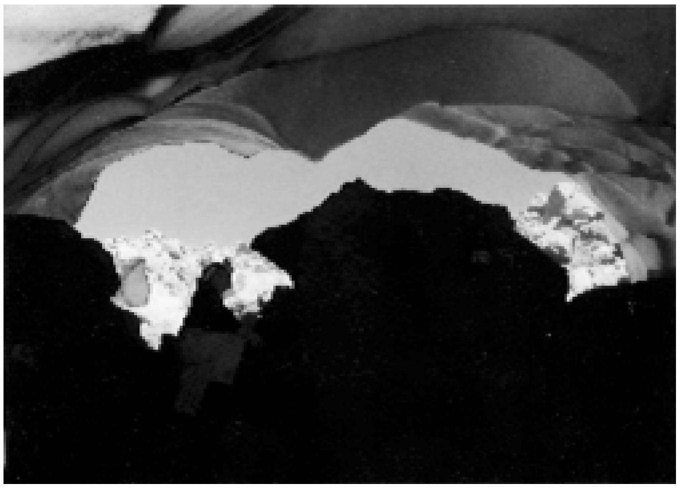

Figure 11. Climbing from an ice cave entrance with the lava dome in the background. Photo by Charles H. Anderson, Jr.

exposed (Fig. 11).

Ridge-like accumulations of rock debris from the lava dome occur in many places on the floor against or near the ice wall of the passage (Fig. 12). They are composed of unsorted, unstratified mud and rock debris derived from the upslope portion of the cave floor. They occur toward the center of the floor in some sites and in others closer to or in contact with the downslope ice wall. They probably represent talus formed against a downslope ice wall. This wall appears to retreat in response to temperature fluctuations. Fluctuation may be due to normal seasonal changes or to changes in volcanic thermal activity.

Ablation Process

Evaporation/sublimation and heat conduction are the major active processes of ablation within the cave (Anderson et al., 1994). Since caves are sheltered from sunlight, radiation from the sun has no effect, but radiant heat from the heated ground and fumaroles may have an appreciable effect. The main control of cave ablation is the amount of air flow against the walls of the cave. Since the crater cave passage networks extend over vertical distances, convective circulation affects the ice cave system, especially volcanic heat sources. The flow rate is greatest in the least restrictive passage morphology. Since the ablation rate is faster where air flow is greatest, trunk passages will be initiated and become dominant.

External Air Communication

As cave ablation and surface ablation continue through a summer season, the cave ceiling often approaches and intersects the ice surface over time. If the ice is fractured, or perhaps after winter snow adds weight to the ceiling, a cave passage may experience ceiling failure. In either case, the cave system suddenly gains a vent to outside air. The effect of venting in summer is to allow cold cave air out and warm outside air in. The effect is reversed in winter. Any superimposed restriction in the system, such as winter snow or rockfall blocking other entrances, exaggerates the importance of ablation vents. The vent entrance is a major means of communication with outside air. When all vents to the surface are closed, ordinary glacier caves become dormant. In crater firn caves that contain internal heat sources, the ablation process can continue by convection even when all external openings are blocked. The system is, therefore, less seasonally dependent and may evolve much faster than an ordinary glacier cave.

Crater Access at Mount St. Helens

Crater access in the Mount St. Helens Administrative Closure Area is through a permit for scientific research issued to the International Glaciospeleological Survey by the United

Figure 12. The lowest cave passge where glacier ice is showing on September 29, 1996. Photo by Charles H. Anderson, Jr.

States Forest Service. Specific application is required by the Forest Service for each crater visit. The crater is closed to public access, and anyone found without a crater permit within closed areas can be arrested and fined.

HAZARDS OF CRATER CAVE STUDY

Since Mount St. Helens is active, there is an ever-present danger of volcanic eruption occurring while exploring the crater area (USGS, 1994). Since November 1986, Mount St. Helens has been relatively quiet except for occasional steam explosions and ash plumes reaching as high as 5.6 km msl (Swanson et al., 1987; Tilling et al., 1990). Even a small eruption of this type would be life threatening to anyone in the crater, if for no other reason than the poisonous nature of volcanic gases. Explosions have thrown rocks more than 1.0 km from the lava dome and have generated small pyroclastic flows in the crater. Although these explosions generated widespread public interest, they have been confined to the crater. In the recent geologic past, when pyroclastic flows encountered an abundant water supply (perhaps snow and ice), they generated volcanic debris flows (lahars) that have been traced more than 16 km from the crater down Mount St. Helens' north flank and connecting valleys (Wolfe & Pierson, 1995).

Inside the crater there are many rockfalls from the crater walls and the lava dome. These rockfalls pose a significant hazard to explorers entering the crater between August and November. In winter, snow avalanches off the crater walls and the lava dome has been large enough to flow out of the crater.

The ice caves themselves present a hazard in the snow field areas. These caves are changing each day and explorers must expect the entrances to collapse as cave passages grow internally by melting. At any time during the hottest time of the day from June through September, roof collapse can occur spontaneously. At any time, day or night, traverse over potentially thin roof ice is dangerous, and should be met with the same caution and preparation as for glacier traverse in the presence of hidden crevasses. Ice caves can also trap SO_2, H_2S, and CO_2 gas emitted by the volcanic fumaroles throughout the lava dome area. Breathable air is displaced by these gases, and people have died entering ice caves formed in these conditions on Mount Hood in Oregon (Kiver & Mumma, 1975).

CONCLUSIONS

The results of this ongoing study will lead to a more thorough understanding of crater firn cave evolution at Mount St. Helens or any locale where ice accumulation interacts with geothermal energy. Cave formation was initiated above fumaroles located along fractures in and adjacent to the lava dome. Cave passages gradually enlarge by ablation, caused by outside air circulation and by geothermal sources beneath the ice. Passages grow laterally and vertically toward the surface, spawning ceiling collapse. The network of fumaroles have produced a ring of relatively horizontal passage connected to the surface by a number of ascending entrance passages.

An ice body is forming and expanding in the Mount St. Helens crater. Its mean density is increasing with each passing year, and the transition from snow to firn to glacier ice (with active crevasses) has been observed. Net budget balances have been positive in the crater since 1986, when the snowpack was first subjectively recognized to be growing.

Trends and changes in geothermal activity in the crater of Mount St. Helens have become noticeable through cave passage observation and remapping. Our detailed mapping and investigations of the crater cave system should furnish a more sensitive indicator of geothermal activity than is furnished by remote surveys.

ACKNOWLEDGMENTS

The authors are grateful to IGS members and to staff of the U.S. Forest Service of Mount St. Helens National Volcanic Monument. Special thanks are given to Peter Frenzen (Monument Scientist), James Quiring (U.S. Forest Service), and Don Swanson (U.S. Geological Survey).

REFERENCES

Anderson, C.H. Jr., Vining, M.R., & Nichols, C.M. (1994). Evolution of The Paradise/Stevens Glacier Ice Caves. *National Speleological Society Bulletin 56*(2): 70-81.

Kiver, E.P. & Mumma, M.D. (1975). Mount Baker Firn Caves, Washington. *The Explorers Journal 53*: 84-87.

Kiver, E.P. & Steel, W.K. (1975). Firn Caves in the volcanic craters of Mount Rainier, Washington. *National Speleological Society Bulletin* 37: 45-55.

Pringle, P.T. (1993). Roadside geology of Mount St. Helens National Monument and vicinity. *Washington Department of Natural Resources Division of Geology and Earth Resources Information Circular* 88: 24-29.

Sharp, R.P. (1960). *Glaciers*. Eugene, Oregon. University of Oregon Books: 78 p.

Swanson, D.A., Dzurisin, D., Holcomb, R.T., Iwatsubo, E.Y., Chadwick, W.W. Jr., Casadevall, T.J., Ewert, J.W., & Heliker, C.C. (1987). Growth of the lava dome at Mount St. Helens, Washington (USA), 1981-1983. In Fink, J.H. (ed.) *The Emplacement of Silicic Domes and Lava Flows. Geological Society of America Special Paper 212*: 1-16.

Swanson, D.A. & Holcomb, R.T. (1990). Regularities in growth of the Mount St. Helens dacite dome, 1980-1986. In Fink, J.H. (ed.) *Lava Flows and Domes: Emplacement Mechanisms and Hazard Implications.* International Association of Volcanology and Chemistry of the Earth's Interior, *Proceedings in Volcanology 2*, Springer Verlag: 3-24.

Tilling, R I., Topinka, L. & Swanson, D A. (1990). *Eruptions of Mount St. Helens: Past, Present, and Future*. U.S. Geological Survey general interest publication (no publication number): 56 p.

USGS. (1994). *Preparing for the Next Eruption in the Cascades*. United States Geological Survey Open-File Report 94-585.

Wolfe, E. W. & Pierson, T. C. (1995). *Volcanic-Hazards Zonation for Mount St. Helens, Washington, 1995*. USGS Open File Report 95-497.

HYDROBASALUMINITE AND ALUMINITE IN CAVES OF THE GUADALUPE MOUNTAINS, NEW MEXICO

VICTOR J. POLYAK
Department of Geosciences, Texas Tech University, Lubbock, Texas 79409-1053 USA

PAULA PROVENCIO
Sandia National Laboratories, Albuquerque, New Mexico 87185 USA

Hydrobasaluminite, like alunite and natroalunite, has formed as a by-product of the H_2S-H_2SO_4 speleogenesis of Cottonwood Cave located in the Guadalupe Mountains of New Mexico. This mineral is found as the major component of white pockets in the dolostone bedrock where clay-rich seams containing kaolinite, dickite, and illite have altered during speleogenesis to hydrobasaluminite, amorphous silica, alunite, and hydrated halloysite (endellite). Gibbsite and amorphous silica are associated with the hydrobasaluminite in a small room of Cottonwood Cave. Opalline sediment on the floor of this room accumulated as the cave passage evolved. Jarosite, in trace amounts, occurs in association with the opalline sediment and most likely has the same origin as hydrobasaluminite and alunite. The hydrobasaluminite was found to be unstable at 25ºC and 50% RH, converting to basaluminite in a few hours. Basaluminite was not detected in the cave samples.

Aluminite has precipitated as a secondary mineral in the same small room where hydrobasaluminite occurs. It comprises a white to bluish-white, pasty to powdery moonmilk coating on the cave walls. The bedrock pockets containing hydrobasaluminite provide the ingredients from which aluminite moonmilk has formed. It appears that recent cave waters have removed alumina and sulfate from the bedrock pocket minerals and have deposited aluminite and gypsum along the cave wall. Gypsum, amorphous silica and sulfate-containing alumina gels are associated with the aluminite moonmilk.

We report the occurrence of hydrobasaluminite as a by-product of speleogenesis and aluminite as a secondary deposit (moonmilk) in Cottonwood Cave of the Guadalupe Mountains in New Mexico. A description of the depositional setting and mineralogy, and a brief discussion on the origin of these two hydrated aluminum sulfate minerals are presented.

Hydrobasaluminite, $Al_4SO_4(OH)_{10}\cdot(12\text{-}36)H_2O$, has been previously reported only in Alum Cave, Sicily, Italy (Forti, 1997). Its origin is related to the oxidation of fumarole gas (containing minor H_2S) and acid weathering of volcanic ash and tuff (Hill & Forti, 1997). Two occurrences of basaluminite, $Al_4SO_4(OH)_{10}\cdot 7H_2O$, have been reported in caves of Japan and South Africa (Hill & Forti, 1997). Basaluminite in the South African cave was reported as a product of evaporation of ore-derived solutions (Martini et al., 1997). In non-cave environments, basaluminite and hydrobasaluminite in association with allophane, goethite, halloysite, gypsum, aragonite, and calcite (rock-milk) have been reported as a coating in fractures, cement in narrow fissures, and as a matrix constituent of brecciated rock in south-central England (Hollingsworth & Bannister, 1950). Srebrodol'skiy (1969) detected basaluminite and gypsum in the oxidized zone of a former U.S.S.R. sulfur deposit. It was reported as coatings in fractures of dolostone. Frondel (1968) noted a similar occurrence of basaluminite with meta-aluminite in association with gypsum along the periphery of a brecciated zone containing pyrite in Utah. Tien (1969) reported hydrobasaluminite and basaluminite associated with iron oxides between Pennsylvanian marine shale and coal in Kansas. Sunderman and Beck (1969) and Ambers and Murray (1995) describe a similar occurrence of hydrobasaluminite between Pennsylvanian limestone and siliclastic materials in Indiana. Basaluminite was reported with gypsum in clay masses within Cretaceous rocks in Maryland (Mitchell, 1970), and as coatings and joint infillings in Eocene shales of the Polish Flysch Carpathians (Wieser, 1974).

The occurrence of aluminite, $Al_2(SO_4)(OH)_4\cdot 7H_2O$, in caves is apparently also rare. Hill and Forti (1997) note only one report by Martini et al. (1997) who describes the aluminite as white, chalky efflorescences on gypsum in an eastern Transvaal, South African cave as an evaporation product of ore-derived solutions. Reports of aluminite occurring in non-cave environments are moderately few as well. The mineral is found in bauxitic deposits and as fissure or joint fillings in brecciated zones. Deposits of aluminite were first noted around 1730 near Halle, Germany (Bassett & Goodwin, 1949). Gedeon (1954) identified aluminite associated with gypsum, calcite, boehmite, limonite, and quartz in a pyritic blue-mottled clay of a bauxite deposit in Hungary. Bárdossy and Sajgó (1968) also reported aluminite in a bauxite deposit in Hungary. Aluminite and basaluminite were reported with gibbsite, nord-

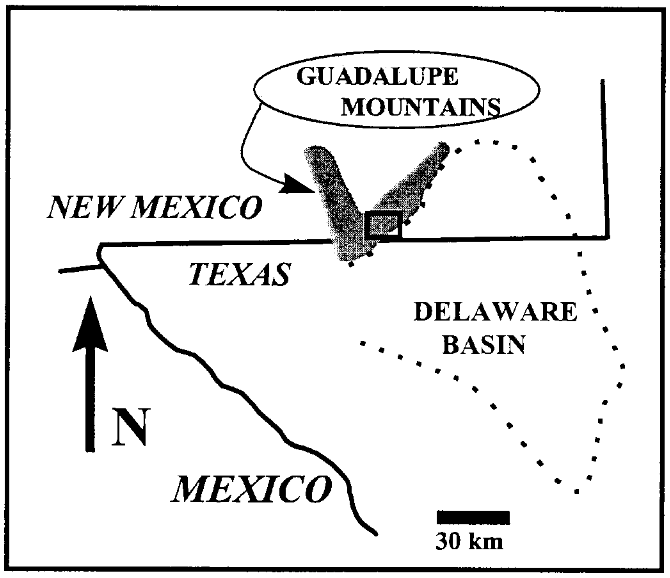

Figure 1. Study area in the Guadalupe Mountains is shown by an open rectangle.

strandite, and bayerite in sediments of solution pipes within Tertiary clays and chalk in southeast England (Wilmot & Young, 1985). The depositional environments of the brecciated rocks, fissures, and joints are similar to the cave environment.

DEPOSITIONAL SETTING

Hydrobasaluminite and aluminite occur in a small room of Cottonwood Cave in the Guadalupe Mountains, New Mexico. The study area is shown in Figure 1. This cave is located in the

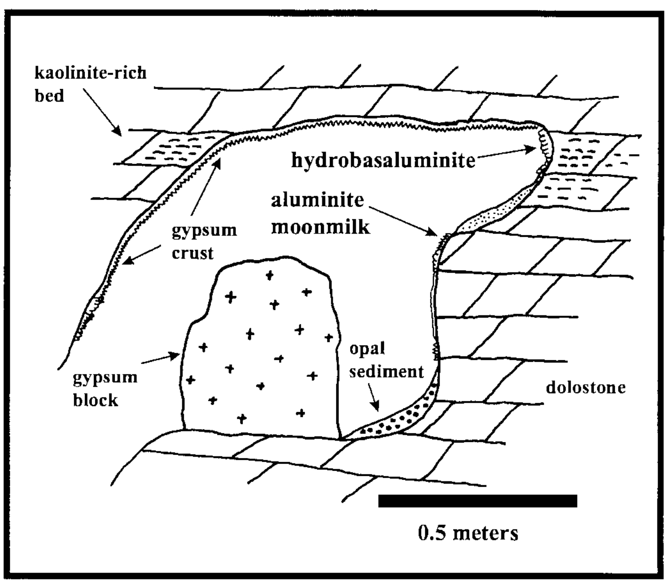

Figure 2. Profile of the small room in Cottonwood Cave where hydrobasaluminite and aluminite occur.

Permian dolostones and limestones of the Capitan Reef Complex, the same group of carbonate rocks in which Carlsbad Cavern is located. Hydrobasaluminite is found in areas of altered bedrock referred to as bedrock pockets by Polyak and Güven (1996). It resembles globules or blebs with the consistency of toothpaste, or loosely to moderately indurated materials with the consistency of a cookie. Aluminite is found as a bright to brilliant white and bluish-white, pasty to powdery, finely crystalline deposit on the cave walls. Carbonate speleothems which are numerous in Guadalupe Mountain caves are lacking in this room. The floor contains a relatively large block of gypsum. Figure 2 shows a profile of the small room where hydrobasaluminite and aluminite are reported. This section of the cave is located stratigraphically within a clay-rich pisolitic dolostone of the Permian Seven Rivers Formation (Jagnow, 1977). A 10-cm thick bed of kaolinite located near the ceiling appears to be a source bed for the hydrobasaluminite. Temperature and relative humidity in this room were measured as 11ºC and 95% during the spring of 1994.

METHODS

X-ray diffraction (XRD), electron microscopy, and energy dispersive spectroscopy (EDS) were used to identify all mineral phases. XRD of random powders and suspended mounts were performed using Cu-Kα radiation. Samples were kept moist until XRD analyses were performed. Moist hydrobasaluminite was packed into a 2-mm deep sample chamber and x-rayed immediately at 1°2θ per minute. The 2-mm thickness prevented rapid dehydration of the hydrobasaluminite. Aluminite moonmilk was examined scanning electron microscopy (SEM) on a Hitachi S-570 at Texas Tech University. Scanning transmission electron microscopy (STEM) and EDS were used to determine semiquantitative elemental compositions on a JEM-100CX analytical electron microscope at Texas Tech University. Transmission electron microscopy (TEM) on a JEM-1200EX at Sandia National Laboratory was used to determine crystal morphology, single crystal quality, and existence of other fine-grained components such as opal. Hydrobasaluminite and aluminite samples were prepared for TEM by suspending powders in deionized water and settling powders onto holey carbon, copper grids. Monoclinic unit-cell parameters reported by Clayton (1980) were used with the Appleman and Evans (1973) indexing and least-squares powder diffraction computer program revised for the PC by Benoit (1987) to index our XRD data. The optical binocular polarizing microscope was used for direct observations of the mineral morphologies.

RESULTS

Hydrobasaluminite occurs in bedrock pockets in dolostone. The mineralogy of the bedrock consists of dolomite, quartz, mica, illite, kaolinite, and dickite. The dolostone is locally rich

Table 1. List of X-ray diffraction data for hydrobasaluminite from Cottonwood Cave.

hkl	*dmeas* (nm)	*dcalc* (nm)	*Imeas*
001	1.259	1.266	100
110	0.808	0.808	4
-111	0.766	0.762	3
002	0.633	0.633	11
-202	0.5920	0.5924	13
-112	0.5623	0.5630	9
012	0.5328	0.5342	3
201	0.5265	0.5272	15
020	0.5002	0.4981	1
120	0.4705	0.4686	24
112	0.4520	0.4516	3
121	0.4218	0.4220	16
-113	0.4152	0.4139	2
202	0.3969	0.3970	19
013	0.3893	0.3885	5
212	0.3690	0.3688	44
-411	0.3477	0.3474	8
-322	0.3409	0.3404	3
130	0.3226	0.3229	19
302	0.3162	0.3187	1
-323	0.3094	0.3095	7
131	0.3062	0.3064	8
312	0.3040	0.3036	2
-230	0.3004	0.2992	1
-422	0.2954	0.2957	14
-511	0.2817	0.2820	15
-513	0.2753	0.2752	1
not indexed	0.2734		5
223	0.2640	0.2638	2
232;-333	0.2544	0.2547	25
-613	0.2385	0.2379	21
240	0.2345	0.2343	9
403	0.2276	0.2279	2
610	0.2242	0.2241	7
340;-621	0.2187	0.2190	7
242	0.2114	0.2110	8
620	0.2090	0.2088	5
432	0.2064	0.2065	12
-711	0.2028	0.2028	18
621	0.1953	0.1954	17
250	0.1914	0.1914	1
612	0.1905	0.1902	2
433;-543	0.1878	0.1879	4
-813; 720	0.1833	0.1833	5
-253; 343	0.1816	0.1817	13
252;-353	0.1780	0.1781	14
153;-823	0.1749	0.1750	1
721	0.1729	0.1729	16
-821	0.1696	0.1696	1
253	0.1677	0.1678	2
542	0.1664	0.1664	2
-902	0.1640	0.1640	1
641;-743	0.1616	0.1616	22
-741; 353	0.1594	0.1593	1
-831; 261	0.1585	0.1585	1
-362	0.1564	0.1564	5
732	0.1518	0.1518	3
-460;-843	0.1494	0.1496	11
362	0.1472	0.1473	6
-752, 651	0.1454	0.1454	7
911	0.1442	0.1442	5

Note: the unit-cell parameters for hydrobasaluminite are: a=1.4930(5)nm, b=0.9963(3)nm, c=1.3695(11)nm, β=112.43(3)º, **V**=1.882(1)nm^3, indexed and compared to the monoclinic unit-cell of Clayton (1980). The numbers in parentheses for the values represent the uncertainties of the last digits.

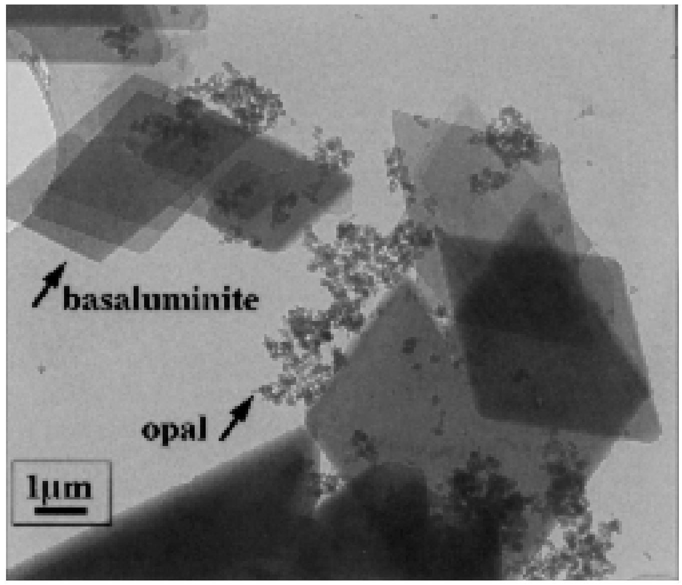

Figure 3. TEM micrograph showing rhomb-shaped platelets of hydrobasaluminite. The platelets have dehydrated to probably basaluminite due to the vacuum of the electron microscope.

in kaolinite in the small room in which hydrobasaluminite and aluminite are found. Weathered bedrock in this area contains pockets that are commonly blackened by manganese mineralization. In other caves of the Guadalupe Mountains, these areas of altered bedrock, usually associated with manganese mineralization, are referred to as bedrock pockets by Polyak and Güven (1996) and contain significant amounts of alunite and hydrated halloysite. In Cottonwood Cave, gibbsite and amorphous silica are abundant in the bedrock pockets containing hydrobasaluminite.

Powder diffraction data for hydrobasaluminite from Cottonwood Cave are listed in Table 1. Unit-cell parameters and powder data for hydrobasaluminite were compared with those of Clayton (1980), and the parameters were determined to be a=1.4930(5)nm, b=0.9963(3)nm, c=1.3695(11)nm, β=112.43(3)°, **V**=1.882(1)nm^3. We note, however, that hydrobasaluminite is insufficiently described in the literature, and further study is needed to find the correct structure and unit-cell for this mineral. The hydrobasaluminite was allowed to dehydrate at 25ºC and 50% RH for 30 hours. XRD results showed that the sample completely converted to basaluminite and the conversion was irreversible when the sample was remoistened. Basaluminite was not found in the cave samples.

Hydrobasaluminite (which dehydrates to basaluminite quickly under the vacuum of the TEM) interspersed with submicron, gel-like, amorphous silica was observed by TEM from powder samples. The rhomb-shaped platelets of hydrobasaluminite, shown in Figure 3, are characteristic of this mineral (Sunderman & Beck, 1969; Tien, 1969; Clayton, 1980; Ambers & Murray, 1995). The amorphous silica occurs as accumulations of submicron gel-like spheres (Fig. 4), or as

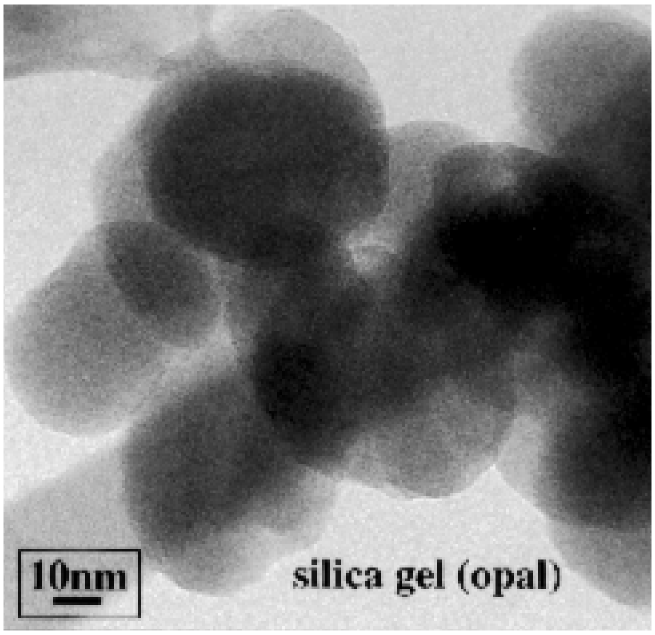

Figure 4. TEM micrograph showing the amorphous silica gel-like material that is associated with hydrobasaluminite.

deci-micron single spheres.

Aluminite occurs as a moonmilk on cave walls where bedrock is exposed. The walls of this small room, however, are mostly covered with a macrocrystalline coating of secondary gypsum. Associated with the aluminite and gypsum coatings are globules of dull white gypsum moonmilk. The floor consists of opal sediment mixed with an accumulation of fallen wall deposits. Faint blue-green to green nodules of opal also occur in the aluminite moonmilk.

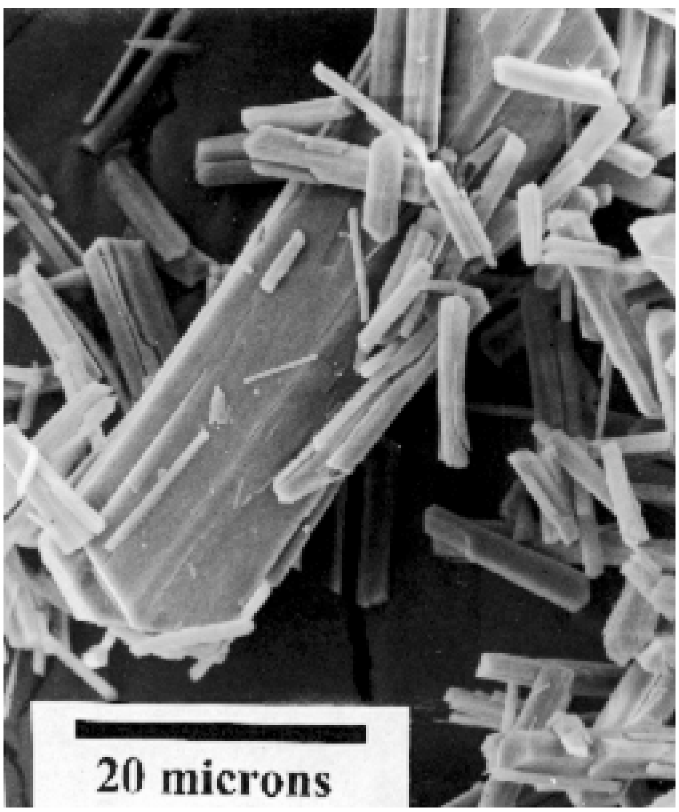

Figure 5. SEM micrograph of aluminite laths.

Unit-cell parameters and powder data for aluminite were compared with those of Sabelli and Ferroni (1978) and Farkas and Werner (1980), and the parameters were determined to be a=0.7419(4)nm, b=1.5791(7)nm, c=1.1650(4)nm, β=110.32(2)°, **V**=1.2783(6)nm^3.

TEM reveals that the aluminite moonmilk is made up of aluminite laths, gypsum prisms, submicron amorphous sulfate-containing alumina spheres (gels), and some amorphous silica spheres. Aluminite crystals are micron to decimicron-sized slender, rod-like to slightly flattened, euhedral laths (Fig. 5). Spheres of sulfate-containing amorphous alumina were observed as branching chains of gel-like spheres with an outer sheath as shown in Figure 6a. The outer sheath is probably an artifact caused by the tertiary butylamine which was used in sample preparation. When the gels dehydrated without the organic coating, they crystallized as fibrous radiating clusters as shown in Figure 6b. Gypsum crystals in the moonmilk are decimicron-sized, stubby, euhedral prisms.

Alunite, gibbsite, hydrated halloysite, and jarosite were identified by XRD, electron microscopy, and EDS. Alunite and hydrated halloysite in caves of the Guadalupe Mountains have been described by Polyak and Güven (1996). Black to dark brown, nearly pure gibbsite was located along a ledge directly below or adjacent to the hydrobasaluminite. Gibbsite was also found to occur in bedrock pockets below Wonderland in Cottonwood Cave, and at the top of the Four O'clock Staircase in Virgin Cave. Gibbsite crystals are decimicron-sized laths. The jarosite was found as small (<mm-sized) yellow pods in the floor opal. Jarosite crystals are micron-sized cube-like rhombs, similar in morphology to alunite.

DISCUSSION

Bedrock pockets in this area of Cottonwood Cave are identical to those of Carlsbad Cavern and Lechuguilla Cave described by Polyak and Güven (1996) which formed by the H_2S-H_2SO_4 speleogenesis mechanism. Pockets of alteration in Cottonwood Cave differ from those noted by Polyak and Güven (1996) by consisting mostly of hydrobasaluminite with only minor amounts of alunite and hydrated halloysite, rather than predominantly alunite and hydrated halloysite. The bedrock pockets are 5 to 50 cm in diameter and show a black (probably hydrous) manganese oxide that stains the pocket margins. The most obvious evidence of H_2S-H_2SO_4 speleogenesis in Cottonwood Cave are remnant "primary" gypsum blocks in the area of the bedrock pockets and other areas of the cave (Hill, 1987; Buck et al., 1994). These blocks are rarely observed in direct contact with the bedrock pockets. Hydrated halloysite (endellite) has also been reported as a H_2SO_4-indi-

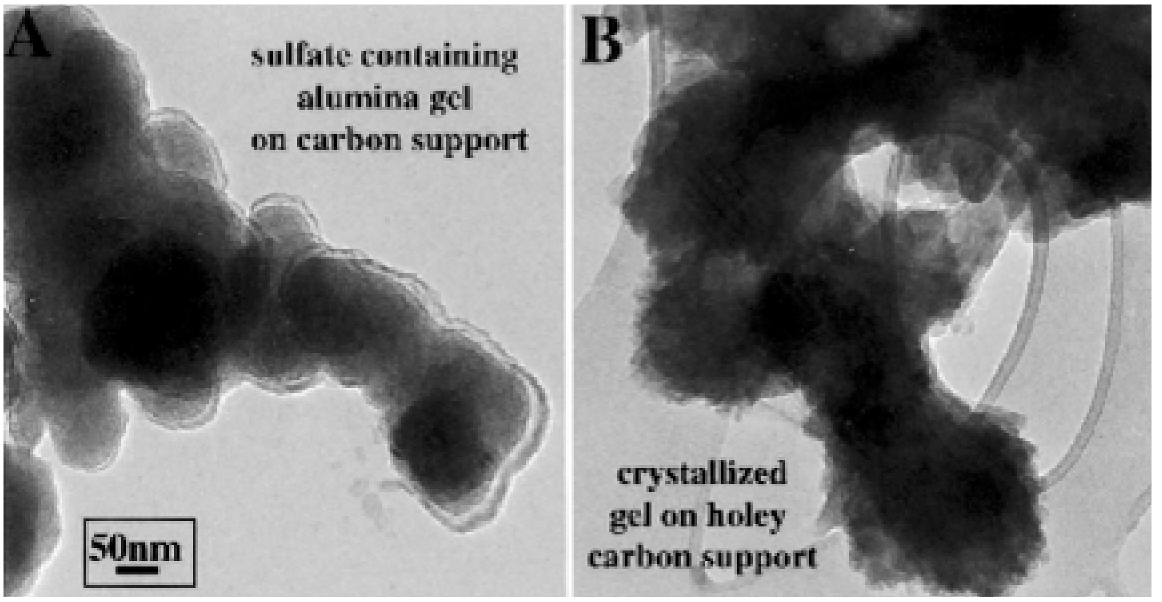

Figure 6. TEM micrograph showing sulfate-bearing alumina gel. (a) A sheath has formed on the alumina gel from tertiary butylamine which is used to disperse small particles during sample preparation. The tertiary butylamine apparently prevents further crystallization of the gel materials during preparation. (b) The alumina gel, without tertiary butylamine, crystallizes upon preparation.

cator mineral in Cottonwood and other caves of the Guadalupe Mountains (Hill, 1987). The bedrock pockets containing alunite, hydrated halloysite (Polyak & Güven, 1996), and hydrobasaluminite are additional evidence of H_2S-H_2SO_4 speleogenesis.

Hydrobasaluminite, like alunite, is an aluminum sulfate and commonly forms from the interaction of kaolinite with H_2SO_4 (Hollingsworth & Bannister, 1950; Adams & Hajek, 1978; Bassett & Goodwin, 1949; Ambers & Murray, 1995; Beecroft et al., 1995). The Cottonwood Cave hydrobasaluminite probably formed in the same way where H_2SO_4-bearing waters altered the kaolinite-rich bed in the dolostone bedrock by the reaction

$$H_2SO_4 + 2[Al_2Si_2O_5(OH)_4] + nH_20 \rightarrow$$
$$Al_4SO_4(OH)_{10}\cdot (n\text{-}4x)H_20 + 4[SiO_2\cdot xH_20],$$

where n≈16-40 and x≈1-5. This reaction suggests that, other than hydrobasaluminite, silica should also be a by-product of the alteration process. Sparsity of K-bearing clay minerals such as illite and smectite favored the production of hydrobasaluminite over alunite as demonstrated experimentally by Adams and Hajek (1978).

Gibbsite and amorphous silica, which are both commonly associated with the hydrobasaluminite, probably have more complex origins. Gibbsite could have formed during H_2S-H_2SO_4 reactions; however, Adams and Hajek (1978) showed that gibbsite is favored by low SO_4/Al and high OH/Al ratios. During speleogenesis the SO_4/Al ratio was probably too high for production of gibbsite. It is possible that the gibbsite formed by the alteration of hydrobasaluminite during higher pH conditions (Ambers & Murray, 1995 and Beecroft et al., 1995). In Cottonwood Cave gibbsite was found close to the kaolinite bed. It was also identified in another area of Cottonwood Cave and in nearby Virgin Cave where it appears to be a product of altered bedrock pockets containing alunite and hydrated halloysite. Formation of gibbsite in this setting would therefore more likely be secondary from seepage and condensation cave waters.

Amorphous silica in Cottonwood Cave probably formed with the hydrobasaluminite during speleogenesis from excess silica produced by the reaction noted above. Amorphous silica spheres were observed with the hydrobasaluminite platelets under the optical and electron microscopes. Silica in the form of chert in Endless Cave and in another area of Cottonwood Cave probably formed in a similar way. In these other locations the chert is near occurrences of alunite and hydrated halloysite rather than hydrobasaluminite. The opal sediment found on the floor immediately below the aluminite moonmilk is indicative of the removal of silica from clays during the development of the cave passage.

The evolution of the cave passage where hydrobasaluminite occurs in Cottonwood Cave, offered in Figure 7, is based on mineralogy and locations of deposits. We propose that gypsum replacement of dolostone bedrock occurred initially along joints or zones of higher permeability. Ascending H_2SO_4-bearing water reacted with kaolinite-rich seams in the dolostone bedrock. Replacement of dolostone by gypsum probably occurred by a process similar to the subaqueous replacement process described by Buck et al. (1994). As replacement of the dolostone by gypsum progressed, so did conversion of kaolinite to hydrobasaluminite and amorphous silica. We envision there was little open cave passage when the gypsum replacement and clay alterations took place. After descent of the water table, seepage and condensate waters began to slowly remove the replacement gypsum, hydrobasaluminite, and

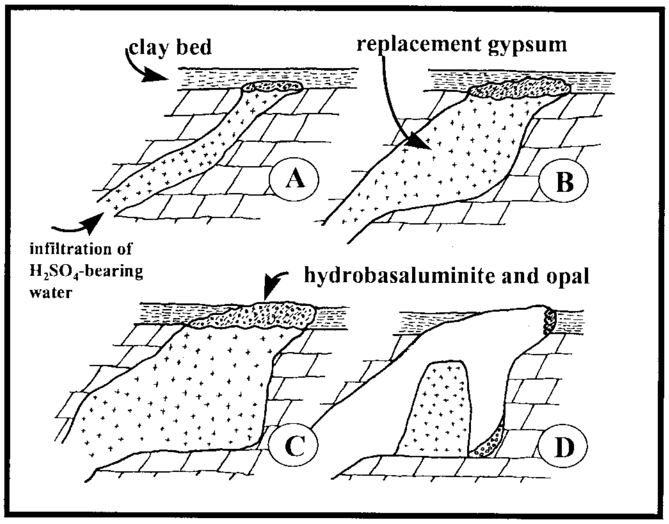

Figure 7. Proposed progression of cave development showing the origin of the cave passage and associated minerals. (A) Initial gypsum replacement of dolostone bedrock occurs along joints or zones of higher permeability. (B) The kaolinite-rich bed serves as a temporary barrier, but is eventually altered to hydrobasaluminite and amorphous silica. (C) Maximum replacement has occurred. (D) After sulfuric acid speleogenesis, seepage and condensate water removed most of the gypsum, hydrobasaluminite, and amorphous silica, forming the open cave passage as it is seen today.

amorphous silica, and eventually formed open cave passage. The absence of drip waters in the area of the hydrobasaluminite has resulted in the protection of these primary features (the remnant gypsum block and hydrobasaluminite globules) since the opening of the cave passage. Except at the bedrock pocket in the clay bed, the alumina phases have since been removed; but the opal has fallen and accumulated on the floor directly below the clay bed. This progression of cave development is illustrated in Figure 7 (A-D).

Aluminite is a secondary deposit of moonmilk on the bedrock surface. The aluminum and sulfate ions for formation of aluminite were supplied by the weathering of hydrobasaluminite, alunite, and gibbsite which are located above in bedrock pockets.

CONCLUSIONS

Hydrobasaluminite is a H_2SO_4-indicator mineral like the primary gypsum, alunite, natroalunite, and hydrated halloysite (endellite) in the caves of the Guadalupe Mountains. Hydrobasaluminite is a product of the interaction of H_2SO_4-bearing waters with a kaolinite-rich bed and other clay minerals in the dolostone bedrock during the formation of Cottonwood Cave.

Aluminite makes up a pasty to powdery deposit (moonmilk) on the cave wall immediately below the hydrobasaluminite and gibbsite deposits. It is a late-stage precipitate, and not a direct by-product of sulfuric acid speleogenesis.

ACKNOWLEDGMENTS

The authors thank Ransom Turner, Kevin Glover, Mike Baskerville, and Mike Harrison of the Lincoln National Forest Service for the collection permits and field assistance. We are very grateful to Necip Güven and Candace H. Haigler of Texas Tech University for use of lab resources. Mark J. Grimson and Anish Kumar assisted with scanning electron microscopy. We thank Carol A. Hill and an anonymous reviewer for reviewing the manuscript. Cyndi J. Mosch and Mike Goar are also thanked for field assistance.

REFERENCES

Adams, F. & Hajek, B.F. (1978). Effects of solution sulfate, hydroxide, and potassium concentrations on the crystallization of alunite, basaluminite, and gibbsite from dilute aluminum solutions. *Soil Science 126*(3): 169-173.

Ambers, C.P. & Murray, H.H. (1995). The role of carbonate bedrock in the formation of Indianaite halloysitic clays. *Indiana Geological Survey Bulletin 65*: 29 p.

Appleman, D.E. & Evans, H.T. (1973). Job 9214: Indexing and least-squares refinement of powder diffraction data. U.S. Geological Survey, Computer Contribution 20, U.S. National Technical Information Service, Document PB2-16188.

Bárdossy, G. & Sajgó, C. (1968). Aluminit in Den Bauxitlagerstätten Von Szoc, Ungarn. *Acta Geologica Academiae Scientiarum Hungaricae 12*: 3-10.

Bassett, H. & Goodwin, T.H. (1949). The basic aluminum sulfates. *Journal of the Chemical Society 1949*: 2239-2279.

Beecroft, J.R.D., Koether, M.C. & vanLoon, G.W. (1995). The chemical nature of precipitates formed in solutions of partially neutralized aluminum sulfate. *Water Resources 29*(6): 1461-1464.

Benoit, P.H. (1987). Adaption to microcomputer of the Appleman-Evans program for indexing and least-squares refinement of powder-diffraction data for unit-cell dimensions. *American Mineralogist 72*: 1018-1019.

Buck, M.J., Ford, D.C., & Schwartz, H.P. (1994). Classification of cave gypsum deposits derived from oxidation of H_2S. In Sasowsky, I.D. & Palmer, M.V. (eds.). *Breakthroughs in Karst Geomicrobiology and Redox Geochemistry*. Special publication 1, Symposium of the Karst Waters Institute; 1994 Feb. 16-19; Colorado Springs, CO. Charlestown, WV. Karst Waters Institute: 5-9.

Clayton, T. (1980). Hydrobasaluminite and basaluminite from Chickerell, Dorset. *Mineralogical Magazine 43*: 931-937.

Farkas, L. & Werner, P. (1980). Powder diffraction studies on aluminite and meta-aluminite. *Zeitschrift fur Kristallographie 151*: 141-152.

Forti, P. (1997). Alum Cave, Vulcano Island, Sicily-Italy. In Hill, C. A. & Forti, P. (eds.). *Cave Minerals of the World*. National Speleological Society, Huntsville, Alabama: 316-318.

Frondel, C. (1968). Meta-aluminite, a new mineral from Temple Mountain, Utah. *American Mineralogist 53*: 717-721.

Gedeon, T.G. (1954). Aluminite (websterite) of Gánt, Hungary. *Acta Geologica Academiae Scientiarum Hungaricae 3*: 27-43.

Hill, C.A. (1987). Geology of Carlsbad Cavern and other caves in the Guadalupe Mountains, New Mexico and Texas. *New Mexico Bureau of Mines and Mineral Resources, Bulletin 117*, 150 p.

Hill, C.A. & Forti, P. (1997). *Cave Minerals of the World*. National Speleological Society, Huntsville, Alabama, 463p.

Hollingworth, S.E. & Bannister, F.A. (1950). Basaluminite and hydrobasaluminite, two new minerals from Northamptonshire. *Mineralogical Magazine 29*: 1-17.

Jagnow, D.H. (1977). *Geologic Factors Influencing Speleogenesis in the Capitan Reef Complex, New Mexico and Texas.* Unpublished M. S. thesis, University of New Mexico, 197 p.

Martini, J.E., Wipplinger, P.E. & Moen, H.F.G. (1997). Mbobo Mkulu Cave, South Africa. In: Hill, C. A. & Forti, P., editors. *Cave Minerals of the World*. National Speleological Society, Huntsville, Alabama: 336-339.

Mitchell, R.S. (1970). An occurrence of basaluminite in Maryland. *Mineralogical Record 1*: 127-128.

Polyak, V.J. & Güven, N. (1996). Mineralization of alunite, natroalunite, and hydrated halloysite in Carlsbad Cavern and Lechuguilla Cave, New Mexico. *Clays and Clay Minerals 44*(6): 843-850.

Sabelli, C. & Ferroni, R.T. (1978). The crystal structure of aluminite. *Acta Crystallographica B34*: 2407-2412.

Sunderman, J.A. & Beck, C.W. (1969). Hydrobasaluminite from Shoals, Indiana. *American Mineralogist 54*: 1363-1373.

Srebrodol'skiy, B.I. (1969). Basaluminite found for the first time in the USSR. Doklady Academy of Sciences, U.S.S.R., *Earth Science Section 180*: 122-123.

Tien, P. (1969). Hydrobasaluminite and basaluminite in Cabaniss Formation (Middle Pennsylvanian), southeastern Kansas. *American Mineralogist 53*: 722-732.

Wieser, T. (1974). Basaluminite in the weathering zone of Carpathian Flysch deposits. *Mineralogia Polonica 5*: 55-64.

Wilmot, R.D. & Young, B. (1985). Aluminite and other aluminum minerals from Newhaven, Sussex: the first occurrence of nordstrandite in Great Britian. *Proceedings of the Geologist Association 96*: 47-52.

BASE-LEVEL CHANGES INFERRED FROM CAVE PALEOFLOW ANALYSIS IN THE LAGOA SANTA KARST, BRAZIL

AUGUSTO S. AULER*

Department of Geography and Geology, Western Kentucky University, Bowling Green, Kentucky 42101 USA
**Current Address: Department of Geography, University of Bristol, Bristol, BS8 1SS, ENGLAND*

The interpretation of flow marks in relict cave passages in two drainage basins in the tropical karst of Lagoa Santa, East Central Brazil was used to characterize past flow routes. Comparison with present groundwater flow deduced from dye tracing was performed in order to assess the evolutionary history of the karst drainage basins. Samambaia Basin's dry caves show that paleoflow in this basin was directed towards other local base levels, suggesting that some fluviokarst features in the basin were generated in a later stage. Paleoflow analysis in the Palmeiras-Mocambo Basin shows that flow direction has not changed significantly since the genesis of today's dry caves. Relict caves can provide useful clues on the paleohydrology of karst areas.

The Lagoa Santa karst area contains two major drainage basins, both possessing underground and subaerial components. Samambaia and Palmeiras-Mocambo basins drain distinct plateaus containing well-developed karst landforms. Although located a few kilometers apart, the basins show distinct paleoflow patterns, suggesting dissimilar histories of drainage basin evolution. A comparative developmental history can be inferred from the analysis of dissolution features in relict caves located inside each basin's boundaries. Local variations in paleoflow direction at the downstream part of Samambaia Basin contrast with the more straightforward evolution of Palmeiras-Mocambo Basin. The data suggest base-level changes during the development of Samambaia Drainage Basin.

The study area is located at Minas Gerais state, East-Central Brazil, about 40 km north from Belo Horizonte, the state capital (Fig. 1). The area lies inside the limits of the municipalities of Lagoa Santa, Matozinhos and Pedro Leopoldo. Several villages occur throughout the area. Limestone quarrying together with agriculture and cattle farming are the main economic activities in the region.

The local geology comprises sequences of Upper Proterozoic limestone of the Sete Lagoas Formation, Bambuí Group, laid over gneiss and migmatite. The karst develops mostly over calcitic limestone with subhorizontal lamination. The limestone is about 200 m thick in the karst plateaus. Cave development is controlled mostly by N75º-85ºE and N-S joints (Beato et al.,1992). Soil cover occurs over most of the karst area. Phyllite and gneiss mark the western limit of the area.

Two major karst plateaus concentrate most of the karst landforms. These elevated areas are separated by a large valley known as Mocambeiro Depression, containing several water-table lakes and a distinct drainage basin. Samambaia Creek and its tributaries drain the southeasternmost karst plateau, whereas Palmeiras-Mocambo Creek drains the karst plateau to the northwest (Fig. 2). The area has a tropical climate with nearly 90% of the yearly rainfall concentrated between October and March. The mean annual rainfall reaches 128 cm at Pedro Leopoldo meteorological station. The mean annual temperature and humidity are 23°C and 68% respectively.

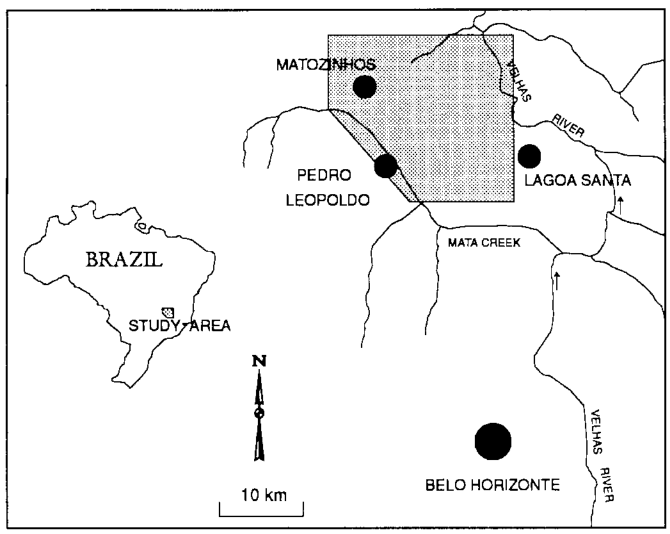

Figure 1. Location map of the study area.

KARST HYDROLOGY

Auler (1994) has made a hydrogeological characterization of the area. Most of the karst water is autogenic, originating as rainfall infiltrating into the limestone. Small allogenic contributions come from the areas of phyllite. Total runoff in the

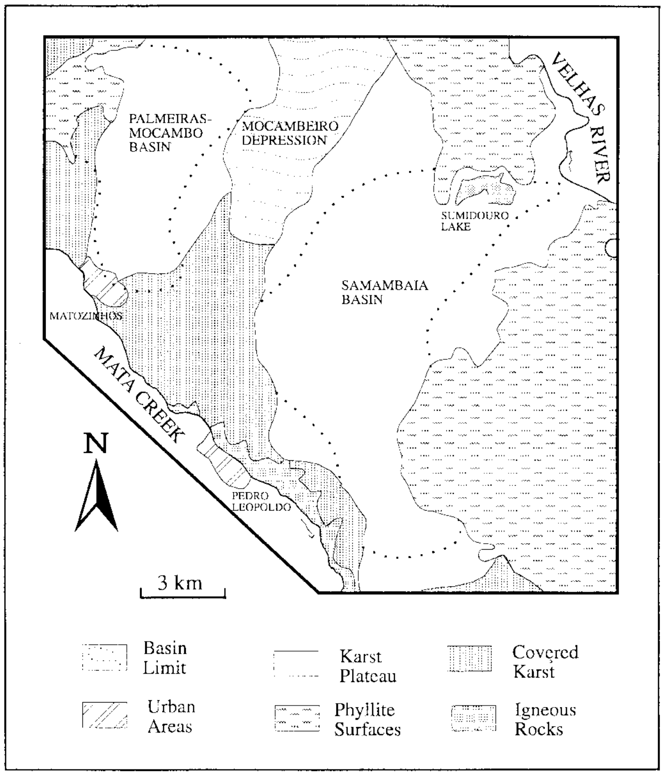

Figure 2. Main physiographical features in the Logoa Santa Karst.

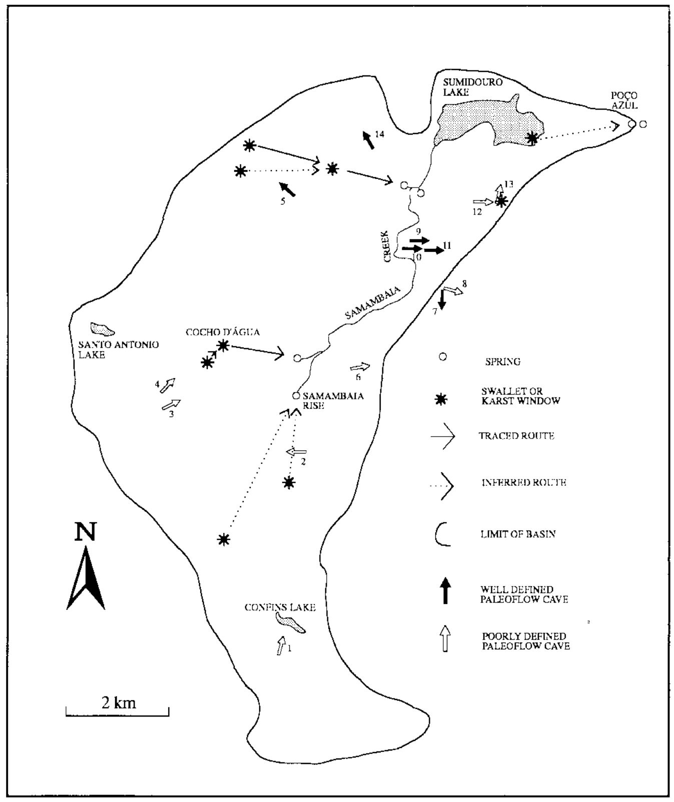

Figure 3. Dye tracing and cave paleoflow results at Samambaia Basin. Caves analyzed are: 1. Galinheiro, 2. Entrada Alta, 3. Borges, 4. Encanação, 5. Baú, 6. Mãe Rosa, 7. Monjolo I, 8. Monjolo II, 9. Lapinha I, 10. Lapinha II, 11. Lapinha III, 12. Corredor de Pedra, 13. Labirinto Fechado, 14. Buraco do Frederico.

karst as measured in springs varies between 1.8 m^3/s for the dry season to about 3.15 m^3/s during the wet months. Velhas River to the northeast is the major base level, draining about 88% of the karst water. The remaining 12% drains towards Mata Creek in the southwest. Dye tracing and discharge measurements have determined that Samambaia and Palmeiras-Mocambo are the largest karst drainage basins in both surface area and discharge. Groundwater flow occurs mainly along joints and lamination bedding, in accordance with the hydraulic gradient.

SAMAMBAIA BASIN

The Samambaia catchment area comprises around 60 km^2 (Fig. 3). The basin's upper section probably includes a large underground catchment area that eventually drains into Samambaia Creek rise. Much of the incoming flow concentrates in four springs along the creek's margin. Samambaia creek has a subaerial run of ~8 km, flowing through a shallow valley limited by gentle soil-covered slopes with some limestone outcrops. The creek discharges into Sumidouro Lake, which is subject to intense evaporation. Sumidouro Lake has a short underground course probably heading toward Poço Azul Spring, located a few meters from the Velhas River channel. Total discharge of the springs that feed Samambaia Creek range from 0.3 m^3/s during the dry season to 0.7 m^3/s during the wet season.

PALMEIRAS-MOCAMBO BASIN

The catchment area for this basin is about 30 km^2. The recharge area includes part of the town of Matozinhos as well as some highly karstified surfaces to the north. The watershed receives water from three different sources (Fig. 4): some small convergent sinks that feeds Bom Jardim Lake, the sink of Palmeiras Creek and the creek at Zé Irene Sinkhole. Except for a small contribution from phyllite surfaces at the source of Palmeiras Creek, all the water comes from diffuse infiltration into the limestone. These three branches have both subaerial and underground sections, discharging at Mocambo Spring. From here, the Mocambo Creek flows through fluviokarst valleys into Velhas River.

The Palmeiras-Mocambo Basin shows a highly segmented drainage route with numerous karst-windows along its course. Subaerial sections occur along the bottom of large collapse sinkholes (karst windows). The discharge at Mocambo Spring varies between 0.4 and 1.0 m^3/s for dry and wet seasons, respectively.

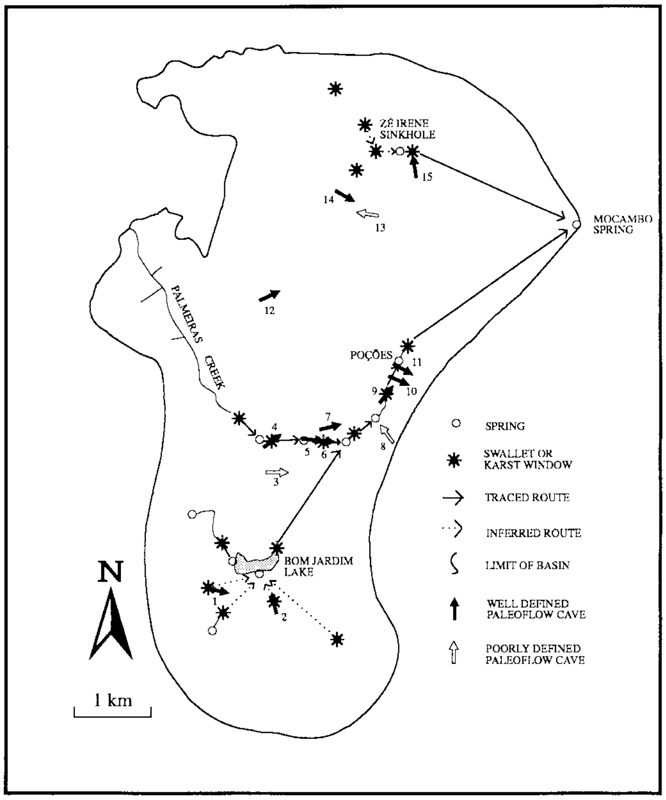

Figure 4. Dye tracing and cave paleoflow results at Palmeiras-Mocambo Basin. Caves analyzed are: 1. Faustina, 2. Boca, 3. Itapucú, 4. Milagres, 5. Periperi I, 6. Periperi II, 7. Pallet, 8. Chapéu, 9. Poções, 10. Poções Cliff I, 11. Poções Cliff II, 12. Escadas, 13. Caieiras, 14. Cacimbas, 15. Esquecida.

PALEOFLOW ANALYSIS

Over 300 caves have been identified in the Matozinhos-Pedro Leopoldo Karst. Lakes play a significant role in the speleogenesis in the area (Auler, 1995). According to Piló (1986), 55% of the caves in the area are dry, aborted from the regional hydrology. Observed hydrological processes inside some of these caves are restricted to dripping from percolation water or invasion runoff during severe storms. The dry caves usually have entrances associated with cliff walls, located above valleys and sinkhole floors. The caves are fragments of larger systems, dissected by surface lowering or by clastic and chemical sediment chokes. They show a complex history of paragenetic development followed by sediment removal.

Solutional forms in the relict caves can provide useful information on the paleohydrology and evolution of an area (Kastning, 1983; Lauritzen, 1982). Scallops have long been recognized as indicators of paleoflow direction in caves (Coleman, 1949). Studies of paleohydrology based on analyses of scallops have been performed in some settings, especially in the Mammoth Cave area, Kentucky, USA (Drake & Borden, 1981 and White & Deike, 1989). Theoretical equations and the hydraulic mechanics of the development of scallops are given by Curl (1974) and Gabriel (1986). Moreover, scallops can potentially be used to estimate drainage-basin area (Lauritzen, 1989).

Observations made in 47 caves inside both drainage basins allowed the determination of the general flow directions of the past. It also provided an insight on the relative evolution of the two karst drainage systems. The studied caves did not experience a synchronous evolution, having become dry at different periods. Absolute ages for cave development have not yet been determined.

In this study, analysis of several sections of cave walls were performed in the sampled caves. The longest possible section of cave passage was always considered in the determination of flow direction, in order to avoid non-representative data from segmented meanders. In some caves, the walls are smooth and scallops are not well defined. Dissolution by water vapor or under a covering of sediment may have played a role in masking scallop morphology.

Preservation of scallops in the dry caves is highly variable. In some caves scallops are not visible at all, whereas in others, the direction of paleoflow varies, suggesting backflooding or changing directions. Some caves show non-prominent scallops where flow direction was determined with some uncertainty. The remaining caves have a well defined paleoflow direction, due to well preserved scallops.

Flow directions were plotted on the maps of the drainage basins as distinct single vectors for either well defined paleoflow caves or poorly defined paleoflow caves, together with the cave reference number. Non-defined paleoflow caves were not taken into account. Due to the segmented nature of many caves, paleoflow vectors were assumed to be acceptable representations of ancient flow directions. Present groundwater flow routes were also represented as approximations, based on inputs and outputs of dye traces. Dye tracing was performed using fluorescein and is described in detail in Auler (1994).

SAMAMBAIA BASIN RESULTS

Figure 3 shows the paleoflow directions in Samambaia Basin. In the upstream section, the paleoflow of the caves studied (1,2,3 & 4) match well with the present underground hydrology. However, the downstream section shows some anomalies, with the paleoflow not pointing towards Samambaia Creek, the present local base level. Flow in some caves, such as caves 6, and 8 to 12 point toward the present regional base level, Velhas River, whereas others (caves 5 & 14) are directed toward the Mocambeiro Depression to the west. Caves 7 and 8 are located just outside of the presumed boundary of the existing drainage basin.

PALMERIRAS-MOCAMBO BASIN RESULTS

Paleoflow in this basin is represented in Figure 4. The great majority of the paleoflow indicators are directed in accordance with the present active hydrogeological routes. In the upstream section, the flow in all analyzed dry caves agree with the existing flow directions. The sole exception occurs in the downstream section of the basin for cave 13 (a cave with poorly defined scallops). Some caves located in the eastern side of this basin (caves 10 & 11) show paleoflow pointing toward the Mocambeiro Depression.

DISCUSSION

Paleoflow data for the downstream part of Samambaia Basin (Fig. 3) shows that there is little concordance between the present-day hydrology and past flow routes. Some caves (5 & 14) point toward the Mocambeiro Depression, showing that the positions of the water divides between the Samambaia Basin and the Mocambeiro Depression basin were perhaps located to the east in the past. Other caves (6,9,10,11 & 12) near Samambaia Creek have paleoflow toward the present location of Velhas River. It seems likely that the Samambaia Creek did not represent a significant base level at the time of genesis of these caves. The groundwater paleoflow does not correlate with the present position of the creek, but is directed instead towards other basins (Mocambeiro) or straight to Velhas River. Figure 5 represents the observed major paleoflow trends at Samambaia Basin. The data suggest that some features of this basin, especially in the downstream section, may be more recent in age.

The dry caves at the Palmeiras-Mocambo Basin (Fig. 4) show a concordant paleoflow direction when compared to the present routes. The general drainage flow pattern has not changed much within the area of the basin. There is convergent paleoflow in the upstream part of the basin and more uniform flow directions with some tributaries (cave 8 for example) in the downstream section. The data show no evidence of a major allogenic paleostream entering this basin as had been suggested by Kohler (1989). The data from active and dry caves point toward multiple autogenic input points that formed the basin in both past and recent times.

CONCLUSIONS

Although located near to each other and having been subject to the same lithologic and climatic controls, the Samambaia and Palmeiras-Mocambo basins have a rather distinct developmental history. Palmeiras-Mocambo Basin seems to be a more mature drainage basin, in the sense that its flow pattern at the time of genesis of today's dry caves closely resembles the present flow pattern. In contrast, the morphology of Samambaia Basin is probably more recent owing to the fact that several dry caves are related to either another distinct local base level (such as the Mocambeiro Depression drainage basin) or to the regional base-level (Velhas River).

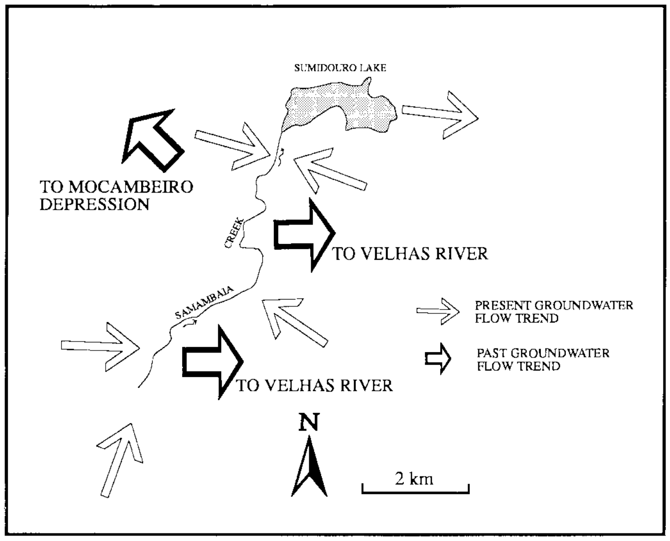

Figure 5. Trends of present and past groundwater flow at Samambaia Basin.

ACKNOWLEDGMENTS

This work has benefited from financial and material support from Western Kentucky University, Richmond Area Speleological Society, Cave Research Foundation and National Speleological Society. My colleagues from Grupo Bambuí de Pesquisas Espeleológicas helped during much of the field work.

REFERENCES

Auler, A. (1994). *Hydrogeological and Hydrochemical Characterization of the Matozinhos-Pedro Leopoldo Karst, Brazil*. MSc Thesis, Western Kentucky University: 110.

Auler, A. (1995). Lakes as a speleogenetic agent in the karst of Lagoa Santa, Brazil. *Cave and Karst Science 21*: 105-110.

Beato, D., Berbert, M., Danderfer, A., Pessoa, P. (1992). Avaliação preliminar do carste de Sete Lagoas - Lagoa Santa e riscos ao meio-ambiente antrópico (Projeto Vida). *Proceedings of the II Simpósio Situação Ambiental e Qualidade de Vida na Região Metropolitana de Belo Horizonte e Minas Gerais*: 56-59.

Coleman, J.C. (1949). An indicator of water-flow in caves. *Proceedings University of Bristol Speleological Society 6*: 57-67.

Curl, R.L. (1974). Deducing flow velocity in cave conduits from scallops. *National Speleological Society Bulletin 36*: 1-5.

Drake, M.E. & Borden, J.D. (1981). Complex groundwater basin migrations in Roppel Cave, Kentucky. *Proceedings of the 8th International Congress of Speleology, Bowling Green*: 28-30.

Gabriel, R. (1986). *Contribució a l'Estudi de les Empremtes de Corrent*. Barcelona, Espeleo Club de Gracia, 78 pp.

Kastning, E.H. (1983). Relict caves as evidence of landscape and aquifer evolution in a deeply dissected carbonate terrain: southern Edwards Plateau, Texas, U.S.A. *Journal of Hydrology 61*: 89-112.

Kohler, H.C. (1989). *Geomorfologia Cárstica na Região de Lagoa Santa, MG*. Doctorate dissertation, Universidade de São Paulo: 113 pp.

Lauritzen, S.E. (1982). The paleocurrents and morphology of Pikhaggrottene, Svartisen, North Norway. *Norsk Geogr. Tidsskr 36*: 184-209.

Lauritzen, S.E. (1989). Scallop dominant discharge. *Proceedings of the 10th International Congress of Speleology, Budapest, Hungary*: 123-124.

Piló, L.B. (1986). *Contribuição ao Estudo do Karst na Micro-Região de Belo Horizonte*. Unpublished report, 10 pp.

White, W.B. & Deike, G.H. (1989). Hydraulic geometry of cave passages. In W.B. White and E.L. White (eds). *Karst Hydrology, Concepts from the Mammoth Cave Area*. New York, Van Nostrand Reinhold: 223-258.

Charles H. Anderson Jr. has received a Gold Medal in the NSS Photo Salon and many Merit and Honorable Mention Awards. He was elected a Fellow of the Explorers Club and has been a member of the NSS for over 28 years. He is the founder and Director of the International Glaciospeleological Survey. He was the leader of the Paradise Ice Caves project and the Leader of the Mount St. Helens Crater Caves project.

Chris J. Behrens is a geologist with over four years of experience as a field geologist with HWA's geotechnical services group. He also has three years of experience as an exploration geologist for major mining and consulting firms. Behrens has worked since 1991 studying ice caves in Washington State. The main locations of these studies have been the crater firn caves at Mount St. Helens, and the Big Four Ice Caves east of Granite Falls, Washington.

Linda Doran is a writer and editor for Sandia National Laboratories in New Mexico, Linda Doran has a professional background in public relations and journalism and a bachelor's degree in anthropology. As a volunteer, she has helped with geological and biological inventory, restoration, and mapping for public agencies that manage cave resources.

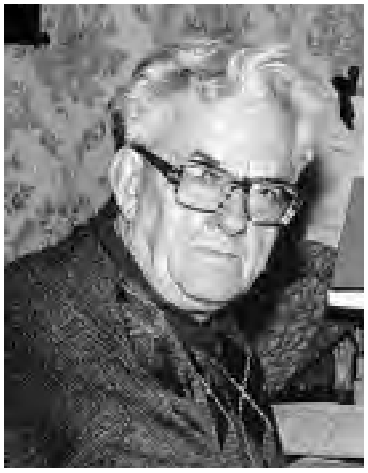

Victor N. Dublyansky was born in 1930. Graduated from Odessa State University (Odessa, Ukraine, 1958). ScD, Professor at the Perm State University (Perm, Russia). Fields of professional expertise: karst geology, hydrogeology, engineering geology, cave climate, regional karst studies (Crimea, Western Ukraine, Caucasus, Central Asia, etc.). Authored more than 400 publications including 28 monographs.

Yuri V. Dublyansky was born in 1960. Graduated from Odessa State University (Odessa, Ukraine, 1982). PhD, Senior Scientist at the United Institute of Geology, Geophysics and Mineralogy, Russian Academy of Sciences (Novosibirsk). Fields of professional expertise: hydrothermal karst, cave mineralogy, paleohydrogeology. Authored more than 50 publications including 1 monograph.

Gary Floyd is a Fellow Member of the International Glaciospeleological Survey. He is a member of the Crater team of Mount St. Helens from 1994 to present. He has worked at Mount St. Helens Volcanic Monument in the Wildlife and Watershed Departments. He is a Registered Environmental Assessor, State of California. He is an Instructor in Environmental Technology of City College of San Francisco and has a MS in Environmental Management from the University of San Francisco.

David H. Jagnow is a Consulting Geologist and President of Venture Capital Information, Los Alamos, NM. Caving since 1960, he joined the NSS in 1965 and became a member of CRF in 1972. B.A. in Geology at University of Iowa (1970) and M.S. in Geology at University of New Mexico (1977). He has conducted bat studies in Oklahoma and New Mexico since 1987. He is an NSS Fellow, recipient of the NSS Conservation Award, and currently NSS Conservation Chairman.

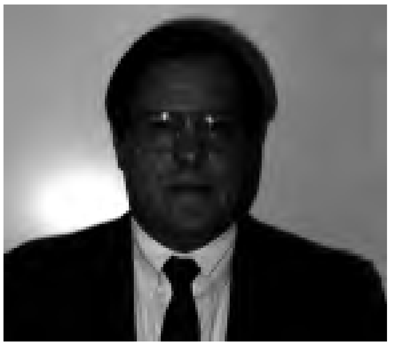

For for than 25 years, Carol Hill has studied the geology of Carlsbad Cavern, the Delaware Basin, and the western part of the Permian Basin in the south-western United States. Among the books she has published are *Cave Minerals of the World*, *Geology of the Delaware Basin*, and *Geology of Carlsbad Cavern and Other Caves in the Guadalupe Mountains*. (No Photo)

Mark R. Vining has been in the Paradise Ice Caves over 170 times. He is the Chief Scientist of the International Glaciospeleological Survey. He worked for Exxon Company, USA and Exxon Production Research through the 1980s and early 1990s as a petroleum geologist in Texas, New Mexico, Florida, Saudi Arabia, and Abu Dhabi. In 1997 he completed a PhD dissertation in geosciences, mathematics, and engineering on development of a watershed evolution computer model at Texas Tech University. Currently he is a Research Fellow with the University of Texas at Austin, Bureau of Economic Geology. (Photo on Front Cover)

National Speleological Society
2813 Cave Avenue
Huntsville, Alabama 35810-4431